AN INVESTIGATION OF THE INVISCID SPATIAL INSTABILITY OF COMPRESSIBLE MIXING LAYERS

Thesis by

Mei Zhuang

In Partial Fulfillment of the Requirements

for the Degree of

Doctor of Philosophy

California Institute of Technology

Pasadena, California

1990

(Submitted May 18, 1990)

To my parents

ACKNOWLEDGEMENTS

This work would not have been possible without the help of a great many people. I wish to express my deep gratitude to my thesis advisor, Professor Paul E. Dimotakis, for his guidance, understanding, and support during my graduate studies. I am truly grateful to Professor Toshi Kubota for his valuable discussions and suggestions during the course of this research project. In addition, discussions with Professor Anthony Leonard, Professor Hans Wolfgang Liepmann and Professor Anatol Roshko were both fruitful and encouraging.

I would like to thank my friends and colleagues in the GALCIT community for their help and encouragement. For many interesting discussions (scientific and otherwise), I would particularly like to thank the members of "the group": Dr. Manooch Koochesfahani, Dr. Rick Miake-Lye, Dr. Dimitri Papamoschou, Cliff Frieler, Jeff Hall, Paul Miller, Phil Tokumaru, Rick Gilbrech and Dr. Henning Rosemann. I am grateful to Dr. Dan Lang for his expertise with computers. For many helpful moments, I am also grateful to Mrs. Judy Kleiner. I owe special thanks to my roommates Jessica Goodfellow, Elaine Kuo, Barbara Wyslouzil and Zheng Zeng for their friendship and support.

Much love and thanks are given to my husband, Wen Jin Meng. We have shared many joys and sorrows during my graduate studies at CALTECH and have accomplished this goal for both of us together. Finally, for making it all possible, and for their encouragement and support in all my educational endeavors,

I dedicate this thesis to my parents.

This work was supported by the Air Force Office of Scientific Research grants No. 83–0213 and 88–0155.

ABSTRACT

The behavior of both unbounded and bounded compressible plane mixing layers with respect to two- and three-dimensional, spatially growing wave disturbances is investigated using linear stability analysis. The mixing layer is formed by two parallel streams with different gases and the flow is assumed to be inviscid and non reacting.

For unbounded mixing layers, the effects of the free stream Mach number, velocity ratio, temperature ratio, gas constant (molecular weight) ratio and the ratios of specific heats on the linear spatial instability characteristics of a mixing layer are determined. A nearly universal dependence of the normalized maximum amplification rate on the convective Mach number is found for two-dimensional spatially growing disturbances. The effects of the mean flow profiles on the instability behavior of the mixing layers are also studied. It is shown that decreasing the thickness of the total temperature profile relative to the mean velocity profile, or adding a wake component in the mean velocity profile can make the normalized amplification rate decrease slower as the convective Mach number increases for both subsonic and supersonic convective Mach numbers.

For an unbounded mixing layer with subsonic convective Mach numbers, there is only one unstable mode propagating with a phase velocity C_{pm}^{*} approximately equal to the isentropically estimated convective velocity of the large scale structures u_{c}^{*}. As the convective Mach number approaches or exceeds unity, there

are always two unstable spatial modes. One is with a phase velocity $C^*_{pm} < u^*_c$ (slow mode) and the other is with a phase velocity $C^*_{pm} > u^*_c$ (fast mode). For the low supersonic convective Mach numbers, the fast mode is more unstable than the slow mode when the heavy gas is on the low speed side and the slow mode is dominant when the heavy gas is on the high speed side.

The effect of parallel flow guide walls on a spatially growing mixing layer is also investigated. It is shown that, in this case, if the convective Mach number exceeds a critical value of approximately unity, there are many supersonic unstable modes. The maximum amplification rates of mixing layers approach an asymptotic value and this maximum amplification rate increases to a maximum value and decreases again as the distance between the walls decreases. For a mixing layer inside parallel flow guide walls, the growth rate of three-dimensional modes is larger than the corresponding two-dimensional mode at high convective Mach numbers. But the growth rate of two-dimensional supersonic instability waves has a larger value than their three-dimensional counterparts for a mixing layer inside a rectangular duct (Tam & Hu [1988], [1989]). Contour plots of the pressure perturbation fields for both unbounded and bounded mixing layers indicate that there are waves propagating outward from the mixing layer along the Mach angle, and that the walls provide a feedback mechanism between the growing mixing layer and this compression/expansion wave system. The bounded mixing layers are more unstable than the corresponding free mixing layers for supersonic convective Mach numbers. The streaklines of the flow confirm that the spreading rate of the mixing layer is unusually small for supersonic disturbances.

TABLE OF CONTENTS

LIST OF FIGURES

LIST OF TABLES

LIST OF SYMBOLS

Symbol	Description
a	Sound of speed
A, A_+, A_-	Complex constants
b	Span of rectangular duct
B	Complex constant
c	Complex phase velocity
c_1, c_2	Constants
c_v	Specific heat per unit mass at constant volume
c_p	Specific heat per unit mass at constant pressure
c_N	Phase velocity of the neutral mode
C_p	Phase velocity of the unstable mode, ω/α_r
C_{pm}	Phase velocity of the most unstable mode, ω_m/α_{rm}
C_δ	Coefficient, given by Eq. 4.3
d	Half distance between flow guide walls, given in Fig. 2.2
D	Binary diffusion coefficient
f	Complex amplitude function of u'
$F(\alpha, \omega)$	Dependent variable, defined by Eq. 2.44
$F(M_{c1})$	Dependent variable, defined by Eq. 4.8
h	Enthalpy per unit mass of gas mixture, given by Eq. 2.7
h_1, h_2	Enthalpy per unit mass of upper and lower streams
h_t	Total enthalpy per unit mass of gas mixture
k	Thermal conductivity

M_1	Mach number of upper stream
$\hat{M}_1$	Free stream Mach number, defined by Eq. 4.13
M_{1cr}	Critical Mach number of upper stream
M_{c1}	Convective Mach number of upper stream
M_{c2}	Convective Mach number of lower stream
p	Pressure
Pr	Prandtl number $c_p^*\mu^*/k^*$
p_0, p_2, p_3, p_4	Constants
q	Complex amplitude of q'
q'	Disturbance of flow quantity
Q	Flow quantity
r	Complex amplitude of ρ'
R	Gas constant
Sc	Schmidt number $D^*\rho^*/\mu^*$
t	Time
t_0	Initial condition of t
T	Temperature
T_t	Total temperature
u_c	Isentropic estimate of the convective velocity
u	Velocity component in the x direction
v	Velocity component in the y direction
w	Normalized wake deficit
x	Streamwise coordinate
x_0	Initial condition of x
y	Cross-stream coordinate
y_0	Initial condition of y

y_1	Constant
Y	Howarth-transformed y coordinate
z	Spanwise coordinate

Greek Letters

α	Streamwise eigenvalue, $\alpha = \alpha_r + i\alpha_i$
α_m	Most unstable streamwise eigenvalue, $\alpha_m = \alpha_{rm} + i\alpha_{im}$
$\hat{\alpha}$	Complex wave number, defined in Eq. 4.12
β	Spanwise eigenvalue, $\beta = \beta_r + i\beta_i$
γ	Ratio of specific heats c_p^*/c_v^*
δ	Mixing layer thickness, defined in Eq. 2.42
δ'	Mixing layer growth rate $d\delta/dx$
ϵ, ϵ_1	Constants
η	Complex amplitude function of χ_1'
θ	Complex amplitude function of T'
ϑ	Angle of an instability wave, $\tan\vartheta = \beta/\alpha$
κ_1, κ_2	Constants
λ	Velocity ratio, $\lambda \equiv (1 - u_2/u_1)/(1 + u_2/u_1)$
λ_+, λ_-	Exponent in asymptotic solution, equation 2.38
Λ_+, Λ_-	$\Lambda_\pm = \lambda_\pm^2$
μ	Viscosity
ν	Mach angle
ζ	Dependent variable, defined in Eq. 3.11
π	Complex amplitude function of p'
ρ	Density

σ	Relative thickness parameter
ϕ	Complex amplitude function of v'
χ_1	Mass fraction of species 1 (upper)
χ_2	Mass fraction of species 2 (lower)
ψ	Stream function
ω	Real disturbance frequency
ω_m	Real disturbance frequency of the most unstable mode

Other Symbols

$()_0$	Incompressible quantity
$()_1$	Upper stream quantity
$()_2$	Lower stream quantity
$()_r$	The ratio of free stream quantity $()_2/()_1$
$()^*$	Dimensional quantity
$\dot{()}$	Derivative $d()/dy$
$\overline{()}$	Mean quantity
$()'$	Disturbance quantity
$\|()\|$	Magnitude

CHAPTER 1

INTRODUCTION

1.1 Historical Background

The aims of the study of hydrodynamic stability were to find how and when laminar flows break down and undergo transition to turbulence or some other laminar flow. The basic problems of hydrodynamic stability were studied and formulated by Helmholtz [1868], Kelvin [1871], Rayleigh [1880] and Reynolds [1883] at the end of the nineteenth century. The hydrodynamic equations were linearized by assuming that the disturbances of the flows were infinitesimally small. The method of normal modes was used. Vivid descriptions of the problems were given by Reynolds through his series experiments on the instability of flow in a pipe.

The first analytic study of two-dimensional hydrodynamic stability was made by Helmholtz [1868] and Kelvin [1871]. They considered the basic flow of incompressible, inviscid fluids in two horizontal parallel infinite streams of different velocities and densities, one stream above the other, and solved the problem of the instability of a wavy disturbance over the surface of discontinuity. It is now called the Kelvin-Helmholtz instability. Later, Rayleigh [1913] studied the instability of incompressible, inviscid parallel flows with continuous velocity distributions across the flows. An important result of his studies is the finding that the existence of an inflection point in the basic velocity profile is a necessary condition for instability.

This result was further enhanced by the work of Tollmien [1935]. He pointed out that this "inflection-point criterion" is not only necessary but also sufficient for flows with a symmetrical or a boundary-layer type velocity distribution. Further development, clarification and physical interpretation of these general results were given by Lin [1944, 1955].

As a result of the increasing importance of the phenomena of gas flow at high speeds, linear stability investigations have been extended to include the effect of compressibility. The first attempt to develop a compressible stability theory was made by Kuchemann [1938]. He studied the stability of a piecewise linear velocity profile representing a boundary layer in a compressible fluid. Later on, the stability of tangential discontinuities in a compressible fluid was treated by Landau [1944]. He showed that tangential discontinuities are stable with respect to infinitesimal disturbances.

Important theoretical investigations of the stability of the compressible laminar free and bounded mixing layers to infinitesimal wave disturbances were made by Lees & Lin [1946]. Their study was in the form of an extension of the principles and techniques already formulated for the study of the stability of incompressible laminar flows to compressible laminar flows. They gave a general stability criterion in terms of the gradient of the product of density and vorticity, analogous to the Rayleigh-Tollmien criterion for the case of an incompressible fluid. The disturbances outside the mixing layers were classified by Lees & Lin as "subsonic," "sonic" and "supersonic" disturbances, according to whether the phase velocity of the wavy disturbance in the direction of the free stream relative to that of the fluid

is less than, equal to, or greater than local velocity of the sound. Also, a detailed consideration to an inviscid theory of compressible mixing layers was given and the possibility that the disturbances in a compressible flow can produce a turbulent transition or lead to the formation of a shock was also pointed out by Lees & Lin.

The instability of inviscid compressible free mixing layers with respect to two- and three-dimensional, temporally growing disturbances was considered by Lessen, Fox & Zien [1965, 1966] for both subsonic and supersonic disturbances. Under the assumption that the flow was iso-energetic, $h_t^* = h^* + u^{*2}/2 = \text{constant}$, they found that the flow is unstable with respect to supersonic disturbances, although the amplification rate is smaller than for subsonic disturbances and the increase of the angle between the disturbance wave number vector and the principle flow direction tends to increase the instability. With spatially growing disturbances, Gropengiesser [1970] studied this instability problem using the Crocco-Busemann relation, $h_t^* = h^* + u^{*2}/2 = \text{fn}(u^*)$, for the mean temperature profile, which would be discussed in detail later, and using the compressible laminar boundary layer velocity profile for the mean velocity distribution across the mixing layers. He carried out the inviscid instability calculations at various free stream Mach numbers and temperature ratios. He found the existence of a second unstable mode and showed that a change in the character of the disturbance may involve the amplification of a second mode. He also noted the high growth rate of three-dimensional waves at high Mach numbers. In order to simplify the stability problems, Blumen and Drazin *et al.* [1970, 1975, 1977] studied the stability problem by assuming that the thermodynamic state of a compressible, inviscid, free mixing layer is constant. They showed that two-dimensional disturbances are unstable at all values of the Mach

number and that there exists a second unstable supersonic mode.

A critical review of the experimental data for developed compressible free turbulent mixing layers was given by Birch & Eggers [1973]. They indicated that although some inconsistency exists among the various experimental investigators, there is a definite trend of decreasing growth rate with increasing free stream Mach number. Experimental evidence of large scale structures in two-stream supersonic turbulent mixing layers were given by Chinzei *et al.* [1986], by Papamoschou & Roshko [1986, 1988] and Papamoschou [1986, 1989]. Papamoschou & Roshko suggested the convective Mach number M_c as the appropriate parameter scaling the effect of compressibility. This is defined, for each stream, as:

$$M_{c1} = \frac{u_1^* - u_c^*}{a_1^*}, \quad M_{c2} = \frac{u_c^* - u_2^*}{a_2^*}, \tag{1.1}$$

where u_1^*, u_2^* and a_1^*, a_2^* are the free stream velocities and speeds of sound. The quantity u_c^* is the convective velocity of the large scale structures. Coles [1981] pointed out that stagnation points must exist in these large scale structures. The convective velocity u_c^* was estimated by Papamoschou & Roshko assuming that the dynamic pressures match at stagnation points in the flow (Coles [1985], Dimotakis [1986]). For compressible isentropic flow with equal static pressures in the two free streams, *e.g.*, Papamoschou & Roshko,

$$\left(1 + \frac{\gamma_1 - 1}{2} {M_{c1}}^2\right)^{\frac{\gamma_1}{\gamma_1 - 1}} = \left(1 + \frac{\gamma_2 - 1}{2} {M_{c2}}^2\right)^{\frac{\gamma_2}{\gamma_2 - 1}}, \tag{1.2}$$

where γ_1, γ_2 are the ratios of the specific heats of the two streams. If γ_1 and γ_2 are equal, u_c^* is given by

$$u_c^* = \frac{a_2^* u_1^* + a_1^* u_2^*}{a_1^* + a_2^*}, \tag{1.3}$$

which, for equal static free stream pressures, reduces to the incompressible expression (Dimotakis [1986]). They suggested that the normalized growth rate of a compressible mixing layer (unity for incompressible flow) might be expressible as a universal function of the convective Mach number M_{c1} which is valid over a wide range of velocity and temperature ratios of a mixing layer. They also indicated that the normalized growth rate decreased significantly with increasing M_{c1}, for subsonic M_{c1}, and reached an asymptotic value for supersonic convective Mach numbers. The same qualitative behavior had been found by Bogdanoff [1983] in his analysis of several previous experimental investigations of supersonic mixing layers.

Using linear spatial instability theory, Ragab & Wu [1988, 1989] studied the influence of velocity ratio on the stability characteristics of compressible free mixing layer. They also investigated the effect of the convective Mach number on the growth rates of mixing layers. Their results indicate that the convective Mach number is a parameter which correlates compressibility effects on the spreading rate of mixing layers. Jackson & Grosch [1988, 1989] presented their results of a study of the inviscid spatial instability behavior of compressible free mixing layers with one stream moving and the other stream stationary. They showed that if the Mach number of the moving stream exceeds a critical value, there are always two groups of unstable waves. One of these groups is fast with normalized phase speeds greater than 1/2, and the other is slow with phase speeds less than 1/2. They also showed that three-dimensional modes have the same general behavior as two-dimensional modes, but with higher growth rates over some range of propagation direction. Recently, Sandham & Reynolds [1989a, 1989b] investigated compressible mixing layers using both linear theory and direct simulation. They showed that lin-

ear theory can be very useful in understanding the physics of free mixing layers and the growth rates of the developed plane mixing layers and that three-dimensional modes are dominant in an unbounded high-speed mixing layer above a convective Mach number of 0.6.

For a compressible boundary-layer, the study of linear instability theory carried out by Mack [1969, 1984] indicated that for supersonic disturbances there are two kinds of neutral waves, inflectional and noninflectional, and that there are always unstable modes in boundary-layers. Mack also noted the high amplification rate of three-dimensional waves at high Mach number.

For a mixing layer inside a rectangular channel, Tam & Hu [1988] showed that the coupling between the motion of the mixing layer and the acoustic modes of the channel produces new instability waves for the spatially growing mixing layers. Greenough *et al.* [1989] considered the effects of walls on a confined compressible, temporally growing mixing layer. They showed that there are two general types of instabilities: confined Kelvin-Helmholtz modes and supersonic wall modes. A class of highly amplified supersonic disturbances are found by Macaraeg & Streett [1989] for high-speed, temporally growing bounded shear flows at high values of the streamwise wave number.

1.2 Present Research Objective

The present studies were undertaken in order to investigate the linear

instability behavior of both unbounded and bounded compressible plane mixing layers with respect to two- and three-dimensional, spatially growing wave disturbances. The purpose of this study is to understand the effect of compressibility on spatially growing plane mixing layers and also the effect of the mean flow profiles on the instability behavior of the mixing layers. The mixing layer is formed by two parallel streams with different gases and the flow is assumed to be inviscid and non reacting.

The convective velocity is estimated by the phase velocity of the most unstable mode C^*_{pm}, since we only consider the amplified disturbances ($\alpha_i < 0$). Therefore, the convective Mach number for each stream is defined here as:

$$M_{c1} = \frac{u^*_1 - C^*_{pm}}{a^*_1}\,, \qquad M_{c2} = \frac{C^*_{pm} - u^*_2}{a^*_2}\,. \tag{1.4}$$

For these amplified disturbances, we think the definition given by Eq. 1.4 is appropriate since we are tracking the most unstable mode. Mack [1975] used the phase velocity of the neutral mode c^*_N as the convective velocity in his stability analysis of the existence of many supersonic neutral waves of supersonic boundary layer. Sandham & Reynolds [1989b] proposed that the large-scale structures found in the mixing layer are associated with neutral instability modes. Therefore, they used the phase velocity of the neutral mode c^*_N to estimate the convective velocity of the large-scale structures in the mixing flow.

For a compressible mixing layer comprised of different gases, the instability calculations were carried out for inviscid wave disturbances, *i.e.*, the effect of viscosity was neglected in the disturbances, and the mean flow profiles were

assumed to vary smoothly across the mixing layer. The disturbances were also assumed to have small amplitudes. Therefore, the linearized equations could be used. The main flow was assumed to be quasi-parallel, *i.e.*, it possessed only a velocity component in the direction of the flow. These assumptions have been justified by previous investigators (*e.g.* Lin [1955]). The assumption of parallel flow provided an even better approximation in the case of compressible mixing layers, since the growth rate of the mixing layer became smaller with increasing free stream Mach number M_1.

The linearized equations for inviscid disturbances were derived and the eigenvalue problem was formulated in Chapter 2. The range of unstable frequencies and wave numbers was numerically calculated using a Runge-Kutta method combined with a shooting technique. The mean flow distributions were either assumed or derived from the boundary layer equations for compressible mixing flow. The details of these mean flow profiles were discussed in Chapter 3.

For compressible, unbounded mixing layers, the influence of free stream Mach number, velocity ratio, temperature ratio and gas constant (molecular weight) ratio, and ratios of the specific heats on the linear spatial instability characteristics of a mixing layer were investigated. The effect of the convective Mach number on the growth rate of the mixing layers was studied. Numerical calculations of linear spatial instability characteristics of the mixing layers with different combinations of the free stream Mach number, velocity ratio, temperature ratio and gas constant ratio were performed in which the free stream Mach number ranged from 0 to 11, the velocity ratio varied from 0.25 to 0.75, the temperature ratio varied

from 0.2 to 5 and the gas constant ratio varied from 0.1 to 5. In order to assess the sensitivity of the details of the mean flow profiles on the instability behavior of the compressible mixing layers, an initial mean velocity profile with a wake component and a total temperature profile with a different thickness relative to the mean velocity profile were also considered.

Finally, for a mixing layer inside parallel flow guide walls, the effects of walls and the distance between the walls on a spatially growing mixing layer were investigated. For a given distance between the parallel flow guide walls, the linear spatial instability characteristics of mixing layers were calculated for different free stream Mach numbers. Contour plots of the pressure perturbation fields indicate that there are waves propagating outward from the mixing layer along the Mach angle, and that reflections of the compression/expansion waves caused by walls provide a feedback mechanism between the growing mixing layer structures and the wave system for supersonic convective Mach numbers. Also, the flow patterns of the mixing layers were obtained by calculating the streaklines of the mixing layers.

CHAPTER 2

MATHEMATICAL FORMULATION

The objectives of this chapter are to derive the linearized disturbance equations for inviscid, compressible plane mixing layers and to formulate the eigenvalue problem of the instability of the mixing layers. The mixing layer is formed by two parallel streams with different perfect gases and is subjected to a two-dimensional spatially growing wave disturbance.

2.1 Equations for Small Disturbances

Consider a two-dimensional compressible mixing layer formed by two parallel streams. Assume that the fluids on each stream of the mixing layer are inviscid and non reacting. In the absence of external forces, the general equations of a two-dimensional, inviscid, compressible flow of a perfect gas can be written in Cartesian co-ordinates as follows:

(a) Equation of continuity:

$$\frac{D\rho^*}{Dt^*} + \rho^*\left(\frac{\partial u^*}{\partial x^*} + \frac{\partial v^*}{\partial y^*}\right) = 0 \tag{2.1}$$

(b) Equations of motion:

$$\frac{\partial u^*}{\partial t^*} + u^*\frac{\partial u^*}{\partial x^*} + v^*\frac{\partial u^*}{\partial y^*} = -\frac{1}{\rho^*}\frac{\partial p^*}{\partial x^*} \tag{2.2}$$

$$\frac{\partial v^*}{\partial t^*} + u^* \frac{\partial v^*}{\partial x^*} + v^* \frac{\partial v^*}{\partial y^*} = -\frac{1}{\rho^*} \frac{\partial p^*}{\partial y^*} \tag{2.3}$$

(c) Equation of energy:

$$\rho^* {c_v}^* \left(\frac{\partial T^*}{\partial t^*} + u^* \frac{\partial T^*}{\partial x^*} + v^* \frac{\partial T^*}{\partial y^*} \right) = -p^* \left(\frac{\partial u^*}{\partial x^*} + \frac{\partial v^*}{\partial y^*} \right) \tag{2.4}$$

(d) Equation of state:

$$p^* = \rho^* R^* T^* \ . \tag{2.5}$$

All quantities in these equations are dimensional, as defined in the List of Symbols.

Since the compressible mixing layers we considered are formed by two different ideal gases, according to the Gibbs-Dalton law, the pressure in a mixture of different gases is equal to the sum of the partial pressures of the different gases, *i.e.*,

$$p^* = \rho^* R^* T^* = p_1^* + p_2^* = \rho_1^* R_1^* T^* + \rho_2^* R_2^* T^* \ , \tag{2.6}$$

and the corresponding expression for enthalpy can be written as

$$h^* = \chi_1 h_1^* + \chi_2 h_2^* = (\chi_1 c_{p1}^* + \chi_2 c_{p2}^*) T^* \ , \tag{2.7}$$

where χ_1 is the mass fraction of species 1 of the gas mixture. The mass fraction, χ_2, of species 2 is equal to $1 - \chi_1$, since only two species exist in the mixing layer. Thus Eqs. 2.6 and 2.7 yield

$$R^* = \chi_1 R_1^* + (1 - \chi_1) R_2^* \ , \tag{2.8}$$

$$c_p^* = \chi_1 c_{p1}^* + (1 - \chi_1) c_{p2}^* \ . \tag{2.9}$$

For perfect gases, a similar expression can be obtained for the specific heat at constant volume c_v^*, *i.e.*,

$$c_v^* = \chi_1 c_{v1}^* + (1 - \chi_1) c_{v2}^* \ . \tag{2.10}$$

Since the mixing layer is formed by two different gases, Eqs. 2.1 to 2.5 do not form a complete set. They have to be supplemented by the species transport equation, which, in the absence of molecular diffusion, is given by

$$\frac{\partial \chi_1}{\partial t^*} + u^* \frac{\partial \chi_1}{\partial x^*} + v^* \frac{\partial \chi_1}{\partial y^*} = 0 \,. \tag{2.11}$$

We consider a time-independent basic flow and a small amplitude, time-dependent disturbance. For a parallel flow, the basic steady state is of the form

$$\overline{Q}^* = \overline{Q}^*(y^*)\, \hat{e}_x \,, \tag{2.12}$$

where $\hat{e}_x$ denotes the unit vector in the x^* direction. The general quantity of the flow can be expressed as

$$Q^*(x^*, y^*, t^*) = \overline{Q}^*(y^*) + Q'(x^*, y^*, t^*) \,, \tag{2.13}$$

where $\overline{Q}^*(y)$ is a mean flow profile, which will be discussed in Chapter 3, and Q' is a small amplitude disturbance. By substituting Eq. 2.13 for each of the variables into Eqs. 2.1 to 2.5 and Eq. 2.11 and neglecting terms quadratic in the small disturbance, we obtain the linearized disturbance equations. With upper stream quantities as the reference and the local layer thickness $\delta^*(x^*)$ as the length scale, the dimensionless variables are defined as follows:

$$t = t^* u_1^* / \delta^*, \quad x = x^*/\delta^*, \quad y = y^*/\delta^*,$$

$$u = u^*/u_1^*, \quad v = v^*/u_1^*,$$

$$\rho = \rho^*/\rho_1^*, \quad T = T^*/T_1^*, \quad R = R^*/R_1^*,$$

$$p = p^*/{p_1}^*, \quad c_p = {c_p}^*/{c_{p1}}^*, \quad c_v = {c_v}^*/{c_{v1}}^*.$$

The non dimensional parameters of the problem are the upper stream Mach number $M_1 = u_1^*/a_1^*$, where a_1^* is the speed of sound of the upper stream, and the ratio of specific heats of the upper stream $\gamma_1 = c_{p1}^*/c_{v1}^*$. The linearized dimensionless disturbance equations are arrived at :

Continuity:

$$\frac{\partial \rho'}{\partial t} + \bar{u}\frac{\partial \rho'}{\partial x} + v'\frac{d\bar{\rho}}{dy} + \bar{\rho}\left(\frac{\partial u'}{\partial x} + \frac{\partial v'}{\partial y}\right) = 0 \tag{2.14}$$

Momentum:

$$\bar{\rho}\left(\frac{\partial u'}{\partial t} + \bar{u}\frac{\partial u'}{\partial x} + v'\frac{d\bar{u}}{dy}\right) = -\frac{1}{\gamma_1 {M_1}^2}\frac{\partial p'}{\partial x} \tag{2.15}$$

$$\bar{\rho}\left(\frac{\partial v'}{\partial t} + \bar{u}\frac{\partial v'}{\partial x}\right) = -\frac{1}{\gamma_1 {M_1}^2}\frac{\partial p'}{\partial y} \tag{2.16}$$

Energy:

$$\bar{\rho}\bar{c}_v\left(\frac{\partial T'}{\partial t} + \bar{u}\frac{\partial T'}{\partial x} + v'\frac{d\overline{T}}{dy}\right) = -(\gamma_1 - 1)\left(\frac{\partial u'}{\partial x} + \frac{\partial v'}{\partial y}\right) \tag{2.17}$$

State:

$$1 = \bar{\rho}\,\overline{R}\,\overline{T}, \quad p' = \frac{\rho'}{\bar{\rho}} + \frac{R'}{\overline{R}} + \frac{T'}{\overline{T}} \tag{2.18}$$

Species transport:

$$\frac{\partial {\chi_1}'}{\partial t} + \bar{u}\frac{\partial {\chi_1}'}{\partial x} + v'\frac{\partial {\chi_1}'}{\partial y} = 0\,. \tag{2.19}$$

In these equations, $\bar{u}$, ..., $\bar{p}$ are dimensionless mean flow quantities and u', ..., p' are the corresponding dimensionless disturbances. Eqs. 2.14 to 2.19 form a system of dimensionless linear partial differential equations for the disturbances. The coefficients are known functions given by the steady mean flow profiles. After linearization, the dimensionless expressions of Eqs. 2.8 to 2.10 become:

$$\overline{R} = \frac{R_2}{R_1} + \left(1 - \frac{R_2}{R_1}\right)\bar{\chi}_1, \qquad R' = \left(1 - \frac{R_2}{R_1}\right){\chi_1}', \tag{2.20}$$

$$\bar{c}_p = \frac{c_{p2}}{c_{p1}} + \left(1 - \frac{c_{p2}}{c_{p1}}\right)\bar{\chi}_1, \qquad c_p' = \left(1 - \frac{c_{p2}}{c_{p1}}\right)\chi_1', \tag{2.21}$$

$$\bar{c}_v = \frac{c_{v2}}{c_{v1}} + \left(1 - \frac{c_{v2}}{c_{v1}}\right)\bar{\chi}_1, \qquad c_v' = \left(1 - \frac{c_{v2}}{c_{v1}}\right)\chi_1'. \tag{2.22}$$

2.2 Normal Mode Solution for a Spatially Growing Mixing Layer

We consider here the disturbance to be a two-dimensional wave propagating in the x-direction. The disturbance quantities in a suitably defined dimensionless form can be expressed as:

$$u', v' = \{f(y), \alpha\phi(y)\} \exp[\, i\alpha(x - ct)\,]; \tag{2.23}$$

$$\rho', T', p' = \{r(y), \theta(y), \pi(y)\} \exp[\, i\alpha(x - ct)\,]; \tag{2.24}$$

$$\chi_1' = \eta(y) \exp[\, i\alpha(x - ct)\,]; \tag{2.25}$$

where, for a spatially growing layer, α is a dimensionless complex wave number and c is a dimensionless complex wave velocity. Each component travels with the dimensionless phase speed $C_p = \omega/\alpha_r$ ($\omega = \alpha c$) and grows or dies away in x like $\exp(-\alpha_i x)$. Therefore the disturbances are amplified, neutral, or damped, according to whether $\alpha_i < 0$, $\alpha_i = 0$, or $\alpha_i > 0$, respectively. It is to be understood that the real part of the disturbances represents the physical quantity in each case.

2.3 Differential Equations for the Complex Amplitude Functions

Using normal mode solutions, we can separate the variables and reduce the linearized disturbance equations from the partial differential equations to

ordinary differential equations. By substituting Eqs. 2.23 to 2.25 into Eqs. 2.14 to 2.19, we obtain a system of ordinary differential equations for determining the amplitude functions $f(y)$, $\phi(y)$, $\rho(y)$, $\theta(y)$, $\pi(y)$ and $\eta(y)$. These are:

Continuity:

$$i(\bar{u} - c)r + \phi\frac{d\bar{\rho}}{dy} + \rho(if + \dot{\phi}) = 0\,, \tag{2.26}$$

Momentum:

$$\rho\left[\phi\frac{d\bar{u}}{dy} + i(\bar{u} - c)f\right] = -\frac{i\pi}{\gamma_1 M_1{}^2}\,, \tag{2.27}$$

$$\rho\alpha^2 i(\bar{u} - c)\phi = -\frac{\dot{\pi}}{\gamma_1 M_1{}^2}\,, \tag{2.28}$$

Energy:

$$\bar{\rho}\,\bar{c}_v\left[i(\bar{u} - c)\,\theta + \phi\frac{d\overline{T}}{dy}\right] = -(\gamma_1 - 1)(if + \dot{\phi})\,, \tag{2.29}$$

State:

$$\frac{\pi}{\bar{p}} = \frac{r}{\bar{\rho}} + \frac{\theta}{\overline{T}} + \frac{1}{\overline{R}}\left(1 - \frac{R_2}{R_1}\right)\eta\,, \tag{2.30}$$

Species Transport:

$$i(\bar{u} - c)\eta + \phi\frac{d\bar{\chi}_1}{dy} = 0\,, \tag{2.31}$$

where dots denote d/dy. These equations for the amplitude functions can be reduced to the following second-order differential equation for the pressure disturbance,

$$\ddot{\pi} - \left[\frac{2\dot{\bar{u}}}{\bar{u} - c} - \left(\frac{\dot{\overline{T}}}{\overline{T}} + \frac{\dot{\overline{R}}}{\overline{R}}\right)\right]\dot{\pi} - \alpha^2\left\{1 - \frac{\gamma_1 M_1{}^2(\bar{u} - c)^2\bar{c}_v/\overline{R}}{\overline{R}\,\overline{T}\left[\bar{c}_v/\overline{R} + (\gamma_1 - 1)\right]}\right\}\pi = 0\,. \tag{2.32}$$

All the other variables can be expressed in terms of π and $\dot{\pi}$ as follows:

$$-f = \frac{1}{\gamma_1 M_1{}^2\bar{\rho}(\bar{u} - c)}\left[\pi + \frac{\dot{\pi}}{\alpha^2(\bar{u} - c)^2}\frac{d\bar{u}}{dy}\right], \tag{2.33}$$

$$\phi = \frac{i\dot{\pi}}{\gamma_1 M_1^2 \alpha^2 \bar{\rho}(\bar{u} - c)} , \tag{2.34}$$

etc.

2.4 Boundary Conditions

Two types of boundary conditions will be considered. One is for unbounded mixing layers and the other is for bounded mixing layers. These will be discussed below.

2.4.1 Unbounded Mixing Layer

The general configuration of a free mixing layer and the variables involved are summarized in Fig. 2.1. The boundary conditions of the eigenfunction $\pi(y)$ are found from Eq. 2.32. With $y \to \pm\infty$, the mean quantities $\bar{u}(y)$, $\overline{T}(y)$, $\overline{R}(y)$ and $\bar{c}_v(y)$ are constants and their corresponding derivatives are zero. In that limit, Eq. 2.32 becomes

$$\ddot{\pi} - \lambda_{\pm}^2 \pi = 0 \tag{2.35}$$

with

$$\lambda_+^2 = \alpha^2[1 - M_1^2(1 - c)^2] = \Lambda_+ = \Lambda_{+r} + i\Lambda_{+i} \tag{2.36}$$

$$\lambda_-^2 = \alpha^2 \left\{ 1 - \frac{\gamma_1 M_1^2 (u_r - c)^2 c_{vr}/R_r}{R_r T_r \left[c_{vr}/R_r + (\gamma_1 - 1) \right]} \right\} = \Lambda_- = \Lambda_{-r} + i\Lambda_{-i} , \tag{2.37}$$

and the solution for large $|y|$ are of the form

$$\pi = A_{\pm} \exp (\pm\lambda_{\pm} y) , \tag{2.38}$$

where $A_{\pm}$ is a complex constant.

Since we are only considering the case of amplified spatially growing disturbances ($\alpha_i < 0$), the boundary conditions for both subsonic and supersonic disturbances require that $\pi(y)$ must be bounded as $y \to \pm\infty$. To define $\lambda_{\pm}$ uniquely, we set the real part of $\lambda_{\pm}$=$\lambda_{\pm r} > 0$ to obtain

$$y = y_{+\infty} \to +\infty \qquad \pi = A_{+} \exp (-\lambda_{+} y) , \tag{2.39}$$

$$y = y_{-\infty} \to -\infty \qquad \pi = A_{-} \exp (+\lambda_{-} y) , \tag{2.40}$$

where

$$\lambda_{\pm} = \lambda_{\pm r} + i\lambda_{\pm i} = \left[\frac{1}{2}\left(|\Lambda_{\pm}| + \Lambda_{\pm r}\right)\right]^{1/2} + i\,\mathrm{sign}(\Lambda_{\pm i})\left[\frac{1}{2}\left(|\Lambda_{\pm}| - \Lambda_{\pm r}\right)\right]^{1/2} . \tag{2.41}$$

2.4.2 Bounded Mixing Layer

The general configuration of a mixing layer inside parallel walls is shown in Fig. 2.2. δ is the dimensionless mixing layer thickness defined in a boundary-layer sense, *i.e.*,

$$\left|\frac{u_1 - u(\delta)}{u_1}\right| < \epsilon \qquad \text{and} \qquad \left|\frac{u_2 - u(-\delta)}{u_1}\right| < \epsilon , \tag{2.42}$$

where ϵ is taken as 0.002. Note that $2d$ is the dimensionless distance between the walls.

In the regions of $\delta < y < d$ and $-d < y < -\delta$, the flow is effectively uniform, *i.e.*, the mean flow quantities, such as velocity, temperature, *etc.* are constants, and Eq. 2.32 reduces to Eq. 2.35. In order to satisfy the boundary conditions at the walls, the vertical velocities of the disturbances should vanish on the solid boundaries and we must have $\dot{\pi}(d) = \dot{\pi}(-d) = 0$. The analytic solutions in Regions 1 and 2 then are

$$\pi = A \cosh[\lambda_+(d-y)], \qquad \pi = B \cosh[\lambda_-(d+y)], \tag{2.43}$$

where λ_+ and λ_- are already given by Eqs. 2.36 and 2.37. A and B are complex constants to be determined by matching to the inner flow region.

2.5 Formulation and Numerical Treatment of the Eigenvalue Problem

The eigenvalue problem of the instability of mixing layers with spatially growing disturbances is defined as follows. We take a real value of the disturbance frequency ω and seek the complex eigenvalue $\alpha = \alpha_r + i\alpha_i$. The dispersion relation can be written in the form

$$F(\alpha, \omega) = 0 . \tag{2.44}$$

For a given real disturbance frequency ω, the complex eigenvalue α is to be determined such that the eigenfunction $\pi(y)$ of Eq. 2.32 satisfies the boundary conditions. This gives a well-defined eigenvalue problem for the amplified disturbances $\alpha_i < 0$. A Runge-Kutta method combined with a shooting technique was used to solve this eigenvalue problem.

For an unbounded mixing layer, Eq. 2.32 is integrated numerically for a fixed value ω starting from the lower boundary $y_{-\infty}$, where the boundary condition is given by Eq. 2.40, to the upper boundary $y_{+\infty}$. This yields $\pi(y_{+\infty})$ and $\dot{\pi}(y_{+\infty})$. By matching the upper boundary condition given by Eq. 2.39, the sum $S(\alpha_r, \alpha_i) = \dot{\pi}(y_{+\infty}) + \lambda_+ \pi(y_{+\infty})$ is evaluated and improved values of α are calculated from the approximated zeros of $S(\alpha_r, \alpha_i)$ by linear interpolation. This procedure is repeated until $|S|$ is sufficiently small.

For a mixing layer inside parallel flow guide walls, we use the analytic solution in Region 2 of Fig. 2.2 as a starting solution and integrate Eq. 2.32 numerically from $y = -\delta$ to $y = \delta$. The correct α is obtained, for a given ω, by matching the numerical solution to the analytic solution at $y = \delta$.

The computations, for both free and bounded mixing layers, were performed using the Runge-Kutta-Fehberg method with automatic estimation of local error and step size adjustment. An error control of 10^{-5} is used for the integrations, iterating until the eigenvalue converges to 10^{-6}.

CHAPTER 3

MEAN FLOW QUANTITIES

In a finite thickness mixing layer, all mean quantities, such as velocity, density, temperature, gas constant (molecular weight), concentration and the ratio of the specific heats, vary gradually across the mixing layer. We consider the two-dimensional motion of a stream of fluid with the velocity u_1^*, density ρ_1^*, temperature T_1^*, gas constant R_1^*, ratio of the specific heats γ_1^*, viscosity μ_1^* and thermal conductivity k_1^*, over a parallel stream described by the corresponding parameters with subscript 2. The main flow is considered to be quasi-parallel and the fluids in the two parallel streams are assumed non-reacting.

A two-dimensional compressible steady mixing flow, comprised of different perfect gases, can be modelled by the compressible boundary layer equations for gas mixture. We take the axis of x^* to be in the direction of motion of the free streams, and the axis of y^* to be in the transverse direction. The velocity components in these directions are u^* and v^*. The origin is taken as the point at which the two fluids first come in contact (see Fig. 2.1). For a steady parallel mixing flow, the disturbance term Q' in Eq. 2.13 is zero, therefore, Eq. 2.13 becomes

$$Q^* = \overline{Q}^*(y^*) \,. \tag{3.1}$$

With zero pressure gradient throughout the entire flow region, the global boundary-layer equations for compressible steady mixing flow are

Continuity equation:

$$\frac{\partial(\rho^* u^*)}{\partial x^*} + \frac{\partial(\rho^* v^*)}{\partial y^*} = 0 \tag{3.2}$$

Momentum equation:

$$\rho^*\left(u^*\frac{\partial u^*}{\partial x^*} + v^*\frac{\partial u^*}{\partial y^*}\right) = \frac{\partial}{\partial y^*}\left(\mu^*\frac{\partial u^*}{\partial y^*}\right) \tag{3.3}$$

Energy equation:

$$\rho^*\left(u^*\frac{\partial h_t^*}{\partial x^*} + v^*\frac{\partial h_t^*}{\partial y^*}\right)$$

$$= \frac{\partial}{\partial y^*}\left\{\mu^*\left[\frac{1}{Pr}\frac{\partial h_t^*}{\partial y^*} + \left(1 - \frac{1}{Pr}\right)u^*\frac{\partial u^*}{\partial y^*} + \left(\frac{1}{Sc} - \frac{1}{Pr}\right)\sum h_i^*\left(\frac{\partial \chi_1}{\partial y^*}\right)\right]\right\} \tag{3.4}$$

Equation of state for ideal gases:

$$p^* = \rho^* R^* T^* \tag{3.5}$$

Species transport equation:

$$\rho^* u^*\frac{\partial \chi_1}{\partial x^*} + \rho^* v^*\frac{\partial \chi_1}{\partial y^*} = \frac{\partial}{\partial y^*}\left(D^*\rho^*\frac{\partial \chi_1}{\partial y^*}\right), \tag{3.6}$$

where μ^* is the viscosity, $Pr = \mu^* c_p^*/k^*$ is the Prandtl number, $Sc = \mu^*/\rho^* D^*$ is the Schmidt number, k^* is the thermal conductivity, and D^* is the binary diffusion coefficient.

3.1 Mean Velocity Distribution

The numerical calculation of the mean velocity distribution for an incompressible mixing layer with $u_2/u_1 \neq 0$, comprised of the same gases was first

provided by Lock [1951]. By introducing a stream function ψ^*, which satisfies the continuity equation of compressible steady flow Eq. 3.2 identically, *i.e.*,

$$\rho^* u^* = \frac{\partial \psi^*}{\partial y^*} , \qquad \rho^* v^* = -\frac{\partial \psi^*}{\partial x^*} , \tag{3.7}$$

and a transformation proposed by L. Howarth [1948],

$$Y^* = \int_0^{y^*} \frac{dy^*}{T^*} , \tag{3.8}$$

the calculation of the mean velocity distribution for compressible steady mixing flows is converted into the corresponding calculation for incompressible flows, if we assume that the viscosity μ^* of the gas is approximately a linear function of the temperature T^* (Gropengiesser [1970]). It was found by Gropengiesser [1970] that the dimensionless velocity distribution $\bar{u}(y)$ for compressible steady mixing flows can be well approximated by the generalized hyperbolic tangent profile with three free constants,

$$\bar{u}(y) = 1 - \left[\frac{1}{2} \left(1 - \tanh \kappa_1 \left(y - y_1 \right) \right) \right]^{\kappa_2} , \tag{3.9}$$

with $\kappa_1 = 0.307257$, $\kappa_2 = 3.695640$, $y_1 = 2.127137$. The dimensionless variable y is equal to $Y^*/\delta^*(x^*)$, where $\delta^*(x^*)$ is the local layer thickness. Therefore, the main flow is considered to be quasi-parallel.

In order to simplify the problem, for the mixing flows considered in the current numerical calculations, we assume that the dimensionless mean velocity profile is described by a hyperbolic tangent profile of the form

$$\bar{u}(y) = \zeta(y) + u_r [1 - \zeta(y)] , \tag{3.10}$$

where $u_r = u_2/u_1$ is the velocity ratio across the mixing layer, and

$$\zeta(y) = \frac{1}{2}[1 + \tanh(y)] . \tag{3.11}$$

See mean velocity profiles $\bar{u}(y)$ with different values of u_r in Fig. 3.1. It has been known from previous investigators that the percentage difference in amplification rate of the case with a hyperbolic tangent profile relative to the case with a boundary-layer profile is small if the value of the velocity ratio u_r is not too small.

It is known that there is a wake component in the initial evolution of the mixing layer (*e.g.* Lang [1985]). For the incompressible mixing layer, Koochesfahani & Frieler [1987] investigated the linear spatial instability behavior of a mean velocity distribution with a wake component. They showed the existence of two unstable modes, which they called shear layer mode and wake mode. In order to investigate the effect of the wake component on the instability behavior of the compressible mixing layer, we assumed that the mean dimensionless velocity profile is composed of the usual hyperbolic tangent profile plus a wake component (owing to the splitter plate) represented by a Gaussian distribution of the form

$$\bar{u}(y) = \zeta(y) + u_r[1 - \zeta(y)] - w \exp(-y^2) , \tag{3.12}$$

where w is the normalized wake deficit, as was assumed in Koochesfahani & Frieler [1987]. Profiles with different values of w are plotted in Fig. 3.2.

3.2 Mean Temperature Distribution

Two different kinds of temperature profiles have been considered. For

the flow comprised of same gases, according to Crocco [1932] and Busemann [1935], it is possible to satisfy the energy equation identically by assuming that the temperature T^* is dependent only upon the velocity component u^* taken parallel to the direction of the flow. Following the Crocco and Busemann's idea, we assume that the total enthalpy $h_t^* = h^* + u^{*2}/2$ depends only on the velocity component u^* for the mixing flows comprised of different gases, *i.e.* $h_t^* = \text{fn}(u^*)$. By substituting the expressions $h_t^* = h_t^*(u^*)$ into the energy equation 3.4 and by assuming that the Prandtl number $Pr = \mu^* c_p^*/k^*$ and Schimdt number $Sc = \mu^*/\rho^* D^*$ are equal to unity, *i.e.*,

$$\begin{aligned} Pr &= 1 \\ Sc &= 1, \end{aligned} \tag{3.13}$$

and using the momentum Eq. 3.3, Eq. 3.4 can be reduced to

$$\frac{d^2 h_t^*}{du^{*2}} = \frac{d^2(h^* + u^{*2}/2)}{du^{*2}} = 0\,. \tag{3.14}$$

Thus the mean static temperature profile can be represented by

$$\bar{c}_p^*(y^*)\,\overline{T}^*(y^*) = -\frac{\bar{u}^{*2}(y^*)}{2} \;+\; c_1\,\bar{u}^*(y^*) \;+\; c_2 \tag{3.15}$$

where c_1 and c_2 are constants determined by the boundary conditions on the mean temperature profile and we also assumed that $c_p^* \neq fn(T^*)$ within the range of the temperatures in the flow and c_p^* is only a function of the fraction of species of the gas mixture. The dimensionless mean temperature profiles $\overline{T}(y)$ with a fixed M_1, or a fixed temperature ratio T_2/T_1, are shown in Figs. 3.3 and 3.4, respectively. Equations 3.10 and 3.15 yield the dimensionless total temperature profile $T_t(y)$ for the mixing flows formed by same gases,

$$T_t(y) = \zeta(y) + T_{tr}\,[\,1 \,-\, \zeta(y)\,]\,, \tag{3.16}$$

where $T_{tr} = T_{t2}/T_{t1}$ is the ratio of the total temperature across the mixing layer. The profile given by Eq. 3.16 has the same thickness relative to the dimensionless mean velocity profile given by Eq. 3.10. A question, then remains as to how this relative thickness affects the instability behavior of the compressible mixing layer. To consider this question, $\zeta(y)$ is replaced by $\zeta(y/\sigma)$ in Eq. 3.16, where σ adjust the thickness of the total temperature profile relative to the velocity profile. The dimensionless total temperature profiles as a function of the total temperature interface thickness σ are shown in Fig. 3.5.

An alternate dimensionless mean temperature profile considered was obtained by assuming that the profile can also be represented by a hyperbolic tangent profile, *i.e.*,

$$\overline{T}(y) = \zeta(y) + T_r\,[1 - \zeta(y)]\,, \tag{3.17}$$

where $T_r = T_2/T_1$ is the ratio of the temperature across the mixing layer. Comparing Eq. 3.17 with Eq. 3.15, we see that the profile given by Eq. 3.17 is only a function of the temperature ratio T_r. Therefore, for both subsonic and supersonic flows, we have the same dimensionless mean temperature profiles for the same T_r (see Fig. 3.6).

3.3 Mean Concentration Distribution

Since the mixing layer we considered may be formed by different gases, the mean mass fractions $\bar{\chi}_1$ and $\bar{\chi}_2$ may vary gradually across the mixing layer, just like the mean velocity and temperature. Following the way we specify the

dimensionless mean velocity, we assume that the mean concentration profile $\bar{\chi}_1(y)$ is also described by a hyperbolic tangent profile of the form

$$\bar{\chi}_1(y) = \frac{1}{2}\left[1 + \tanh(y)\right]. \tag{3.18}$$

Since $\bar{\chi}_1 + \bar{\chi}_2 = 1$, Eq. 3.18 yields

$$\bar{\chi}_2(y) = \frac{1}{2}\left[1 - \tanh(y)\right]. \tag{3.19}$$

Substituting Eq. 3.18 into Eqs. 2.20 to 2.22, the dimensionless mean gas constant and specific heat profiles can be written as:

$$\overline{R}(y) = \zeta(y) + R_r\left[1 - \zeta(y)\right], \tag{3.20}$$

$$\bar{c}_p(y) = \zeta(y) + c_{pr}\left[1 - \zeta(y)\right], \tag{3.21}$$

$$\bar{c}_v(y) = \zeta(y) + c_{vr}\left[1 - \zeta(y)\right], \tag{3.22}$$

where $\zeta(y)$ was given by Eq. 3.11, R_r, and c_{pr}, c_{vr} are the ratio of the gas constant and the ratios of the specific heats at constant pressure and at constant volume respectively. The dimensionless mean profile $\overline{R}(y)$ is shown in Fig. 3.7 for different values of R_r.

CHAPTER 4

THE INSTABILITY BEHAVIOR OF A COMPRESSIBLE FREE MIXING LAYER

In this chapter, the linear, spatial instability behavior of a compressible, laminar, mixing layer, comprised of different gases, is investigated with respect to two- and three-dimensional, spatially amplified, wave disturbances. The fluctuating amplifying flow is assumed to be inviscid and non reacting. The perturbations in the flow are taken as possessing small amplitudes. All flow quantities mentioned in this chapter are defined as dimensionless quantities, using the dimensionless variables defined in Chapter 2. The effects of free stream Mach number, velocity ratio, temperature ratio, gas constant (molecular weight) ratio and the ratio of specific heats on the linear spatial instability characteristics of the compressible mixing layers are examined. The behavior of eigenfunctions of the disturbed mixing layers is discussed for both subsonic and supersonic disturbances. The instability characteristics of compressible mixing layers with spatially growing oblique wave disturbances are also studied. The influence of adding a wake component to the mean velocity profile and decreasing the thickness of the total temperature profile relative to the mean velocity profile on the linear spatial instability behavior of compressible mixing layers is also considered.

4.1 Free Stream Conditions

The instability characteristics of compressible mixing layers can be calculated numerically using Eq. 2.32, with given boundary conditions and mean flow conditions. The mean flow distributions of mixing layers were already described in Chapter 3. For a plane mixing layer having the mean velocity profile Eq. 3.10, the mean temperature profile Eq. 3.15 and the mean concentration profile Eq. 3.18, the instability behavior of mixing layers with two-dimensional, spatially growing disturbances was studied in the range of free stream Mach number $0 \leq M_1 \leq 11.0$, velocity ratio $0.25 \leq u_2/u_1 \leq 0.75$, temperature ratio $0.2 \leq T_2/T_1 \leq 5.0$, gas constant ratio $0.1 \leq R_2/R_1 \leq 5.0$ for given ratios of specific heats γ_1, γ_2. The lists of the combinations of the free stream conditions described above are presented in Tables 4.1 – 4.3.

The mean temperature distribution across the mixing layer is also approximated by a hyperbolic tangent profile Eq. 3.17. The mean flow conditions for this hyperbolic tangent mean temperature profile are given in Table 4.4.

Table 4.1 The free stream conditions for mixing flows formed by the same gases

$R_2/R_1 = 1.0, \quad \gamma_1 = 1.4, \quad \gamma_2 = 1.4$			
Case	M_1	u_2/u_1	T_2/T_1
1	$0 \rightarrow 2.5$	0.00	1.00
2	$0 \rightarrow 3.0$	0.25	0.50
3	$0 \rightarrow 3.5$	0.25	1.00
4	$0 \rightarrow 4.0$	0.25	1.50
5	$0 \rightarrow 4.0$	0.50	0.20
6	$0 \rightarrow 4.5$	0.50	0.50
7	$0 \rightarrow 5.5$	0.50	1.00
8	$0 \rightarrow 5.5$	0.50	1.50
9	$0 \rightarrow 8.0$	0.50	5.00
10	$0 \rightarrow 9.0$	0.75	0.50
11	$0 \rightarrow 10.$	0.75	1.00
12	$0 \rightarrow 11.$	0.75	1.50

Table 4.2 The free stream conditions for different values of R_1 and R_2

$T_2/T_1 = 1.0, \quad \gamma_1 = 1.4, \quad \gamma_2 = 1.4$			
Case	M_1	u_2/u_1	R_2/R_1
13	$0 \rightarrow 4.0$	0.50	0.20
14	$0 \rightarrow 5.0$	0.50	0.50
15	$0 \rightarrow 8.0$	0.50	5.00

Table 4.3 The free stream conditions for different values of γ_1 and γ_2

$u_2/u_1 = 0.5, \quad T_2/T_1 = 1.0, \quad R_2/R_1 = 1.0$			
Case	M_1	γ_1	γ_2
16	$0 \rightarrow 5.0$	1.67	1.40
17	$0 \rightarrow 5.5$	1.40	1.67

Table 4.4 The free stream conditions for hyperbolic tangent mean temperature distribution

$R_2/R_1 = 1.0, \quad \gamma_1 = 1.4, \quad \gamma_1 = 1.4$			
Case	M_1	u_2/u_1	T_2/T_1
18	$0 \rightarrow 4.5$	0.50	0.67
19	$0 \rightarrow 5.0$	0.50	1.00
20	$0 \rightarrow 5.5$	0.50	2.00

The instability characteristics were calculated for each combination of the mean flow conditions, yielding the most unstable eigenvalue α_m ($\alpha_m = \alpha_{rm} + i\,\alpha_{im}$), its corresponding frequency ω_m and phase velocity

$$C_{pm} = \omega_m/\alpha_{rm} \; . \tag{4.1}$$

The convective Mach numbers M_{c1}, M_{c2}, corresponding to these spatially growing waves, can be then obtained from Eq. 1.4.

4.2 Effect of the Free Stream Mach Number M_1

The inviscid solutions of the instability characteristics of compressible mixing layers were calculated for various free stream Mach numbers M_1 for a fixed velocity ratio u_2/u_1, temperature ratio T_2/T_1, gas constant ratio R_2/R_1 and ratio of the specific heats γ_1, γ_2.

For a free mixing layer with subsonic convective Mach numbers, there is only one group of unstable waves. The amplification rate $-\alpha_i$ is shown in

Figs. 4.1a, 4.2a and 4.3a for Cases 2, 15 and 4 (see Tables 4.1 and 4.2), as a function of the amplified disturbance frequency ω and the free stream Mach number M_1. The maximum amplification rate $-\alpha_{im}$ attains its biggest value for an incompressible mixing layer ($M_1 = 0$) and falls off sharply with increasing free stream Mach number M_1. The band of amplified frequencies becomes much narrower with increasing free stream Mach number M_1. These results are in agreement with Gropengiesser's [1970] numerical calculations, who considered a laminar velocity profile with the velocity ratio $u_2/u_1 = 0$. It should also be noticed in Figs. 4.1a, 4.2a and 4.3a that for a constant free stream Mach number M_1, the amplification rate $-\alpha_i$ increases monotonically with increasing amplified disturbance frequency ω, up to a maximum value, and then drops off gradually to zero as the neutral disturbance frequency is reached. The corresponding phase velocities $C_p = \omega/\alpha_r$ of these instability characteristics are given in Figs. 4.1b, 4.2b and 4.3b against the amplified disturbance frequency ω for different free stream Mach numbers M_1. The phase velocity C_p decreases with increasing amplified disturbance frequency ω, down to a minimum value, then increases slightly till the neutral disturbance frequency is reached. For a mixing layer with subsonic disturbances, the phase velocity of the most unstable wave C_{pm} is shown in Fig. 4.4 as a function of the free stream Mach number M_1. From this figure, we can see that C_{pm} is independent of the free stream Mach number M_1. It is approximately equal to the isentropically estimated convective velocity u_c defined in Eq. 1.3, which depends only on the velocity ratio u_2/u_1, temperature ratio T_2/T_1, density ratio ρ_2/ρ_1 and the gas constant ratio R_2/R_1 for $\gamma_1 = \gamma_2$ (see Fig. 4.4).

As the free stream Mach number M_1 approaches or exceeds a critical

value M_{1cr}, the mixing flow becomes supersonic relative to its disturbances, which means the convective Mach number M_{c1} or M_{c2} is greater than unity. Jackson & Grosch [1988] showed that for a single stream ($u_2/u_1 = 0$) supersonic free mixing layer, there are always two groups of unstable waves. One is slow with a scaled phase velocity less than 1/2, and the other is fast with a scaled phase velocity greater than 1/2. They classified these two unstable waves as a slow supersonic mode and a fast supersonic mode respectively. The linear instability investigations performed here indicate that for a supersonic free mixing layer with the velocity ratio $u_2/u_1 \neq 0$, there are also two unstable waves. One is with the phase velocity $C_{pm} < u_c$ (slow mode) and the other is with the phase velocity $C_{pm} > u_c$ (fast mode), where, as noted above, u_c is the isentropically estimated convective velocity (Eq. 1.3). The convective Mach number M_{c1} is always greater than unity and M_{c2} is usually smaller than unity for the slow supersonic mode and vice versa for the fast supersonic mode.

The instability characteristics of supersonic mixing flows were calculated for both unstable supersonic waves. The amplification rate $-\alpha_i$ is plotted in Figs. 4.5a, 4.6a and 4.7a for Cases 2, 15 and 4 at a given free stream Mach number $M_1 > M_{1cr}$. The bands of the amplified disturbance frequencies ω of the two supersonic unstable waves overlap for some range of the frequencies. Therefore, two unstable modes can exist at the same time for some given amplified disturbance frequencies. The corresponding variation of the phase velocity is given in Figs. 4.5b, 4.6b and 4.7b. The phase velocities of the most unstable mode of these two supersonic waves C_{pm} are shown in Figs. 4.8a, 4.9a and 4.10a as a function of the free stream Mach number $M_1 > M_{1cr}$, for Cases 2, 15 and 4. From these figures, we

understand that the phase velocity of the most unstable mode C_{pm} decreases for a slow mode and increases for a fast mode with increasing free stream Mach number M_1. Therefore, the convective Mach number M_{c1} or M_{c2}, defined by Eq. 1.4, increases as the free stream Mach number increases. The maximum amplification rates $-\alpha_{im}$ of both supersonic unstable modes are shown in Figs. 4.8b, 4.9b and 4.10b as a function of the free stream Mach number $M_1 > M_{1cr}$. For the low supersonic disturbances, the fast mode ($M_{c2} > 1$) is more unstable than the slow mode ($M_{c1} > 1$) when the heavy gas is on the low speed side (Case 2) and the slow mode ($M_{c1} > 1$) is dominant when the heavy gas is on the high speed side (Case 4 and Case 15). This might suggest that if there is a shock wave in the mixing flow, the shock would be borne by the heavy gas stream for the low supersonic convective Mach numbers. If the convective Mach numbers are high enough, the maximum amplification rate of the two supersonic modes are comparable. Therefore, the flow might support shocks in both streams for the high convective Mach numbers.

For an incompressible mixing layer with a Blasius mean velocity profile, Monkewitz & Huerre [1982] found that the maximum amplification rate $-\alpha_{im}$ is nearly proportional to the velocity ratio λ, defined as

$$\lambda \equiv (1 - u_2/u_1)/(1 + u_2/u_1) \, . \tag{4.2}$$

Instead of using the Blasius mean velocity profile, the hyperbolic tangent mean velocity profile Eq. 3.10 was used in the current calculations. Other mean flow profiles of the mixing layers were obtained from Eqs. 3.15 and 3.18. Sandham & Reynolds [1989b] showed that the differences in the velocity profile are generally small when the two streams have equal densities.

In order to study the effect of the free stream Mach number M_1 on the function $-\alpha_{im}(\lambda)$, the maximum amplification rate $-\alpha_{im}$ was computed as a function of the velocity ratio λ for the density ratio $\rho_2/\rho_1 = 1.0$, temperature ratio $T_2/T_1 = 1.0$ and the ratio of specific heats $\gamma_1 = \gamma_2 = 1.4$, at different free stream Mach numbers M_1. The result shown in Fig. 4.11 indicates that the relation between the maximum amplification rate $-\alpha_{im}$ and the velocity ratio λ is approximately linear for incompressible mixing flow with equal density and temperature in both mixing streams and that this linear relation becomes nonlinear as the free stream Mach number M_1 increases.

4.3 Effect of the Velocity Ratio u_2/u_1

It is known from turbulent mixing layer experiments that the mixing layer spreading rates are significantly smaller for supersonic mixing flows than those observed in subsonic experiments. Although the effect of compressibility on the growth rate is the major cause for the lower spreading rate, which will be discussed later in Section 4.7, the effect of other flow parameters, such as the velocity ratio u_2/u_1 should also be studied. Using linear spatial instability analysis, the effect of the velocity ratio u_2/u_1 on the instability characteristics of mixing layers was considered. For a temperature ratio $T_2/T_1 = 0.5$, gas constant ratio $R_2/R_1 = 1.0$ and a ratio of specific heats $\gamma_1 = \gamma_2 = 1.4$, the instability characteristics of the mixing layers with different velocity ratios u_2/u_1 (Cases 2, 6 and 10) are shown in Figs 4.12a, 4.12b, 4.12c and 4.12d at different convective Mach numbers M_{c1} or M_{c2}, which can be obtained from Eq. 1.4. For both subsonic and supersonic convective Mach numbers, the band of unstable frequencies ω becomes wider and

the maximum amplification rate $-\alpha_{im}$ becomes smaller as the velocity ratio u_2/u_1 increases. The phase velocities C_{pm} of these unstable waves are plotted in Fig. 4.13 against the velocity ratio u_2/u_1. Fig. 4.13 demonstrates that the phase velocity C_{pm} is approximately a linear function of the velocity ratio u_2/u_1, at a given convective Mach number M_{c1}, or M_{c2}, and other free stream parameters T_2/T_1, R_2/R_1, γ_1 and γ_2. The solid line in Fig. 4.13 is the isentropic estimate of the convective velocity, Eq. 1.3, $u_c(u_2/u_1)$, which is independent of the convective Mach number M_{c1} or M_{c2}. For subsonic convective Mach numbers, the slope of the linear function $C_{pm}(u_2/u_1)$ is the same as the slope of the linear function $u_c(u_2/u_1)$. For supersonic disturbances, there are two groups of unstable waves. Even though the linear relationship between the phase velocity C_{pm} and the velocity ratio u_2/u_1 exists for each unstable wave, the slope of the function $C_{pm}(u_2/u_1)$ is greater than that of the isentropic $u_c(u_2/u_1)$ for the slow supersonic mode ($C_{pm} < u_c$) and is smaller for the fast supersonic mode ($C_{pm} > u_c$).

4.4 Effect of the Density Ratio ρ_2/ρ_1 or the Temperature Ratio T_2/T_1

Plane turbulent mixing between two parallel streams of different densities was studied experimentally by Brown & Roshko [1974] for incompressible mixing layers. The effect of density on turbulent mixing in incompressible flow was investigated. A comparison of the results for the growth of the vorticity thickness in incompressible flow against density ratio with the results of Maydew & Reed [1963] in supersonic flow was made in Fig. 15 of Brown & Roshko [1974]. In the current investigations of the linear instability behavior of inviscid mixing flows, laminar mixing of the two parallel streams, comprised of the same gas ($R_2/R_1 = 1.0$,

$\gamma_1 = \gamma_2$), was considered. The effect of density on laminar mixing in both subsonic and supersonic flows was studied. Figure 4.14 shows the maximum amplification rate $-\alpha_{im}$ as a function of the density ratio ρ_1/ρ_2 for different free stream Mach numbers M_1 at the velocity ratio $u_2/u_1 = 0$. As the density ratio ρ_1/ρ_2 increases, the maximum amplification rate $-\alpha_{im}$ decreases monotonically for an incompressible mixing flow ($M_1 = 0$). For a compressible mixing flow, $-\alpha_{im}$ increases up to a maximum value, then decreases gradually with increasing density ratio ρ_1/ρ_2. The value of the density ratio ρ_1/ρ_2, which corresponds to the maximum value of the maximum amplification rate $-\alpha_{im}$, shifts to larger values of the density ratio ρ_1/ρ_2 as the free stream Mach number M_1 increases. The experimental results of the growth in both incompressible and compressible mixing flows by Brown & Roshko and by Maydew & Reed are also given in Fig. 4.14. The numerical calculations, however, were based on linear instability theory while the experimental results were obtained from the experiments of turbulent mixing layers. We can see that the trend of the instability calculations is comparable to that of the experimental data.

It was shown in Section 4.2 that, for incompressible mixing layers with equal density on both mixing streams and a hyperbolic tangent mean velocity profile, the maximum amplification rate $-\alpha_{im}$ is approximately a linear function of the velocity ratio $\lambda = (1-u_2/u_1)/(1+u_2/u_1)$. For incompressible mixing layers, the effect of the density ratio ρ_2/ρ_1 on the maximum amplification rate $-\alpha_{im}$ is shown in Fig. 4.15. For a density ratio ρ_2/ρ_1 equal to, or less than, unity, the maximum amplification rate $-\alpha_{im}$ is still approximately a linear function of the velocity ratio λ and $-\alpha_{im}$ rises with increasing density ratio ρ_2/ρ_1 for $0 \leq \lambda \leq 1$. For a density ratio ρ_2/ρ_1 greater than unity, the function $-\alpha_{im}(\lambda)$ becomes nonlinear and the

maximum amplification rate $-\alpha_{im}$ falls with increasing density ratio ρ_2/ρ_1 for some values of the velocity ratio λ. For incompressible mixing flows, Dimotakis [1986, 1989] proposed an expression for the spatially growing mixing layer growth rate given by

$$\frac{\delta_0}{x}(u_r, \rho_r; M_1 \to 0) \simeq C_\delta \frac{(1-u_r)(1+\rho_r^{1/2})}{2(1+\rho_r^{1/2}u_r)} \left\{ 1 - \frac{(1-\rho_r^{1/2})/(1+\rho_r^{1/2})}{1+2.9(1+u_r)/(1-u_r)} \right\}, \quad (4.3)$$

where the coefficient C_δ is independent of the velocity ratio u_r and/or the density ratio ρ_r. A comparison of the current numerical results for $\rho_r = 7,\ 1/7$ with the experimental values of Brown & Roshko [1974] and with the Dimotakis [1986, 1989] prediction for the spatially growing mixing layer at the value of $C_\delta = 0.16$ is made in Fig. 4.16.

It was shown in Section 4.3 that the phase velocity of the most unstable mode C_{pm} of the mixing layer is approximately a linear function of the velocity ratio u_2/u_1 at a given convective Mach number M_{c1} or M_{c2} and other free stream parameters T_2/T_1, R_2/R_1, γ_1 and γ_2. Since the temperature ratio T_2/T_1 is one of the important parameters for mixing layers, the effect of changing the temperature ratio T_2/T_1 on the phase velocity C_{pm} was examined. For a mixing layer, comprised of the same gas ($R_2/R_1 = 1.0$, $\gamma_1 = \gamma_2 = 1.4$), the phase velocity C_{pm} was calculated as a function of the velocity ratio u_2/u_1, at a given T_2/T_1, and M_{c1} or M_{c2}. The effect of the temperature ratio T_2/T_1 on the function $C_{pm}(u_2/u_1)$ is shown in Fig. 4.17a for subsonic disturbances. The slope of the approximately linear function $C_{pm}(u_2/u_1)$ decreases as the temperature ratio T_2/T_1 increases. Also, it should be noted that the phase velocity C_{pm} increases with increasing temperature ratio T_2/T_1, at a fixed velocity ratio u_2/u_1. For a mixing layer ($R_2/R_1 = 1.0$, $\gamma_1 = \gamma_2 = 1.4$) with supersonic convective Mach numbers, there are two supersonic unstable modes: the

slow supersonic mode with the phase velocity $C_{pm} < u_c$, and the fast supersonic mode with the phase velocity $C_{pm} > u_c$. The functions $C_{pm}(u_2/u_1)$ for the two supersonic unstable modes are given in Fig. 4.17b and 4.17c respectively. Compared with the subsonic mode, the slope of the approximately linear function $C_{pm}(u_2/u_1)$ is greater for the slow supersonic mode $C_{pm} < u_c$ and is smaller for the fast supersonic mode $C_{pm} > u_c$. The effect on the function $C_{pm}(u_2/u_1)$ of each supersonic mode, however, is the same as that of the subsonic mode when the temperature ratio T_2/T_1 is changed.

4.5 Effect of the Ratios of Specific Heats γ_1, γ_2

In experiments on gas phase turbulent mixing layers, a layer may be formed by two gases with different ratios of specific heats γ_1 and γ_2. The effect of the ratios of specific heats γ_1, γ_2 on the instability characteristics of mixing layers could be important. Here we studied this effect using linear instability analysis.

The instability characteristics of mixing layers were calculated for Cases 7, 16 and 17. For incompressible mixing layers, the instability characteristics are not affected by the difference between γ_1 and γ_2 (see Fig. 4.18a). For subsonic mixing layers with $M_{c1} \neq 0$, the band of the amplified disturbance frequencies ω becomes wider and the maximum amplification rate $-\alpha_{im}$ increases if the high-speed stream has the lower value of the ratio of specific heats (see Fig. 4.18b). The effect of the ratios of specific heats γ_1, γ_2 on the instability behavior of the slow supersonic mode $C_{pm} < u_c$ is the same as for the subsonic unstable mode

(see Fig. 4.19a). On the other hand, the band of amplified disturbance frequencies becomes narrower and the maximum amplification rate $-\alpha_{im}$ becomes smaller for the fast supersonic mode $C_{pm} > u_c$, when the high-speed stream has the lower value of the ratio of specific heats (see Fig. 4.19b).

4.6 Eigenfunction Behavior

For a given eigenvalue α, the eigenfunction $\pi(y)$ for the pressure disturbances, corresponding to amplified disturbances ($\alpha_i < 0$), can be evaluated by integrating Eq. 2.32. The eigenfunctions of subsonic and supersonic mixing flows were calculated for Case 2. The eigenfunction $\pi(y)$ of the most amplified eigenvalue α_m is shown in Fig. 4.20a and 4.20b for subsonic mixing layers with free stream Mach numbers $M_1 \to 0$ and $M_1 = 2.0$, respectively. The solid lines in these figures are the real part of $\pi(y)$ and the dashed lines are the imaginary part of $\pi(y)$. As can be seen from the equation, both real and imaginary parts of the eigenfunctions $\pi(y)$ decay exponentially away from the mixing layers in both the high- and low-speed streams. For supersonic mixing layers, the pressure eigenfunction $\pi(y)$ of the most amplified eigenvalue α_m radiates into the high-speed stream for the slow supersonic mode $C_{pm} < u_c$ and radiates into the low-speed stream for the fast supersonic mode $C_{pm} > u_c$. But for these two supersonic unstable modes, the pressure eigenfunctions $\pi(y)$ display an oscillatory decay in the stream with supersonic disturbances and an exponentially decay in the stream with subsonic disturbances (see Fig. 4.21a and 4.21b).

4.7 The Universal Dependence

The paper by Bogdanoff [1983] and the experimental results on turbulent mixing layers by Chinzei *et al.* [1986] and by Papamoschou & Roshko [1986, 1988] suggest that the isentropically estimated convective Mach number (defined by Eq. 1.1) is the appropriate parameter for scaling the effect of compressibility. Having defined the convective Mach number of the turbulent mixing layers, Papamoschou & Roshko argued that the expression of the growth rate

$$\delta' = \mathrm{fn}(\frac{u_2}{u_1}, \frac{\rho_2}{\rho_1}, M_1, M_2, \gamma_1, \gamma_2) \tag{4.4}$$

can be reduced into the simpler expression

$$\delta' = \mathrm{fn}(\frac{u_2}{u_1}, \frac{\rho_2}{\rho_1}, \gamma_1, \gamma_2, M_{c1}) \,, \tag{4.5}$$

if compressibility effects can be expressed in terms of a single parameter M_{c1}. After uncoupling the effect of the convective Mach number M_{c1}, they suggested that the growth rate of a compressible mixing layer might be generally expressed as

$$\frac{\delta'}{\delta'_0} \simeq F(M_{c1}) \,, \tag{4.6}$$

where δ'_0 is the growth rate of the corresponding incompressible mixing layer and F is a nearly universal function, over a wide range of velocity ratios, density ratios, and ratios of specific heats.

In the numerical investigations of the linear instability of an inviscid, compressible plane mixing layer, we considered a two-dimensional, spatially growing wave disturbance of the form

$$q' = q(y)\, e^{i\alpha(x-ct)} \,, \tag{4.7}$$

where α is a complex wave number and c is a complex wave velocity. The disturbance propagates as $e^{-\alpha_i x} e^{i(\alpha_r x - \omega t)}$, where ω is a real disturbance frequency. The linear instability characteristics of mixing layers with mean flow profiles described in Eqs. 3.10, 3.15 and 3.18 were calculated for the mean flow conditions given in Tables 4.1 – 4.3. The phase velocity of the most unstable mode C_{pm} was obtained from Eq. 4.1. This yields the convective Mach numbers M_{c1} and M_{c2} from Eq. 1.4.

It was shown in Section 4.2 that there are always two unstable waves for supersonic mixing layers. One is with the phase velocity $C_{pm} < u_c$ (slow mode), and the other is with the phase velocity $C_{pm} > u_c$ (fast mode). Since the slow supersonic mode $C_{pm} < u_c$ is more unstable than the fast supersonic mode $C_{pm} > u_c$ for most cases given in Tables 4.1 – 4.3, only the slow mode was considered for supersonic convective Mach numbers. Results shown in Figs. 4.22a – 4.22h, which were obtained from different mean flow conditions listed in Tables 4.1 – 4.3, indicate that if the most unstable eigenvalue for a compressible mixing layer is normalized by its value corresponding to an incompressible mixing layer (at the same velocity ratio, density ratio and the ratio of the specific heats), the ratio is approximated as a function of the convective Mach number only for the free stream conditions given in Tables 4.1 – 4.3., *i.e.*,

$$\frac{\delta'(M_{c1})}{\delta'(M_{c1}=0)} \simeq \frac{\max\left\{-\alpha_i(u_2/u_1, \rho_2/\rho_1, \gamma_1, \gamma_2, M_{c1})\right\}}{\max\left\{-\alpha_i(u_2/u_1, \rho_2/\rho_1, \gamma_1, \gamma_2, M_{c1}=0)\right\}} \simeq F(M_{c1}). \qquad (4.8)$$

The solid line estimate of $\delta'(M_{c1})/\delta'(M_{c1}=0)$ in Figs. 4.22a – 4.22h was computed using all the data corresponding to the seventeen different mean flow conditions listed in Tables 4.1 – 4.3, and least squares fitting the normalized maximum amplification rate *vs.* the convective Mach number M_{c1}, for the range of M_{c1} from 0 to

2 with a function of the form (see Fig. 4.23)

$$\frac{\delta'(M_{c1})}{\delta'(M_{c1}=0)} = \frac{1 + p_0\left[e^{-(p_2 M_{c1}^2 + p_3 M_{c1}^3 + p_4 M_{c1}^4)} - 1\right]}{1 + x^{p_1}}\,, \tag{4.9}$$

where

$$p_0 = 0.758\,, \qquad p_1 = 1.902\,, \qquad p_2 = 0.523\,,$$
$$p_3 = -2.196\,, \qquad p_4 = 3.710\,.$$

Note that $\delta'(M_{c1} \rightarrow \infty)/\delta'(M_{c1} = 0) \rightarrow 0$, *i.e.*, the normalized maximum amplification rate of unbounded mixing layers decreases continuously with increasing convective Mach number in the supersonic region. Note also that these results suggest that $(dF/dM_{c1})_{M_{c1}=0} = 0$, as might have been argued *a priori*. Finally, we note that the quality of the fit, assuming the $p_1 = 2$ (exactly), which yielded slightly different values for the remainder of the fit parameters, was essentially the same. The results, shown in Figs. 4.22a – 4.22h, also suggest that the normalized maximum amplification rate decreases significantly with increasing M_{c1} for subsonic convective Mach numbers. In the region $1 < M_{c1} < 2$, this normalized amplification rate decreases slowly, but continuously as the convective Mach number M_{c1} is increased.

In the second set of calculations, the mean temperature profile was assumed to be a hyperbolic tangent profile and was obtained from Eq. 3.17. The normalized amplification rate was calculated for different values of the temperature ratio (Cases 18, 19 and 20) as a function of the convective Mach number M_{c1} from 0 to about 2.0, for a velocity ratio $u_2/u_1 = 0.5$ and a gas constant ratio $R_2/R_1 = 1.0$. The results, shown in Fig. 4.24, substantiate the convective Mach number as the relevant compressibility parameter and also display good agreement

with the plot of $\delta'(M_{c1})/\delta'(M_{c1}=0)$ obtained from Eq. 4.9, even though these two mean temperature profiles are very different at supersonic convective Mach numbers (see Figs. 3.4 and 3.6).

A comparison of the estimate of $\delta'(M_{c1})/\delta'(M_{c1}=0)$ with Ragab & Wu's numerical data and with Papamoschou & Roshko's experimental data is made in Fig. 4.25. The result of our linear instability calculations is in close agreement with Ragab & Wu's result, which was also based on linear instability calculations, but using a laminar velocity profile at the velocity ratio $u_2/u_1 = 0$. Also, Ragab & Wu used the isentropically estimated convective velocity u_c to approximate the convective velocity of the spatially growing wave disturbances instead of the phase velocity of the most unstable mode C_{pm}, as was done here. The difference between C_{pm} and u_c, though not small in the region of supersonic convective Mach numbers, does not affect the results, since the normalized amplification rates are very small in this region. According to Papamoschou & Roshko's experimental data, the growth rate of the mixing layer approaches an asymptotic value as the convective Mach number becomes supersonic. As opposed to the experimental findings, however, the growth rate of the unbounded shear layers, based on linear instability calculations, decreases continuously in the supersonic convective Mach number region.

4.8 Oblique Wave Disturbances

The numerical calculations described above were carried out by assuming that the disturbances in the mixing layers are two-dimensional and spa-

tially growing. In the work of Gropengiesser [1970], Ragab & Wu [1988], Jackson & Grosch [1988] and Sandham & Reynolds [1989], it was found that a mixing layer with three-dimensional wave disturbances has the same general behavior as that with two-dimensional wave disturbance but with higher growth rates over some range of the propagation direction for the high-speed mixing layers.

If a mixing layer is subjected to a small, three-dimensional, spatially growing wave disturbance of the form

$$q'(x,y,z,t) = q(y)e^{i(\alpha x + \beta z - \omega t)} , \tag{4.10}$$

where q is the disturbance amplitude, α and β are the complex wave numbers in the downstream x and cross-stream z directions respectively, and ω is the real disturbance frequency. If we substitute these three-dimensional disturbances into the linearized three-dimensional basic equations, the second-order differential equation for the pressure disturbance, similar to Eq. 2.32, is obtained

$$\ddot{\pi} - \left[\frac{2\dot{\bar{u}}}{\bar{u}-c} - \left(\frac{\dot{\overline{T}}}{\overline{T}} + \frac{\dot{\overline{R}}}{\overline{R}}\right)\right]\dot{\pi} - \left\{\alpha^2 + \beta^2 - \frac{\alpha^2\gamma_1 M_1^2(\bar{u}-c)^2\bar{c}_v/\overline{R}}{\overline{R}\,\overline{T}\left[\bar{c}_v/\overline{R} + (\gamma_1 - 1)\right]}\right\}\pi = 0 , \tag{4.11}$$

where $c = \omega/\alpha$ is the complex phase velocity. The following transformations, which are due to Squire [1933], are introduced

$$\hat{\alpha}^2 = \alpha^2 + \beta^2 , \qquad \hat{\alpha}\hat{M}_1 = \alpha M_1 , \qquad \hat{\alpha}\hat{\pi} = \alpha\pi . \tag{4.12}$$

Thus,

$$\alpha = \hat{\alpha}\cos(\vartheta) , \qquad \beta = \hat{\alpha}\sin(\vartheta) , \qquad \hat{M}_1 = M_1\cos(\vartheta) . \tag{4.13}$$

Using these transformations, Eq. 4.11 can be cast into the same form as those for the flow with two-dimensional wave disturbances, *i.e.*,

$$\ddot{\pi} - \left[\frac{2\dot{\bar{u}}}{\bar{u}-c} - \left(\frac{\dot{\overline{T}}}{\overline{T}} + \frac{\dot{\overline{R}}}{\overline{R}}\right)\right]\dot{\pi} - \hat{\alpha}^2\left\{1 - \frac{\gamma_1\hat{M}_1^2(\bar{u}-c)^2\bar{c}_v/\overline{R}}{\overline{R}\,\overline{T}\left[\bar{c}_v/\overline{R} + (\gamma_1 - 1)\right]}\right\}\pi = 0 . \tag{4.14}$$

The instability characteristics of the three-dimensional disturbances were studied for compressible mixing layers formed by different perfect gases. The effect of the angle of propagation direction ϑ of three-dimensional disturbances on the instability behavior of mixing layers was considered. For the mean profiles given by Eqs. 3.10, 3.15 and 3.20 with $u_2/u_1 = 0.5$, $T_2/T_1 = 2.0$, $R_2/R_1 = 0.5$ and $\gamma_1 = \gamma_2 = 1.4$, the amplification rate as a function of the propagation angle ϑ is shown in Figs. 4.26a and 4.26b for the cases $M_{c1} = 0.25$ and $M_{c1} = 0.75$ respectively. The maximum amplification rate $-\alpha_{im}$ decreases as the angle ϑ of the disturbance increases for the low-speed mixing layers. Also, the band of unstable frequencies becomes narrower as the angle ϑ of a disturbance increases. For the high-speed mixing layer, the maximum amplification rate is higher than that of the corresponding two-dimensional disturbances over some range of the angle of propagation ϑ. Therefore, the three-dimensional results may provide better agreement with the experimental data for high Mach number mixing layers. Recall, however, that according to Papamoschou & Roshko's experimental data, the growth rate approaches an asymptotic value as the convective Mach number M_{c1} becomes supersonic. Even though the growth rate of the oblique wave disturbances is higher than the corresponding two-dimensional disturbances, it nevertheless decreases continuously as the convective Mach number M_{c1} is increased (see Fig. 4.27).

4.9 Wake-dominated Mixing Flows

Owing to the finite thickness of a splitter plate and the displacement thickness of the splitter plate boundary layers, the initial region of a two-stream mixing flow is wake-dominated. The mean quantities of the developing wake/mixing

layer downstream of a splitter plate can be obtained by numerically solving the laminar, two-dimensional, thin-layer Navier-Stokes equations. In order to simplify the problem, we assumed that the mean velocity profile is composed of the usual hyperbolic tangent profile plus a wake component (due to the splitter plate) represented by a Gaussian distribution (see Eq. 3.12). For incompressible mixing layers, Koochesfahani & Frieler [1987] studied the linear spatial instability characteristics of both uniform and non-uniform density plane mixing layers, taking into account the wake component of the initial velocity profile. They found that there are two unstable waves in incompressible mixing layers. One is the shear layer mode and the other is the wake mode. For compressible mixing layers, the instability behavior of mixing layers was investigated here with a wake component in the mean velocity profile. The shear layer mode and the wake mode corresponding to that of the incompressible mixing flows found by Koochesfahani & Frieler were also found for compressible mixing layers. The instability characteristics of the shear layer mode and the wake mode, with different normalized wake deficits w, are shown in Figs. 4.28a and 4.28b at free stream Mach numbers $M_1 = 1$ and $M_1 = 2$ respectively. As the normalized wake deficit w increases, the mixing layer becomes more unstable and the band of amplified disturbance frequencies ω becomes narrower for both the shear layer mode and the wake mode. A comparison is made in Fig. 4.29 of the normalized growth rate as a function of the convective Mach number M_{c1} of both shear layer mode and the wake mode ($w = 0.4$) with the function $F(M_{c1})$ and with the Papamoschou & Roshko experimental data. For the shear layer mode, the normalized growth rate has a similar behavior as the function $F(M_{c1})$, but with higher values of the normalized growth rate in the region $0 \leq M_{c1} \leq 2$. As the convective Mach number M_{c1} increases continuously in the region of supersonic disturbances, the growth rate of the shear layer mode starts to rise up to a local extremum value

and then falls again. For the wake mode, the amplification rate decreases very slowly in the subsonic convective Mach number region and continuously decreases in the region of supersonic convective Mach numbers. Figure 4.30a shows the effect of the normalized wake deficit w on the normalized maximum amplification rate of the shear layer mode. If the convective Mach number M_{c1} is less than about 0.4, the value of the normalized wake deficit w does not affect the behavior of the normalized maximum amplification rate as a function of the convective Mach number M_{c1}. But in the region $0.4 < M_{c1} < 1.0$, the normalized maximum amplification rate decreases faster for smaller values of w. For supersonic convective Mach numbers, the value of the convective Mach number M_{c1}, which corresponds to the local extremum value, shifts to bigger values as w decreases. For the wake mode, the normalized maximum amplification rate decreases faster as a function of the convective Mach number M_{c1} with increasing wake deficit w (see Fig. 4.30b). Studies of wake-dominated mixing layers suggest that a larger value of the growth rate at large convective Mach number M_{c1} can be obtained by increasing the normalized wake deficit w.

4.10 Effect of the Thickness of the Total Temperature Profile

The thickness of the total temperature profile may be much smaller than that of the mean velocity profile in the initial region of the flow near the splitter plate tip. It is interesting, therefore, to find out how this relative thickness can affect the instability behavior of mixing layers. For incompressible mixing layers, Koochesfahani & Frieler [1987] studied the effect of the density profile thickness on the instability behavior of mixing layers. They found that when the high density

fluid is carried on the low-speed side, the density profile thickness must be smaller than a certain value before the wake mode becomes dominant and that when the high density fluid is on the high-speed side, regardless of the density profile thickness, the shear layer mode is always dominant. For compressible mixing layers, we considered the effect of the thickness of the total temperature profile relative to the mean velocity profile on the amplification rate of mixing layers. In the calculations, the hyperbolic tangent mean velocity profile given by Eq. 3.10 and the total temperature profile given by Eq. 3.16 with $\zeta(y)$ replaced by $\zeta(y/\sigma)$, see Fig. 3.5, were considered, where σ adjusts the thickness of the total temperature profile relative to the mean velocity profile. For the velocity ratio $u_2/u_1 = 0.5$, the total temperature ratio $T_{t2}/T_{t1} = 0.5$ and $\sigma = 1.0,\ 0.8,\ 0.6,\ 0.4$, the variation of the amplification rate $-\alpha_i$, as a function of the amplified disturbance frequencies ω, is shown in Figs. 4.31a – 4.31c for different values of the free stream Mach number M_1. As the thickness of the total temperature decreases, the maximum amplification rate $-\alpha_{im}$ increases and the band of amplified frequencies becomes wider for both subsonic and supersonic mixing layers. The normalized maximum amplification rate as a function of the convective Mach number M_{c1} is shown in Fig. 4.32 for different values of the relative thickness parameter σ. As the thickness of the total temperature profile σ becomes smaller, the normalized maximum amplification rate decreases slower in the subsonic convective Mach number region. For supersonic convective Mach numbers, the larger value of the normalized amplification rate is obtained with decreasing σ.

CHAPTER 5

THE EFFECT OF WALLS ON SPATIALLY GROWING SUPERSONIC MIXING LAYERS

The inviscid instability, with respect to supersonic disturbances, of a spatially growing plane mixing layer inside parallel flow guide walls is investigated here using linear stability analysis. The mixing layer is assumed to be inviscid and formed by the same gases in the two streams. The mean flow is treated as parallel. The purpose of this chapter is to give a description of how the instability characteristics of the mixing layer are affected by the flow guide walls and by the distance between the walls. It is found that the maximum amplification rates of the mixing layers approach an asymptotic value and that this maximum amplification rate increases to a maximum value and decreases again as the distance between the parallel walls decreases continuously. For a mixing layer inside parallel flow guide walls, the growth rate of three-dimensional modes is larger than the corresponding two-dimensional mode at higher convective Mach numbers. But the growth rate of two-dimensional supersonic instability waves is higher than their three-dimensional counterparts for a mixing layer inside a rectangular duct (Tam & Hu [1988, 1989]). All flow quantities used in this chapter are the dimensionless quantities defined in Chapter 2.

5.1 Instability Behavior of Bounded Mixing Layers

The instability characteristics of mixing layers with mean velocity and temperature profiles given by Eq. 3.10 and Eq. 3.15 are determined for two-dimensional, spatially growing disturbances with $u_2/u_1 = 0.5$, $T_2/T_1 = 1.0$, $\delta = 3$ unit lengths (defined in Eq. 2.42) and $d = 4\delta = 12$ unit lengths, at different free stream Mach numbers M_1. The main result, shown in Fig 5.1, is that when the convective Mach number of the flow is supersonic, as was also noted by Mack [1969, 1984] in his analysis of supersonic boundary layer stability, there are many supersonic unstable modes, as opposed to only one for the case of subsonic convective Mach numbers.

The existence of many supersonic instability modes in the case of mixing layers, has been known from the work of Tam & Hu [1988, 1989]. Their results, however, were based on instability calculations inside a three-dimensional rectangular channel. Fig. 5.2 (the normalized maximum amplification rate *vs.* the convective Mach number M_{c1}) indicates that the growth rate of the most unstable supersonic instability mode of a mixing layer with two-dimensional, spatially growing disturbances approaches an asymptotic value as the convective Mach number becomes supersonic, in accord with the previously cited growth rate experiments by Papamoschou & Roshko [1986, 1988]. The convective Mach number here is defined by Eq. 1.4.

If a mixing layer inside parallel flow guide walls is subjected to a small,

three-dimensional, spatially growing disturbance of the form

$$q'(x,y,z,t) = q(y)\exp[i(\alpha x + \beta z - \omega t)], \qquad (5.1)$$

where β is a complex wave number in the z direction and ω is a real disturbance frequency, then the growth rate of the three-dimensional mode is larger than the corresponding two-dimensional mode at high convective Mach numbers over some range of propagation direction (see Fig. 5.3). This result is similar to that of previous studies of a free mixing layer with three-dimensional disturbances by Gropengiesser [1970], Ragab & Wu [1988], Jackson & Grosch [1988] and by Sandham & Reynolds [1989]. For a mixing layer inside a rectangular duct, however, Tam & Hu [1989] considered three-dimensional, spatially growing disturbances of the form

$$p' = \bar{p}(y)\exp[i(\alpha x - \omega t)]\cos(2m\pi z/b); \quad m = 0,\ 1,\ 2,\ \ldots, \qquad (5.2)$$

where p' is the perturbation pressure and b is the span of the rectangular duct. The important result of their investigations was that, for reasonably thick mixing layers, two-dimensional supersonic instability waves have larger spatial growth rates than their three-dimensional counterparts. We conducted similar calculations as part of this investigation. Our results are in agreement with Tam & Hu's results. The instability characteristics of three-dimensional modes are characterized by similar behavior as two-dimensional modes. As a consequence, two-dimensional modes were considered mainly in the work described below.

A comparison of the current results of growth rate with the Papamoschou & Roshko experimental results [1986, 1988] and with the results obtained from the two-dimensional free mixing layer calculations by Zhuang *et al.*

[1988], are made in Fig. 5.4. We can see how the parallel flow guide walls affect the instability of the mixing layer. The existence of walls makes the mixing layer more unstable and keeps the maximum amplification rates from reaching asymptotically small values for supersonic convective Mach numbers, but has no discernible effect on the amplification rate in mixing layers with subsonic convective Mach numbers.

For a fixed high stream Mach number M_1, with the same mean velocity and temperature profiles given as described above, the instability characteristics of mixing layers with two-dimensional spatially growing waves are calculated for different values of d (d = 20, 16, 12, 8 unit lengths). The most unstable supersonic instability mode, which is not the Kelvin-Helmholtz mode, moves to higher frequencies and its maximum amplification rate increases as the distance between two parallel walls decreases (see Fig. 5.5). This maximum amplification rate, however, reaches its maximum value and decreases as the distance between the walls decreases continuously (see Fig. 5.6). The instability characteristics of subsonic mixing layers are not affected by the distance between the walls. The thickness of the mixing layer was chosen as the characteristic length in the calculations, which made the solution of the bounded mixing layer, as $d/\delta \rightarrow \infty$, approach that of the corresponding free mixing layer. Note that if the distance between the parallel walls is chosen as the characteristic length, the growth rate of the supersonic instability waves, scaled to this characteristic length, *decreases* at a fixed frequency as the mixing layer becomes thicker and thicker (Tam & Hu [1989]).

5.2 The Pressure Perturbation Field

With the computed eigenfunction $\pi(y)$, the pressure perturbation fields can be obtained by

$$p'(x,y,t) = \pi(y)\exp\left[i(\alpha x - \omega t)\right]. \tag{5.3}$$

The real part of p' represents the physical quantity of the pressure perturbations. Contour plots of the pressure perturbation fields, which combine the periodic term and the growth term, are shown in Figs 5.7, 5.8, 5.9 and 5.10. Note that the convective Mach numbers of the mixing layers corresponding to these contour plots are either close to, or larger than, unity, so the growth of the mixing layers is small within the extent plotted. Fig. 5.7 shows the flow with the same supersonic convective Mach numbers at both sides of the boundaries ($M_{c1} = M_{c2} = 1.375$). We can see that the compression/expansion waves propagate along the Mach angle $\nu_1 = \arcsin(1/M_{c1})$ or $\nu_2 = \arcsin(1/M_{c2})$ for supersonic convective Mach numbers. By measuring the Mach angle ($\nu_1 = \nu_2 = 45.7°$), I estimated a convective Mach number of $M_{c1} = M_{c2} = 1.397$, in close agreement with M_{c1} and M_{c2} estimated using Eq. (1.4). The variations in the strength of these compression/expansion waves indicate that these waves are reflected by the walls. Fig. 5.8 is the contour plot for the free mixing layer with the upper stream supersonic and the lower stream subsonic ($M_{c1} = 1.81$ and $M_{c2} = 0.94$). The upper flow compression/expansion waves propagate with the Mach angle $\nu_1 = 34.2°$, *i.e.*, $M_{c1} = 1.78$, with no reflections. From these two contour plots we can see that for supersonic disturbances, because of the existence of the walls, the energy carried by the wave system is reflected back to the mixing layer instead of being radiated and lost to the far field. The feedback mechanism between the growing supersonic mixing layer and

the wave system makes the bounded supersonic mixing layer more unstable than the corresponding free supersonic mixing layer, which is losing energy to acoustic radiation to the far field (Mack [1969], Tam [1989] and Dimotakis [1989]). Figs. 5.9 and 5.10 are two other examples of contour plots for bounded mixing layers; one is with the lower stream supersonic and upper stream subsonic, and the other is vice versa. Reflections of the compression/expansion wave system propagating along the Mach angles for supersonic convective Mach numbers can also be seen in those two figures (Zhuang *et al.* [1989]).

5.3 Streaklines of the Disturbed Mixing Layer

In order to describe the flow patterns of the mixing layers, streaklines were calculated for the modes corresponding to the maximum amplification rates. A streakline is the locus of particles which have earlier passed through a prescribed point. In the experiments, the streaklines can be produced and visualized by the continuous release of marked particles (dye, smoke, or bubbles) from a given point. The procedure for the calculation of streaklines is the same as that used by Michalke [1965]. The motion of a particle is given by

$$\begin{aligned} \frac{dx}{dt} &= \epsilon_1 u'(x,y,t) + \bar{u}(y)\,, \\ \frac{dy}{dt} &= \epsilon_1 v'(x,y,t)\,. \end{aligned} \tag{5.4}$$

With appropriate initial conditions, $x(t_0) = x_0$ and $y(t_0) = y_0$, a pathline can be determined. In order to plot each streakline for a fixed time, the pathlines for various initial times, t_0, are calculated. In the calculations, I have chosen $x_0 = 0$, $\epsilon_1 = 0.0005$ for subsonic convective Mach numbers and $x_0 = 0$, $\epsilon_1 = 0.1$ for super-

sonic convective Mach numbers. The results are plotted in Figs. 5.11 and 5.12 and represent streaklines corresponding to supersonic and subsonic disturbances, respectively. These flow patterns show that, for supersonic disturbances, the growth of the mixing layer, as labeled by the streaklines, is much slower than that for subsonic disturbances, and the spreading rate of the mixing layer is small.

CHAPTER 6

SUMMARY AND CONCLUSIONS

An investigation of the linear instability behavior of compressible unbounded and bounded mixing layers with spatially growing wave disturbances has been performed. The mixing layer is formed by two parallel streams with different perfect gases and the flow is assumed to be inviscid and non reacting.

6.1 Results for Unbounded Mixing Layers

For compressible unbounded mixing layers with given ratios of specific heats γ_1, γ_2, the instability characteristics of flows were calculated in which the free stream Mach number M_1 varied from 0 to 11, the velocity ratio u_2/u_1 varied from 0.25 to 0.75, the temperature ratio T_2/T_1 varied from 0.2 to 5.0, the gas constant ratio R_2/R_1 varied from 0.1 to 5. The effect of compressibility on the properties of mixing layers was determined. The sensitivity to the details of the mean flow profiles on the instability behavior of mixing layers was also studied. A summary of the results for unbounded mixing layers is presented below:

1. For a free mixing layer with hyperbolic mean flow profiles, there is only one unstable mode propagating with the phase velocity of the most unstable wave C^*_{pm} approximately equal to the isentropic estimate of the convective velocity of the large scale structures u^*_c for

subsonic convective Mach numbers. As the convective Mach number approaches or exceeds unity, there are always two unstable modes. One with a phase velocity $C_{pm}^* < u_c^*$ (slow mode) and the other with a phase velocity $C_{pm}^* > u_c^*$ (fast mode).

2. For supersonic mixing layers, the phase velocity of the most unstable mode C_{pm}^* decreases for the slow mode and increases for the fast mode with increasing free stream Mach number M_1. The bands of amplified disturbance frequencies ω of these two unstable modes overlap for some range of frequencies. For the low supersonic convective Mach numbers, the fast mode is more unstable than the slow mode when the heavy gas is on the low-speed side and the slow mode is dominant when the heavy gas is on the high-speed side.

3. For a given convective Mach number, the band of unstable frequencies ω becomes wider and the maximum amplification rate $-\alpha_{im}$ becomes smaller as the velocity ratio u_2/u_1 increases. The phase velocity of the most unstable mode C_{pm}^* is a linear function of the velocity ratio u_2/u_1 for both subsonic and supersonic convective Mach numbers.

4. For an incompressible unbounded mixing layer with a hyperbolic mean velocity profile, the maximum amplification rate $-\alpha_{im}$ is approximately a linear function of the velocity ratio $\lambda = (1 - u_2/u_1)/(1 + u_2/u_1)$ and $-\alpha_{im}$ rises with increasing density ratio ρ_2/ρ_1 for all

$0 \leq \lambda \leq 1$ and density ratios $\rho_2/\rho_1 \leq 1$. For density ratios ρ_2/ρ_1 greater than unity, the function $-\alpha_{im}(\lambda)$ becomes nonlinear and the maximum amplification rate $-\alpha_{im}$ falls with increasing density ratio ρ_2/ρ_1 for some values of the velocity ratio λ.

5. The instability characteristics of unbounded mixing layers are not affected by the difference between γ_1 and γ_2 for incompressible flows. For the subsonic mode ($M_{c1} \neq 0$) and the slow supersonic mode $C^*_{pm} < u^*_c$, the band of unstable frequencies ω becomes wider and the maximum amplification rate $-\alpha_{im}$ rises if the high-speed stream has the lower value of the ratio of specific heats. But the band of amplified disturbance frequencies becomes narrower and the maximum amplification rate falls for the fast supersonic mode $C^*_{pm} > u^*_c$ when the high-speed stream has the lower value of the ratio of specific heats.

6. The eigenfunction $\pi(y)$ decays exponentially away from the mixing layers in the stream with subsonic disturbances and displays an oscillatory decay in the stream with supersonic disturbances.

7. A nearly universal dependence of the normalized maximum amplification rate on the convective Mach number is found for two-dimensional, spatially growing wave disturbances, with the normalized maximum amplification rate decreasing significantly with increasing convective Mach numbers in the subsonic region. At high convective Mach num-

bers, the maximum amplification rate $-\alpha_{im}$ of mixing flows with three-dimensional spatially growing disturbances is bigger than that of corresponding two-dimensional disturbances. But for both two-dimensional and three-dimensional disturbances, the maximum amplification rate decreases continuously as the convective Mach number M_{c1} increases.

8. Adding a wake component to the mean velocity profile, or decreasing the thickness of the total temperature profile relative to the mean velocity profile, can make the normalized maximum amplification rate decrease slower for both subsonic and supersonic convective Mach numbers.

6.2 Results for Bounded Mixing Layers

For compressible bounded mixing layers, the inviscid instability with respect to supersonic disturbances, of a spatially growing plane mixing layer inside parallel flow guide walls has been investigated using linear stability analysis. The thickness of the mixing layer was chosen as the characteristic length in the calculations, which made the solutions of the bounded mixing layer, as $d/\delta \to \infty$, approach that of the corresponding unbounded mixing layer. The effects of the parallel walls and the distance between the walls on the instability characteristics of mixing layers were determined. Contour plots of the pressure perturbation fields for both unbounded and bounded mixing layers were calculated. Also, the flow patterns of

the mixing layers were obtained by calculating the streaklines of the mixing layers. A summary of the results for bounded mixing layers is given below:

1. The existence of parallel flow guide walls makes the mixing layer more unstable and keeps the maximum amplification rate $-\alpha_{im}$ from reaching an asymptotically small value for supersonic convective Mach numbers, but has no discernible effect on mixing layers with subsonic convective Mach numbers.

2. The most unstable supersonic instability mode, which is not the Kelvin-Helmholtz mode, moves to higher frequencies and its maximum amplification rate $-\alpha_{im}$ increases to its maximum value and decreases again as the distance between the walls decreases continuously.

3. For supersonic convective Mach numbers, the reflections of the compression/expansion waves caused by the parallel walls provide a feedback mechanism between the growing mixing layer structures and the wave system. Bounded mixing layers are more unstable than the corresponding unbounded mixing layers. The maximum amplification rates $-\alpha_{im}$ of the bounded mixing layers are found to approach an asymptotic value for supersonic convective Mach numbers. The streaklines of the flow confirm that the spreading rate of the mixing layer is unusually small for supersonic disturbances.

REFERENCES

BIRCH, S. L. and EGGERS, J. M. [1973] "A Critical Review of the Experimental Data for Developed Free Turbulent Shear Layers," NASA SP–321, 943–949.

BLUMEN, W. [1970] "Shear Layer Instability of an Inviscid Compressible Fluid," *J. Fluid Mech.* **40**, 769–781.

BLUMEN, W., DRAZIN, P. G. and BILLINGS, D. F. [1975] "Shear Layer Instability of an Inviscid Compressible Fluid. Part 2," *J. Fluid Mech.* **71**, 305–316.

BOGDANOFF, D. W. [1983] "Compressibility Effects in Turbulent Shear Layers," *AIAA J.* **21**(6), 926–927.

BROWN, G. L. and ROSHKO, A. [1974] "On Density Effects and Large Structures in Turbulent Mixing Layers," *J. Fluid Mech.* **64**(4), 775–781.

BUSEMANN, A. [1935] "Gasstromung mit Laminarer Grenzschicht Entlang einer Platte," *ZAMM* **15**, 23–25.

CHINZEI, N., MASUYA, G., KOMURO, T., MURAKAMI, A., and KUDOU, K. [1986] "Spreading of Two-Stream Supersonic Mixing Layers," *Phys. of Fluid*, **29**(5), 1345–1347.

COLES, D. [1981] "Prospects for Useful Research on Coherent Structure in Turbulent Shear Flow," *Proc. Indian Acad. Sci.* **4**(2), 111–127.

COLES, D. [1985] "Dryden Lecture: The Uses of Coherent Structure," AIAA Paper

No. 85–0506.

CROCCO, L. [1932] "Sulla Trasmissione del Calore da una Lamina Piana a un Fluido Scorrente ad alta Velocita," *L' Aerotecnica* **12**, 181–197.

DIMOTAKIS, P. E. [1986] "Two-Dimensional Shear Layer Entrainment," *AIAA J.* **24**(11), 1791–1796.

DIMOTAKIS, P. E. [1989] "Turbulent Free Shear Layer Mixing," AIAA Paper No. 89–0262.

DRAZIN, P. G. and DAVEY, A. [1977] "Shear Layer Instability of an Inviscid Compressible Fluid. Part 3," *J. Fluid Mech.* **82**, 255–260.

GREENOUGH, J., RILEY, J., SOETRISNO, M. and EBERHARDT, D. [1989] "The Effects of Walls on a Compressible Mixing Layer," AIAA Paper No. 89–0372.

GROPENGIESSER, H. [1970] "Study of the Stability of the Boundary Layers in Compressible Fluids," NASA TT–F–12, 786.

HELMHOLTZ, H [1868] "Discontinuous Fluid Motions," *Monatsberichte Konigl. Akad. Wiss. Berlin*, 215–228.

HOWARTH, L. [1948] "Concerning the Effect of Compressibility on Laminar Boundary Layers and Their Separation," *Proc. Roy. Soc., Ser. A*, **194**, 16–42.

JACKSON, T. L. and GROSCH, C. E. [1988] "Spatial Stability of a Compressible Mixing Layer," *ICASE Report* No. 88–33.

JACKSON, T. L. and GROSCH, C. E. [1989] "Inviscid Spatial Stability of a Com-

pressible Mixing Layer," *J. Fluid Mech.* **208**, 609–637.

KELVIN, L. [1871] "Hydrokinetic Solutions and Observations," *Phil. Mag.* (4), **42**, 362–377.

KOOCHESFAHANI, M. M. and FRIELER, C. E. [1987] "Inviscid Instability Characteristics of Free Shear Layers with Non-Uniform Density," AIAA Paper No. 87–0047.

KUCHEMANN, D. [1938] "Storungsbewegungen in einer Gasstromung mit Grenzschicht," *Z.F.A.M.M., Bd.* **18**, Heft 4, 207–222.

LANDAU, L. D. [1944] "Stability of Tangential Discontinuities in Compressible Fluid," *Dokl. Akad. Nauk. SSSR,* **44**, 139–141.

LANG, D. B. [1985] *Laser Doppler Velocity and Vorticity Measurements in Turbulent Shear Layers*, Ph.D. Thesis, California Institute of Technology.

LEES, L. and LIN, C. C. [1946] "Investigation of the Stability of the Laminar Boundary Layer in a Compressible Fluids," NACA Techn. Note No. 1115.

LESSEN, M., FOX, J. A. and ZIEN, H. M. [1965] "On the Inviscid Stability of the Laminar Mixing of Two Parallel Streams of a Compressible Fluid," *J. Fluid Mech.* **23**, 355–367.

LESSEN, M., FOX, J. A. and ZIEN, H. M. [1966] "Stability of the Laminar Mixing of Two Parallel Streams with respect to Supersonic Disturbances," *J. Fluid Mech.* **25**, 737–742.

LIN, C. C. [1944] *On the Development of Turbulence*, Ph.D. Thesis, California Institute of Technology.

LIN C. C. [1955] *The Theory of Hydrodynamic Stability* (Cambridge University Press).

LOCK, R. C. [1951] "The Velocity Distribution in the Laminar Boundary Layer Between Parallel Streams," *Quart. J. Mech. Appl. Math.* **4**, 42–63.

MACARAEG, M. G. and STREETT, C. L. [1989] "New Instability Modes for Bounded, Free Shear Flows," *Phys. Fluids A* **1**(8), 1305–1307.

MACK, L. M. [1969] "Boundary Layer Stability Theory," Jet Propulsion Laboratory, Document No. 900–277, Rev. A.

MACK, L. M. [1975] "Linear Stability and Theory and the Problem of Supersonic Boundary Layer Transition," *AIAA J.* **13**, 278–289.

MACK, L. M. [1984] "Boundary Layer Linear Stability Theory," AGARD Report 709.

MAYDEW, R. C. and Reed, J. F. [1963] "Turbulent Mixing of Compressible Free Jets," *AIAA J.* **1**, 1443–1444.

MICHALKE, A. [1965] "On Spatially Growing Disturbances in an Inviscid Shear Layer," *J. Fluid Mech.* **23**, 521–544.

MONKEWITZ, P. A. and HUERRE, P. [1982] "Influence of the Velocity Ratio on the Spatial Instability of Mixing Layers," *Phys. Fluids* **25**(7), 1137–1143.

PAPAMOSCHOU, D. and ROSHKO, A. [1986] "Observations of Supersonic Free Shear Layers," AIAA Paper No. 86–0162.

PAPAMOSCHOU, D. and ROSHKO, A. [1988] "The Compressible Turbulent Shear Layer: An Experimental Study," *J. Fluid Mech.* **197**, 453–477.

PAPAMOSCHOU, D. [1986] *Experimental Investigation of Heterogeneous Compressible Shear Layers*, Ph.D. Thesis, California Institute of Technology.

PAPAMOSCHOU, D. [1989] "Structure of the Compressible Turbulent Shear Layer," AIAA Paper No. 89–0126.

RAGAB, S. A. and WU, J. L. [1988] "Instabilities in the Free Shear Layer Formed by Two Supersonic Streams," AIAA Paper No. 88–0038.

RAGAB, S. A. and WU, J. L. [1989] "Linear Instabilities in Two-Dimensional Compressible Mixing Layers," *Phys. Fluids A* **1**(6), 957–966.

RAYLEIGH, L [1880] "On the Stability, or Instability, of Certain Fluid Motions," *Scientific Papers* **1**, 474-487 (Cambridge University Press).

RAYLEIGH, L. [1913] "On the Motion of a Viscous Fluid," *Phil. Mag.* (6) **26**, 776–786.

REYNOLDS, O. [1883] "An Experimental Investigation of the Circumstances which Determine Whether the Motion of Water Shall Be Direct or Sinuous, and of the Law of Resistance in Parallel Channels," *Phil. Trans. Roy. Soc.* **174**, 935–982.

SANDHAM, N. and REYNOLDS, W. [1989a] "The Compressible Mixing Layer:

Theory and Direct Simulation," AIAA Paper No. 89–0371.

SANDHAM, N. and REYNOLDS, W. [1989b] "A Numerical Investigation of the Compressible Mixing Layer," Report No. TF–45.

SQUIRE, H. B. [1933] "On the Stability of Three-Dimensional Disturbances of Viscous Flow between Parallel Walls," *Proc. Roy. Soc. A* **142**, 621–628.

TAM, C. K. W. and HU, F. Q. [1988] "Instabilities of Supersonic Mixing Layers Inside a Rectangular Channel," AIAA Paper No. 88–3675–CP.

TAM, C. K. W. and HU, F. Q. [1989] "The Instability and Acoustic Wave Modes of Supersonic Mixing Layers Inside a Rectangular Channel," *J. Fluid Mech.* **203**, 51–76.

TOLLMEIN, W [1935] "A General Criterion for the Instability of Laminar Velocity Distributions," *Nachr. Ges. Wiss. Gottingen, Math.-Phys. Klasse*, 79–114.

ZHUANG, M., KUBOTA, T. and DIMOTAKIS, P. E. [1989] "On the Instability of Inviscid, Compressible Free Shear Layers," *Proceeding, First National Fluid Dynamics Congress*, July 25–28, 1988 (Cincinatti, Ohio), **2**, 768-773. Revised version has been accepted for publication, *AIAA J.*

ZHUANG, M., DIMOTAKIS, P. E. and KUBOTA, T. [1988] "The Effect of Walls on a Spatial Growing Supersonic Shear Layer," *Phys. Fluids* A **2**(4), 599–604.

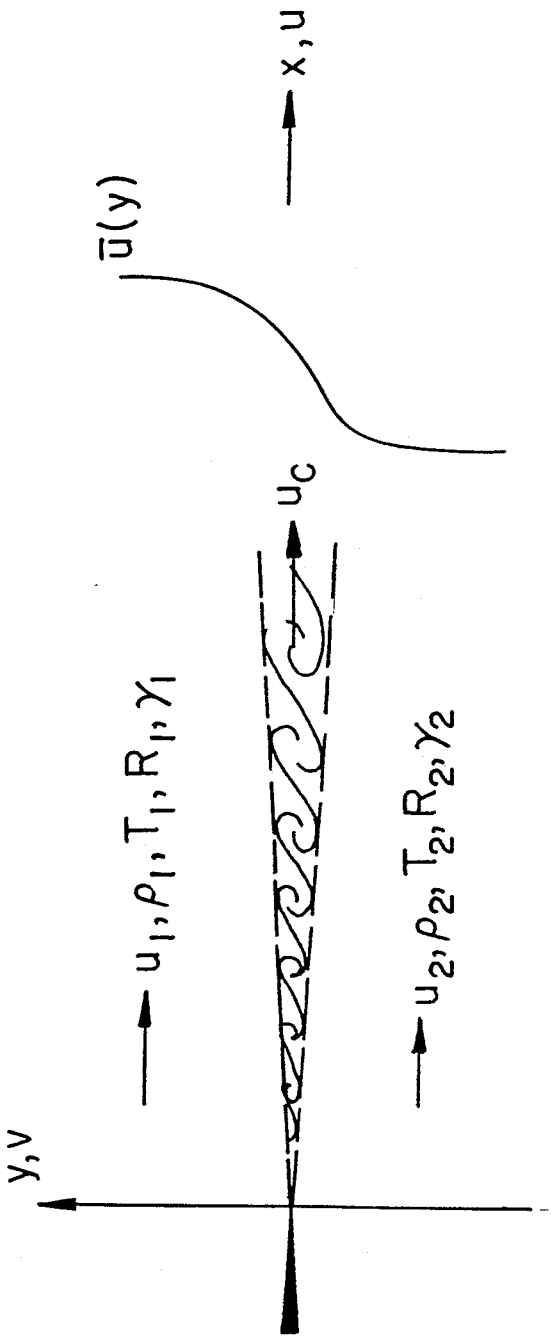

FIG. 2.1 The general configuration of an unbounded mixing layer.

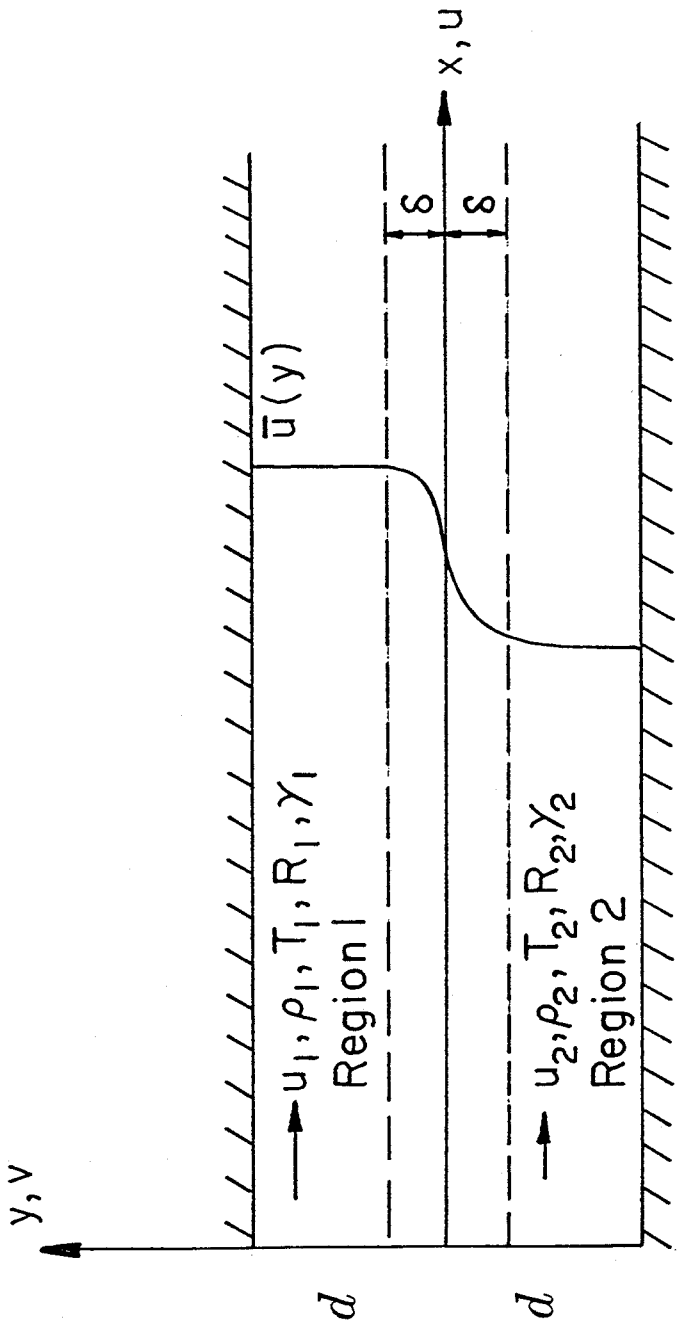

FIG. 2.2 The general configuration of a bounded mixing layer.

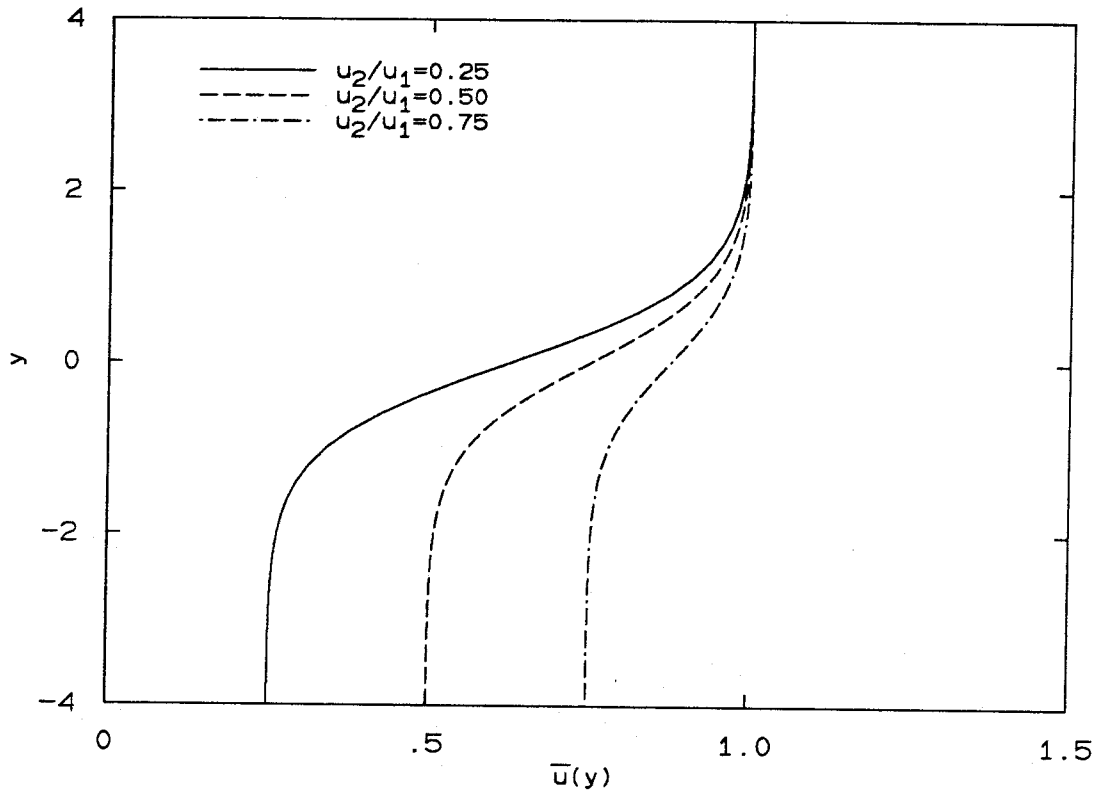

FIG. 3.1 Hyperbolic tangent mean velocity profiles for different values of the velocity ratio u_2/u_1.

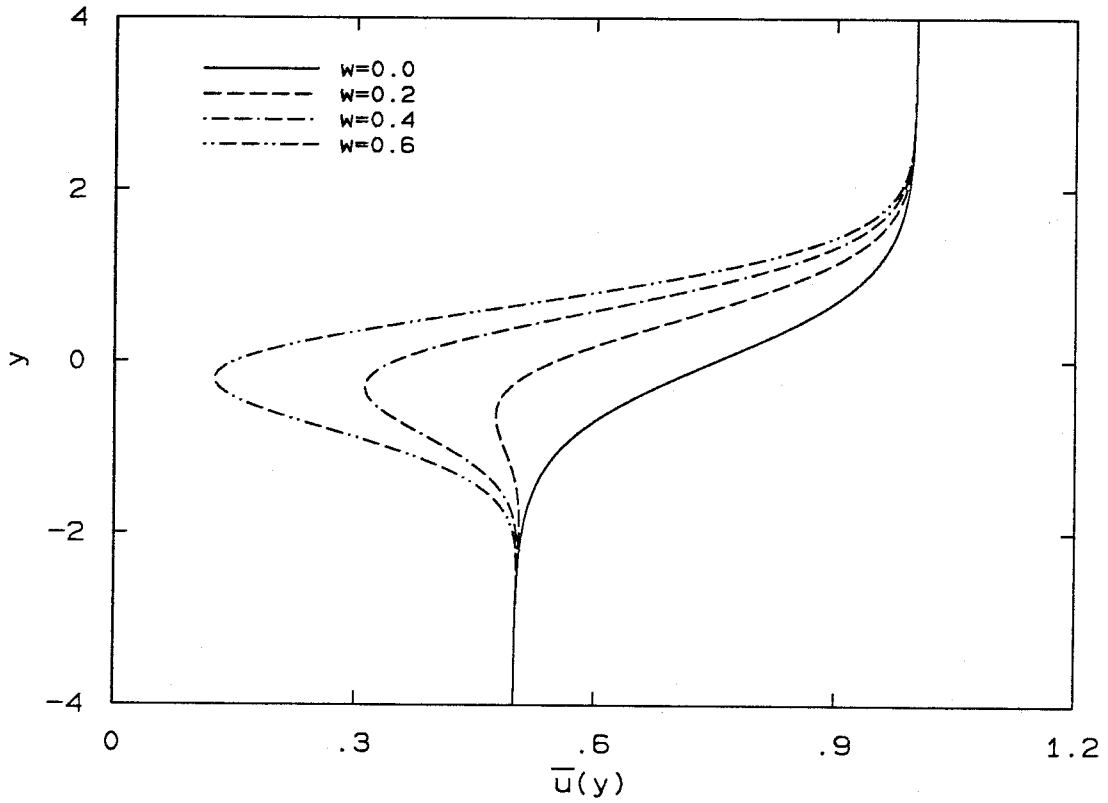

FIG. 3.2 Mean velocity profiles for different values of the normalized wake deficit w at the velocity ratio $u_2/u_1 = 0.5$.

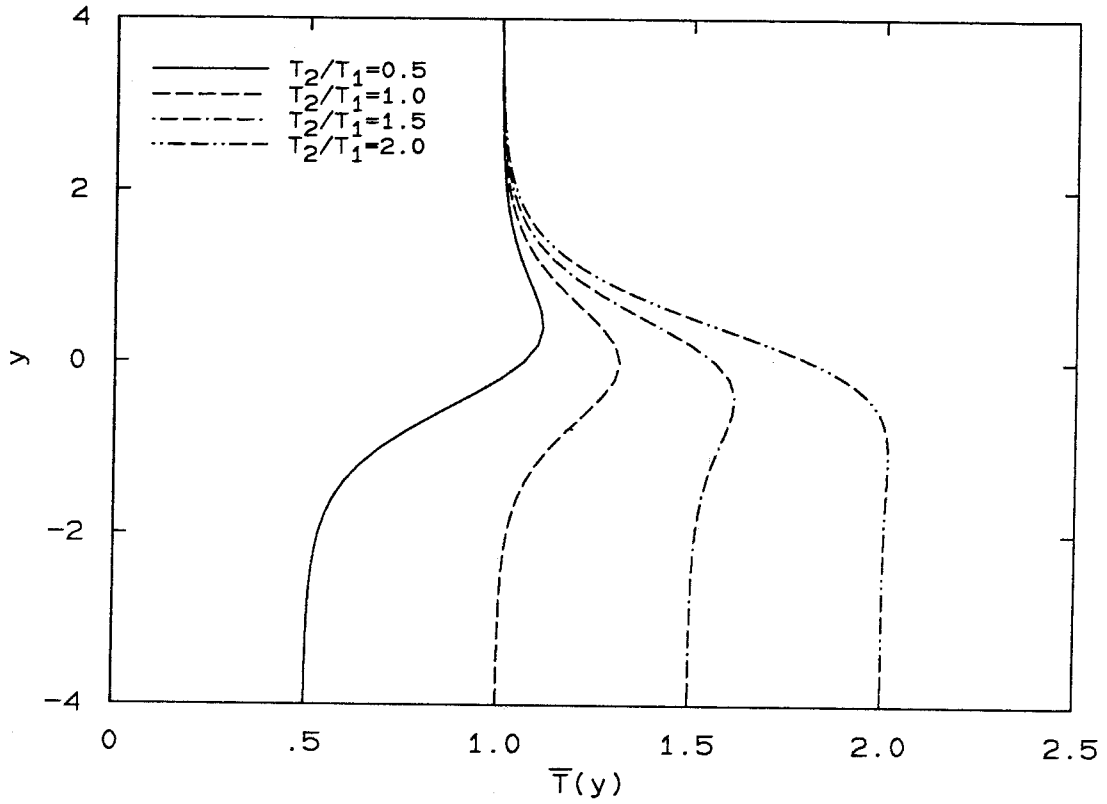

FIG. 3.3 Mean temperature profiles for different values of the temperature ratio T_2/T_1 for the case $u_2/u_1 = 0.5$, $R_2/R_1 = 1.0$ and $M_1 = 5.0$.

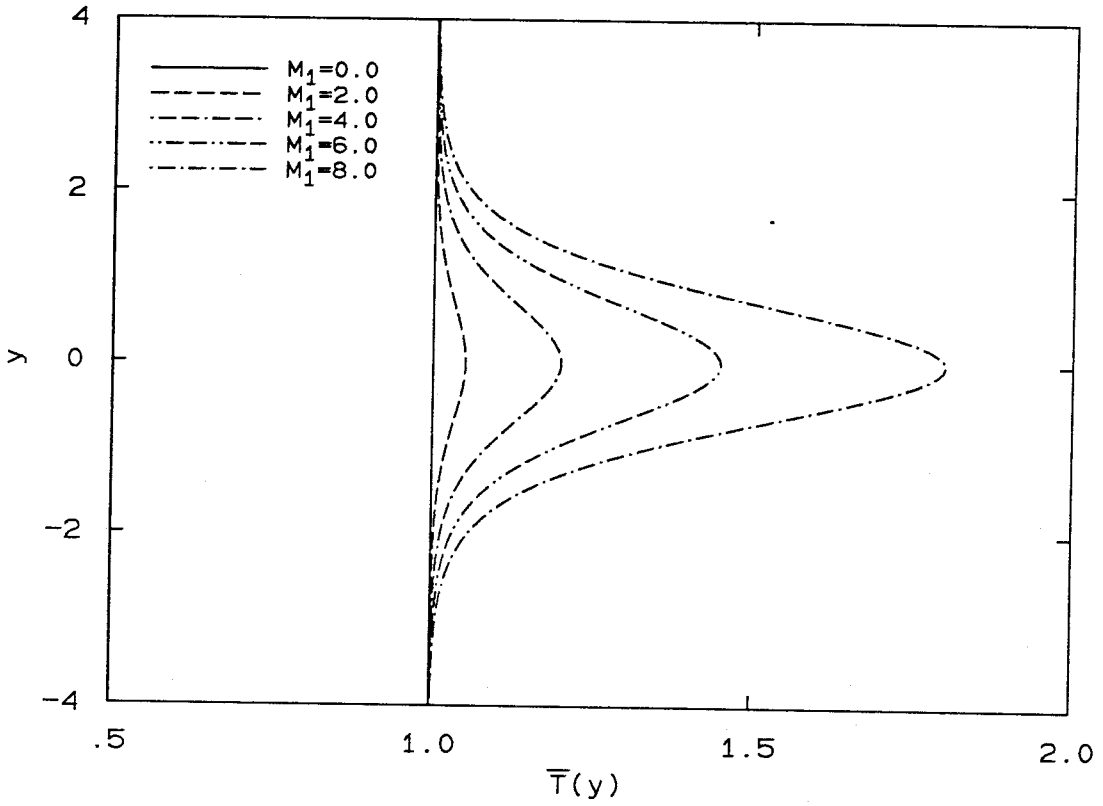

FIG. 3.4 Mean temperature profiles for different values of the free stream Mach number M_1 for the case $u_2/u_1 = 0.5$, $T_2/T_1 = 1.0$ and $R_2/R_1 = 1.0$.

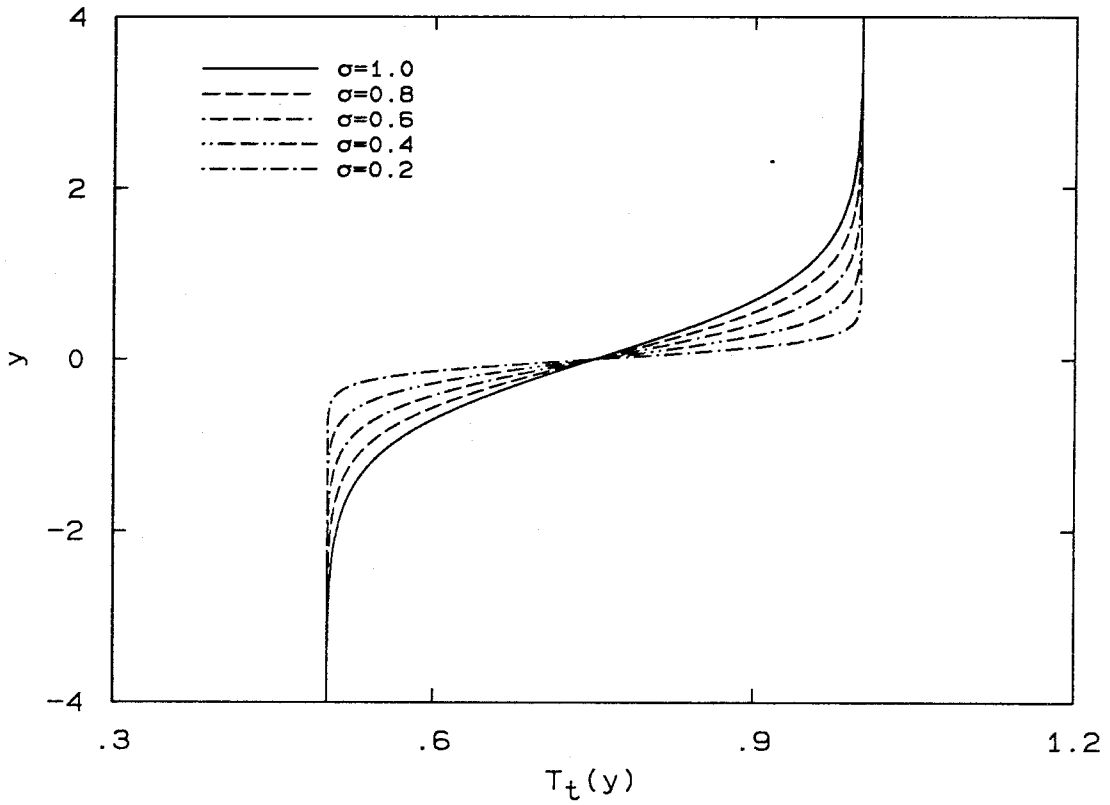

FIG. 3.5 Hyperbolic tangent total temperature profiles for different values of the interface thickness σ at the total temperature ratio $T_{t2}/T_{t1} = 0.5$.

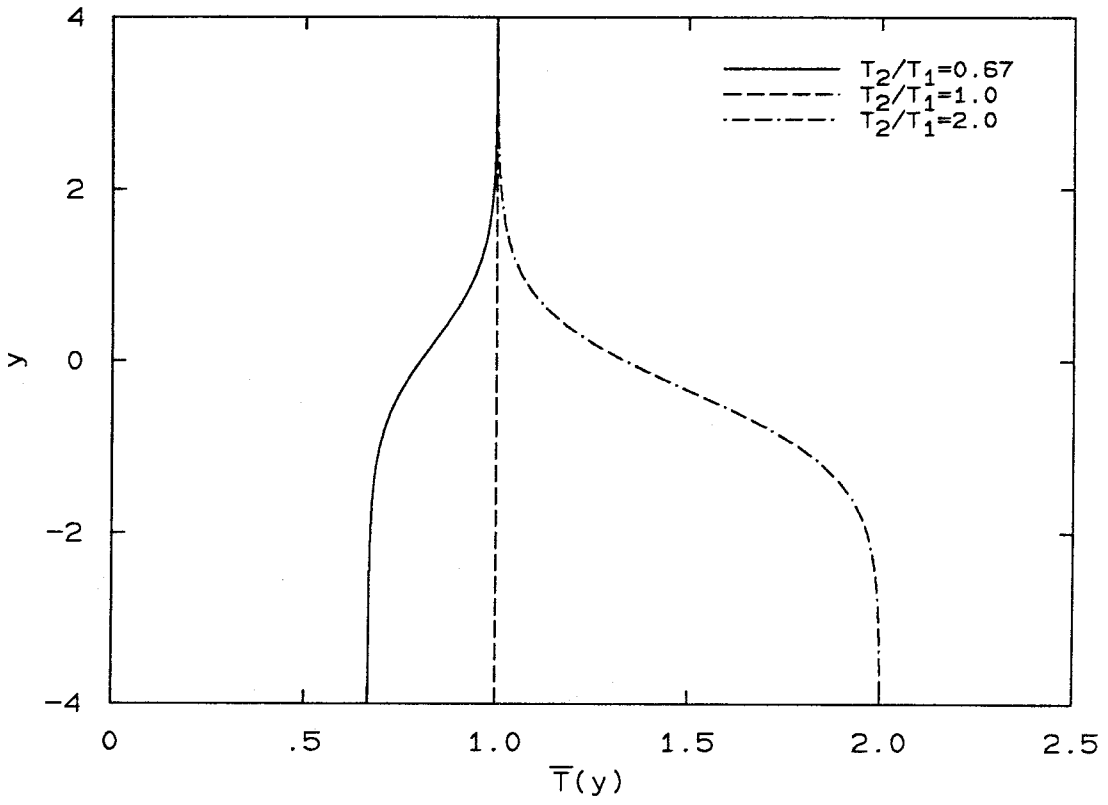

FIG. 3.6 Hyperbolic tangent mean temperature profiles for different values of the temperature ratio T_2/T_1.

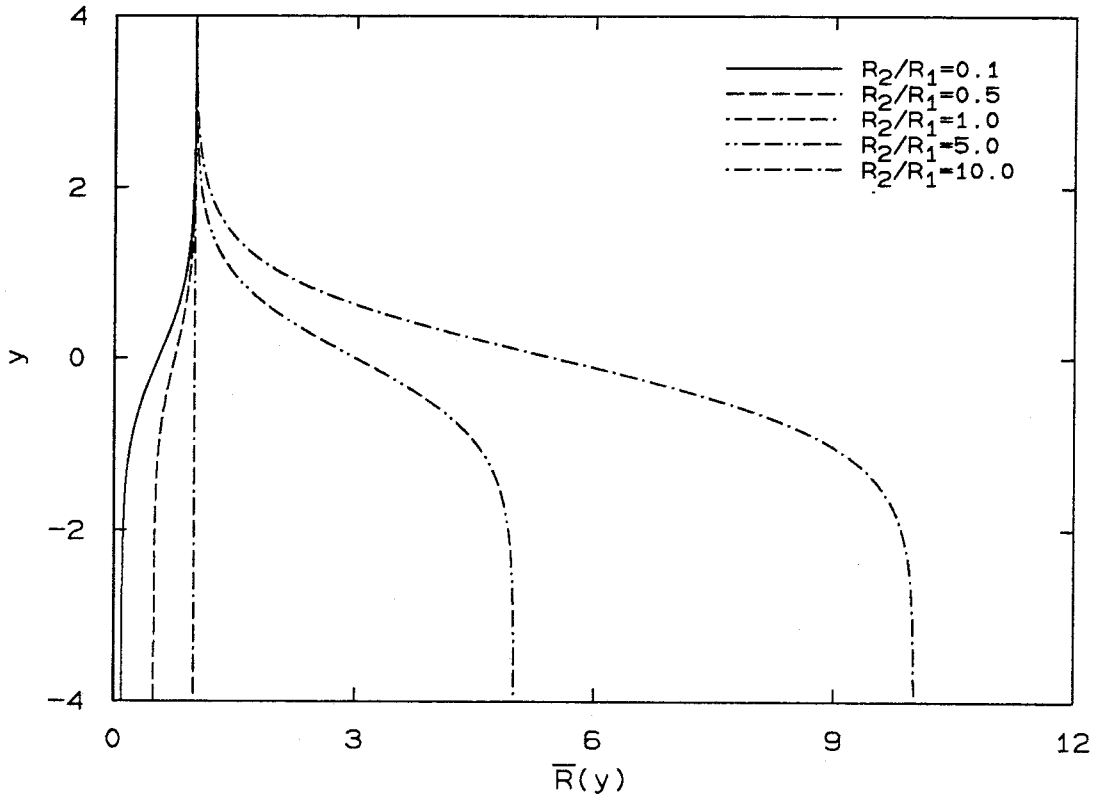

FIG. 3.7 Mean gas constant profiles for different values of the gas constant ratio R_2/R_1.

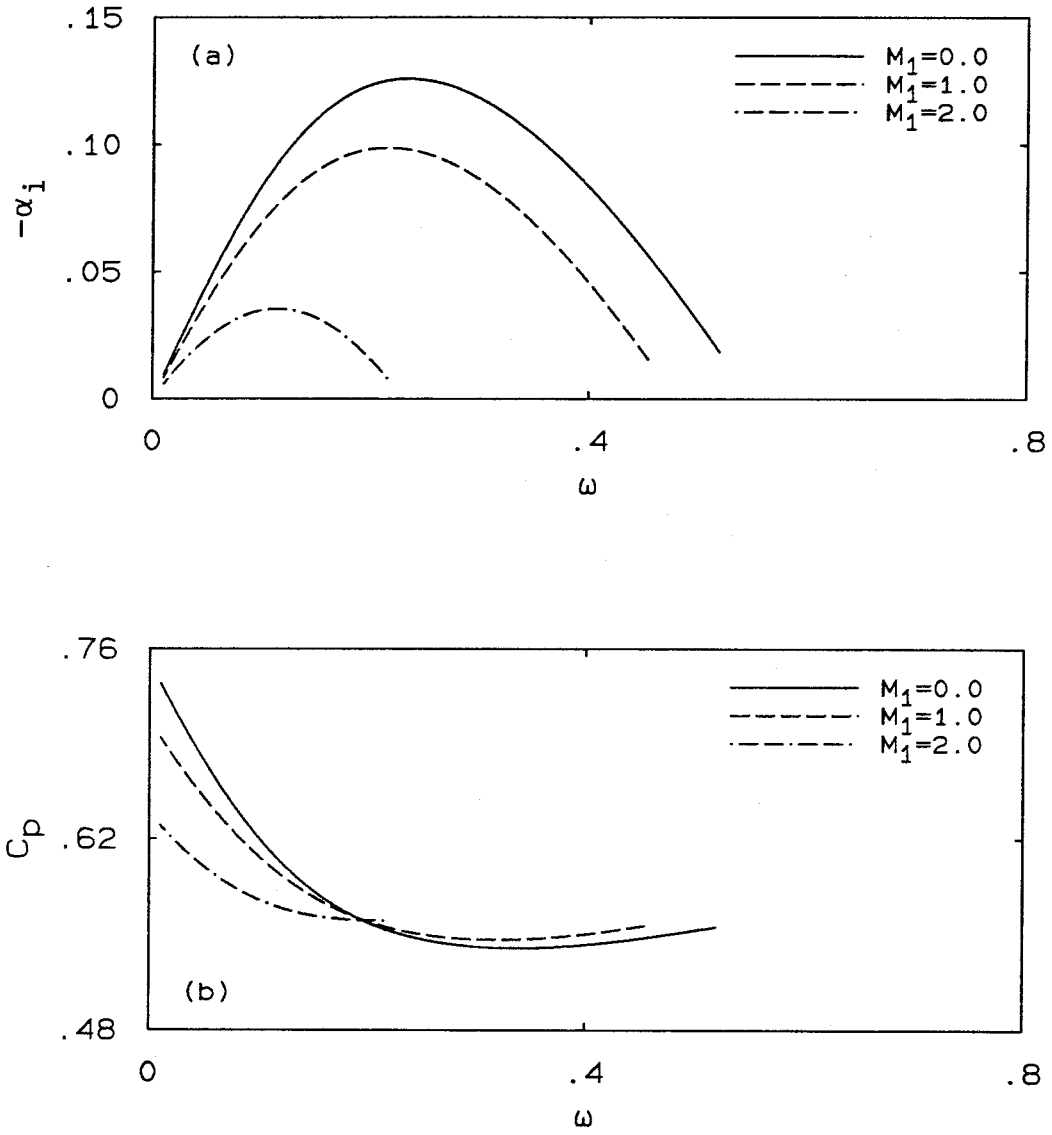

FIG. 4.1 Instability characteristics for the case $u_2/u_1 = 0.25$, $T_2/T_1 = 0.5$ and $R_2/R_1 = 1.0$ at subsonic disturbances. (a) The amplification rate $-\alpha_i$. (b) The phase velocity C_p.

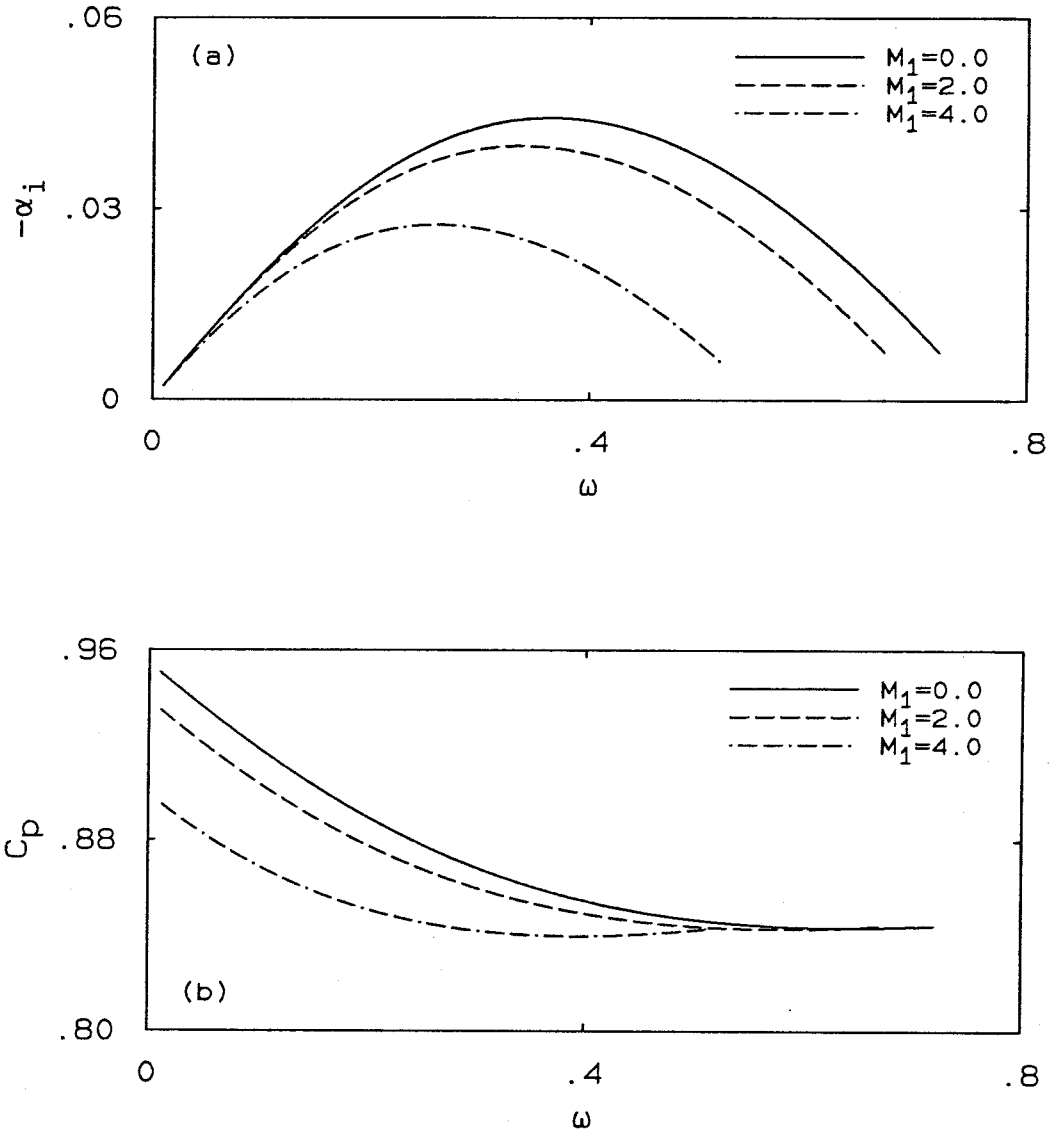

FIG. 4.2 Instability characteristics for the case $u_2/u_1 = 0.5$, $T_2/T_1 = 1.0$ and $R_2/R_1 = 5.0$ at subsonic disturbances. (a) The amplification rate $-\alpha_i$. (b) The phase velocity C_p.

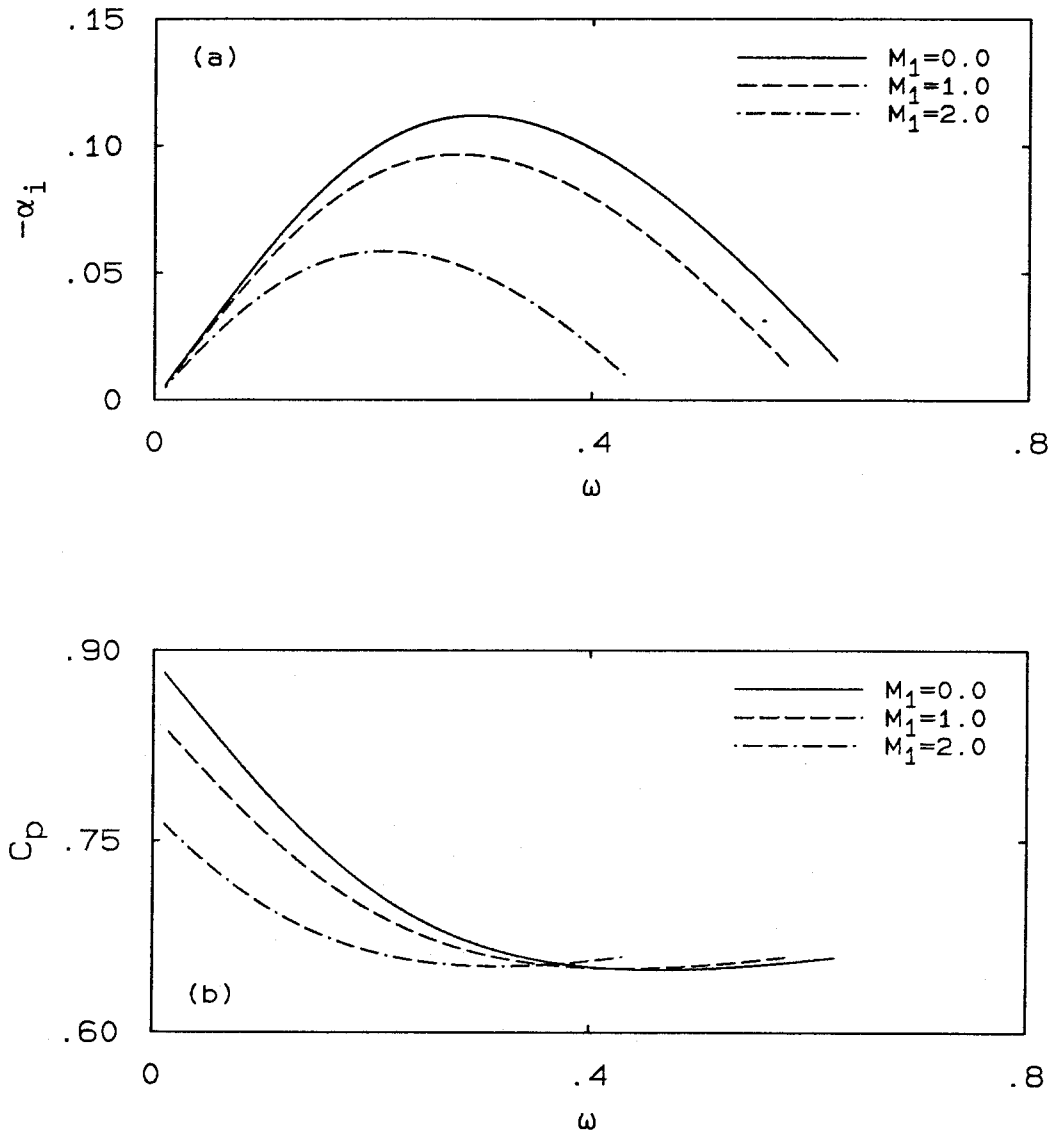

FIG. 4.3 Instability characteristics for the case $u_2/u_1 = 0.25$, $T_2/T_1 = 1.5$ and $R_2/R_1 = 1.0$ at subsonic disturbances. (a) The amplification rate $-\alpha_i$. (b) The phase velocity C_p.

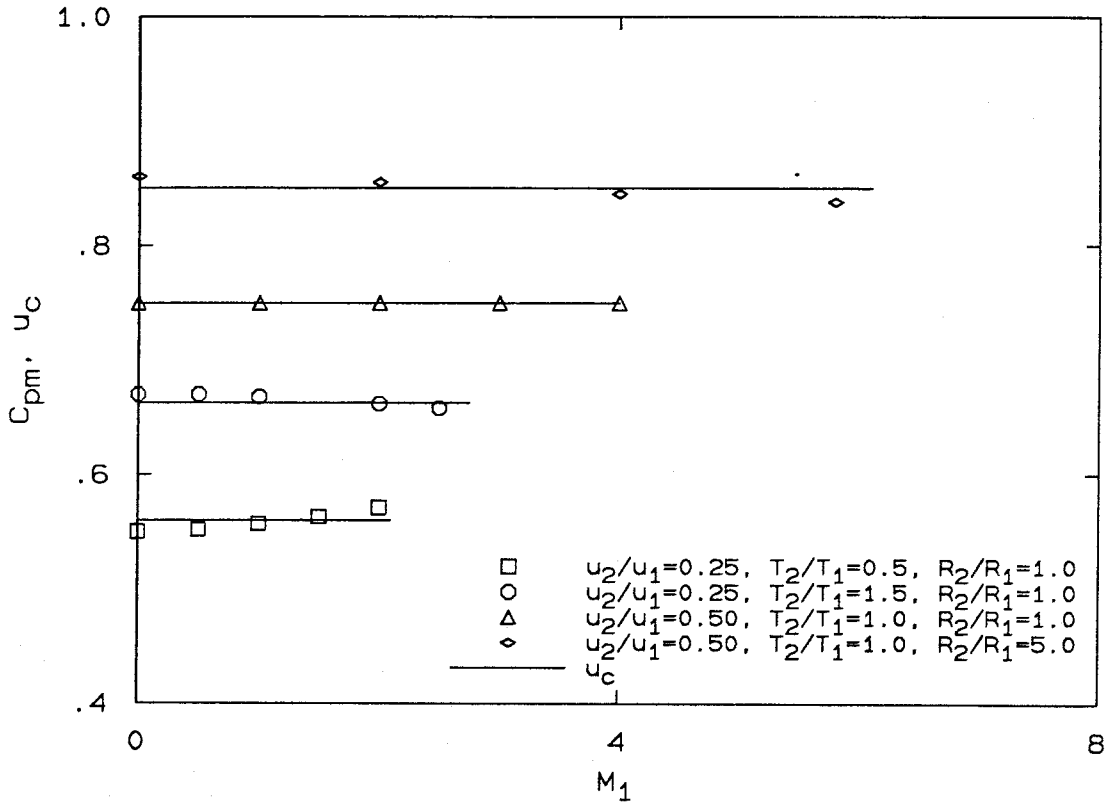

FIG. 4.4 Phase velocity of the most unstable mode C_{pm} and the convective velocity u_c *vs.* the free stream Mach number M_1 for subsonic disturbances.

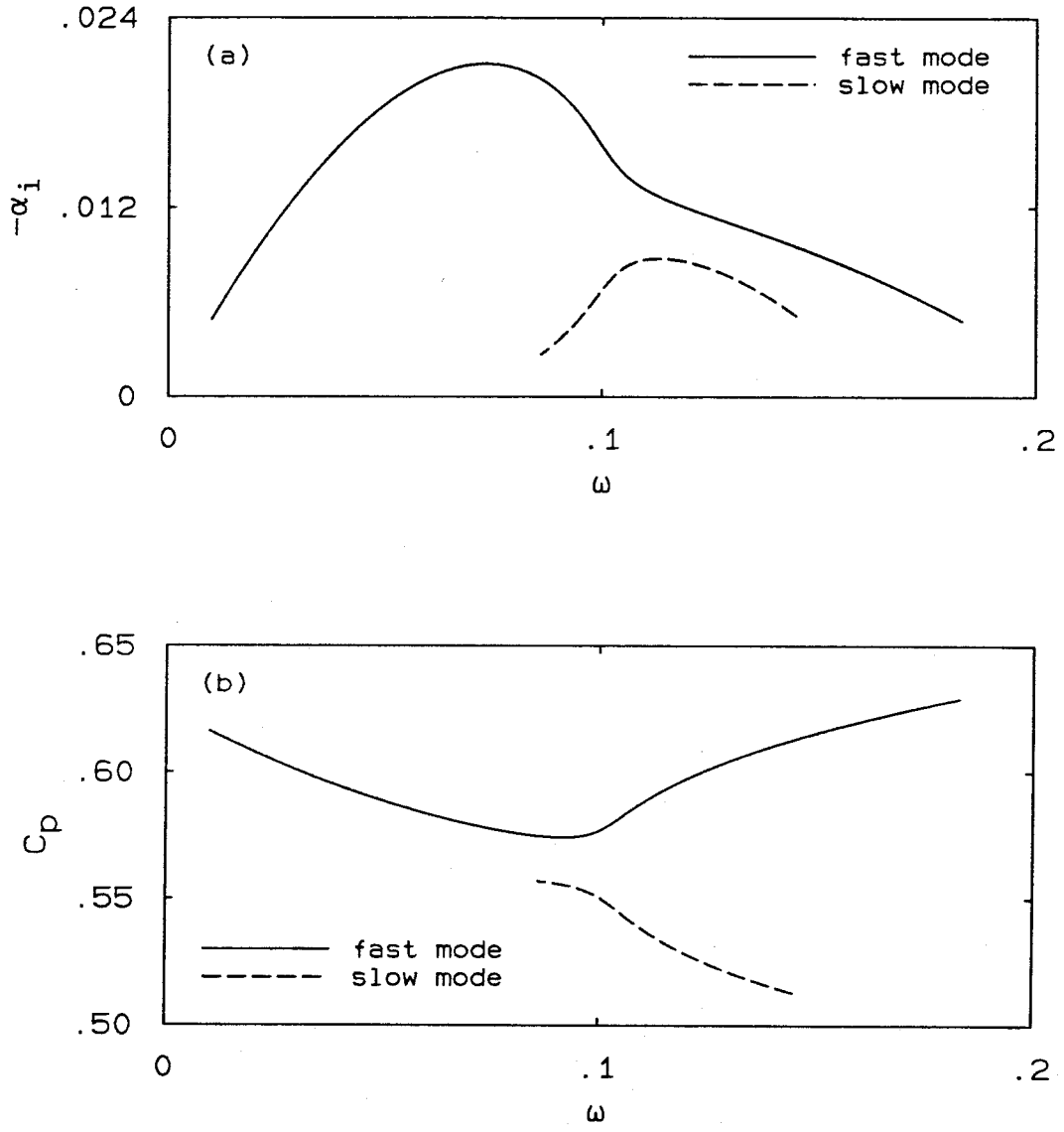

FIG. 4.5 Instability characteristics for the case $u_2/u_1 = 0.25$, $T_2/T_1 = 0.5$, $R_2/R_1 = 1.0$ and $M_1 = 2.25$ at supersonic disturbances. (a) The amplification rate $-\alpha_i$. (b) The phase velocity C_p.

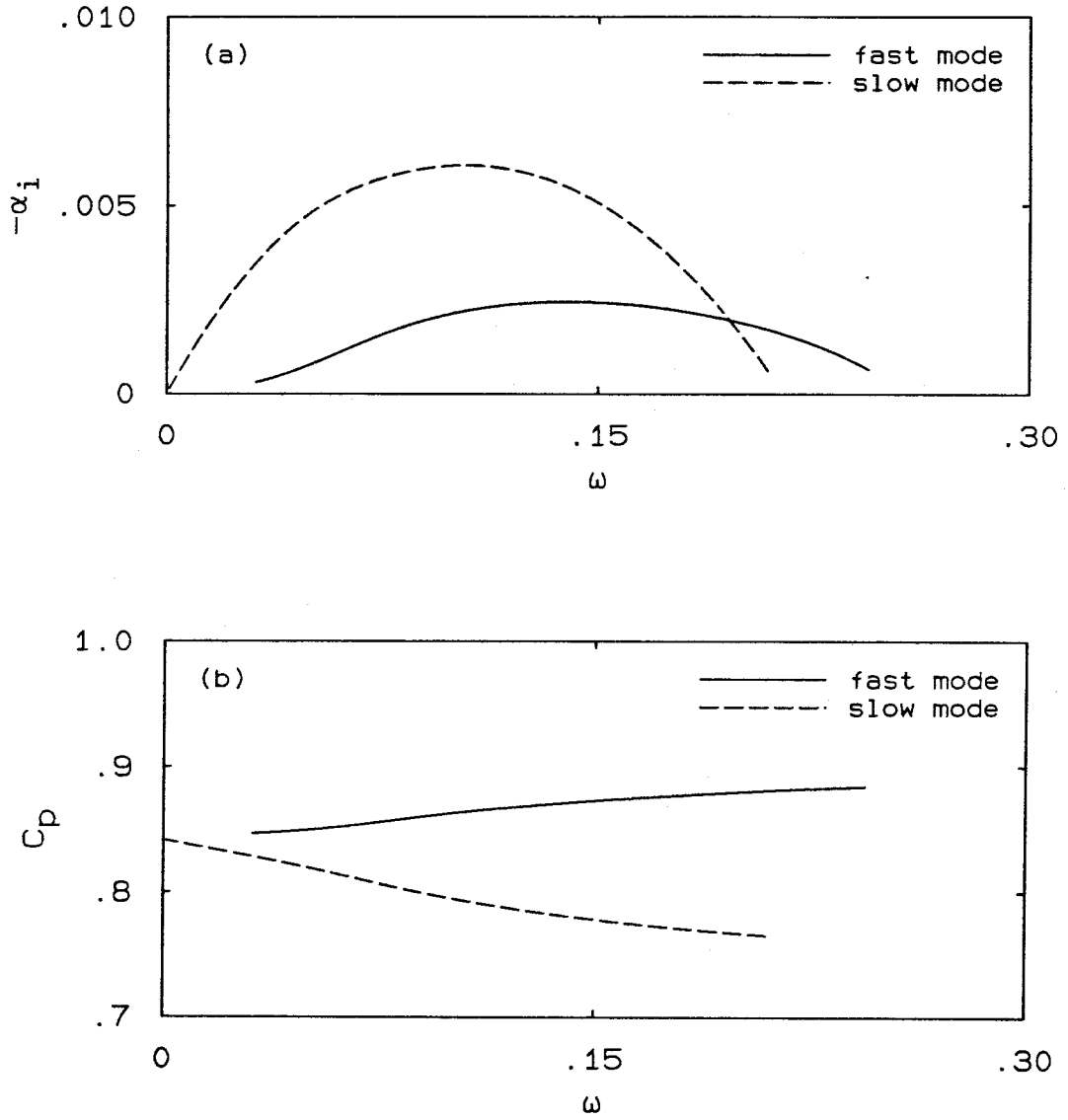

FIG. 4.6 Instability characteristics for the case $u_2/u_1 = 0.5$, $T_2/T_1 = 1.0$, $R_2/R_1 = 5.0$ and $M_1 = 7$ at supersonic disturbances. (a) The amplification rate $-\alpha_i$. (b) The phase velocity C_p.

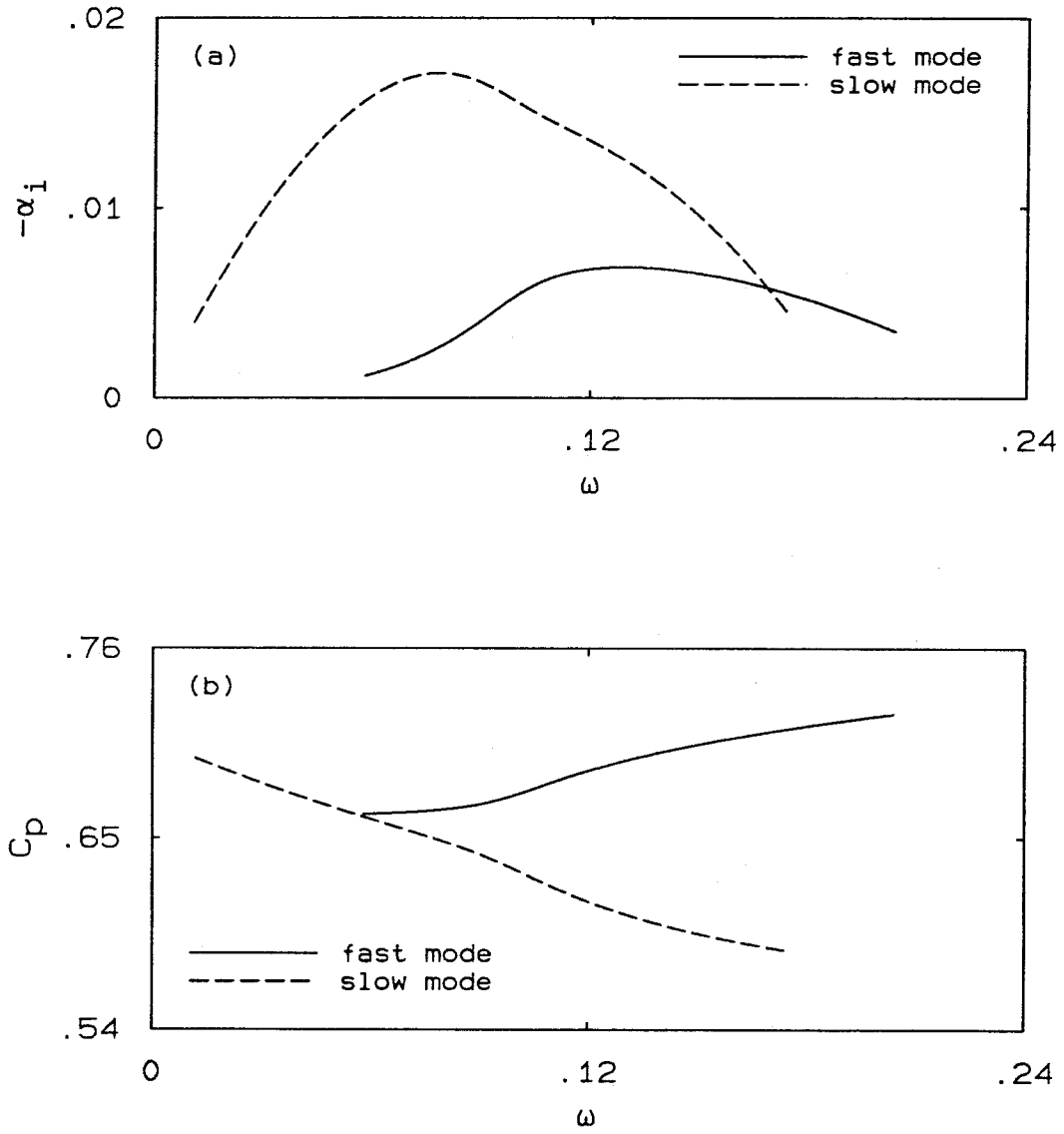

FIG. 4.7 Instability characteristics for the case $u_2/u_1 = 0.25, T_2/T_1 = 1.5, R_2/R_1 = 1.0$ and $M_1 = 3$ at supersonic disturbances. (a) The amplification rate $-\alpha_i$. (b) The phase velocity C_p.

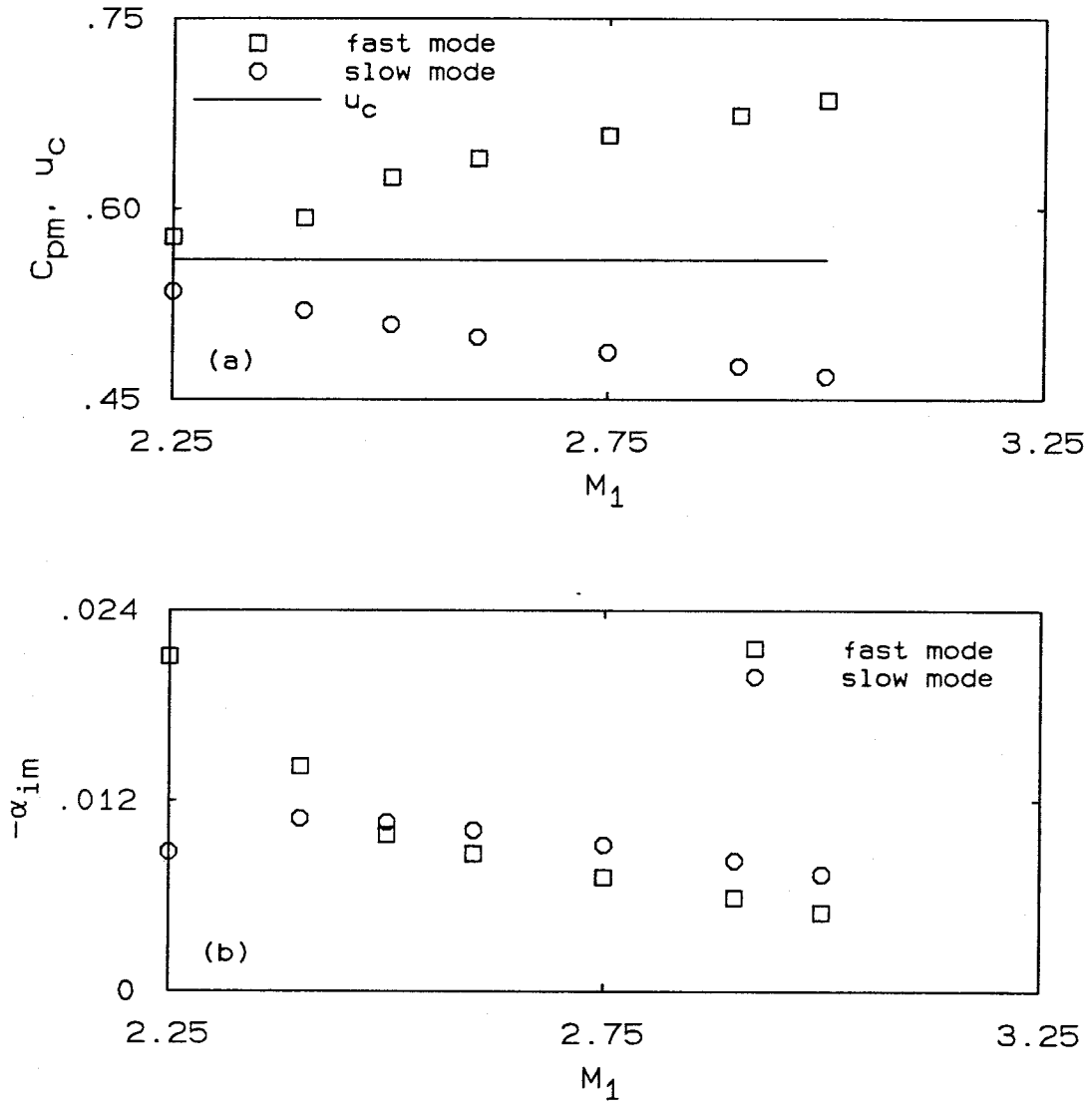

FIG. 4.8 Two-dimensional free mixing layers with supersonic disturbances: $u_2/u_1 = 0.25$, $T_2/T_1 = 0.5$, $R_2/R_1 = 1.0$. (a) The phase velocity of the most unstable mode C_{pm} and the convective velocity u_c *vs.* the free stream Mach number M_1. (b) The maximum amplification rate $-\alpha_{im}$ *vs.* the free stream Mach number M_1.

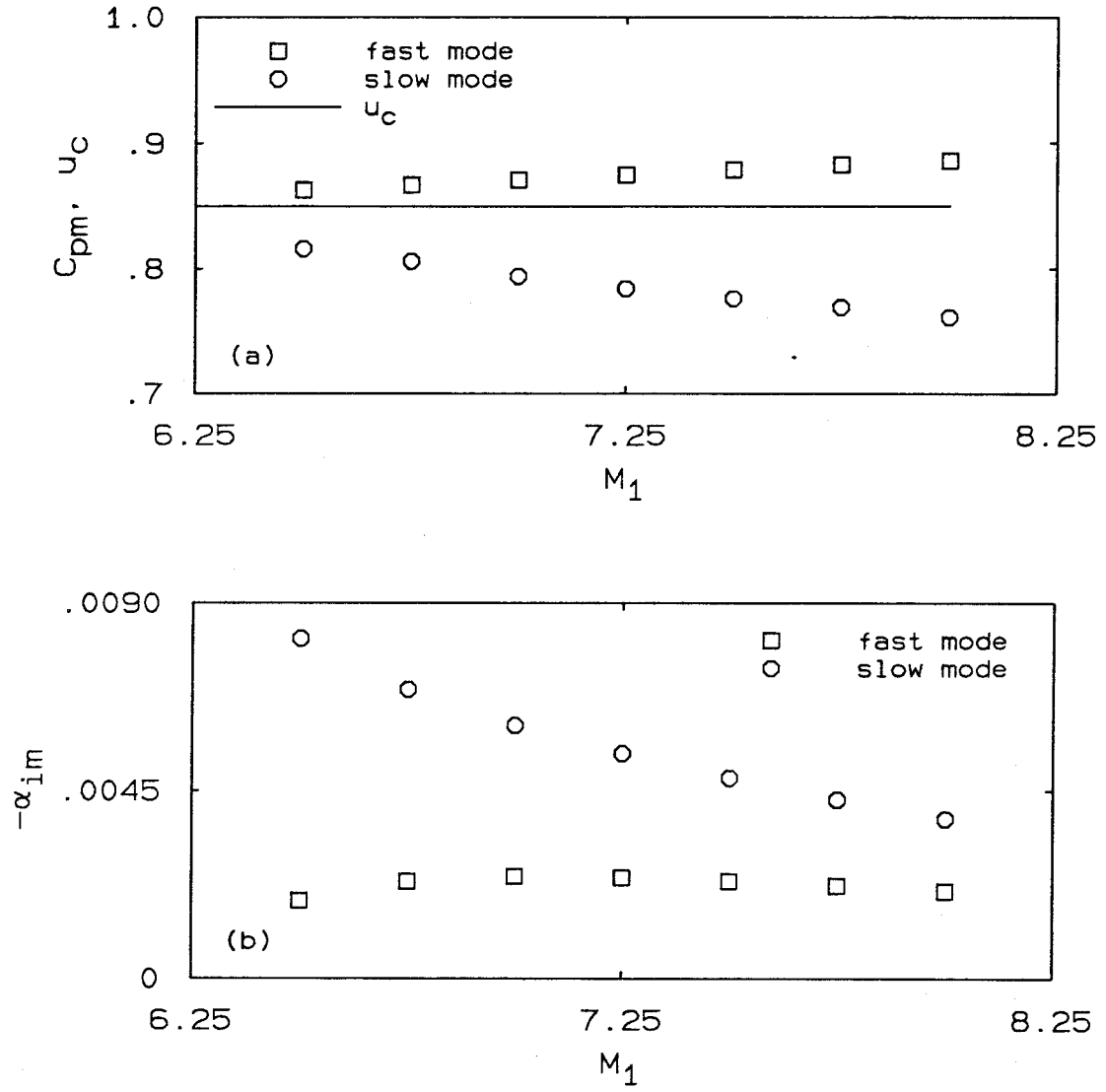

FIG. 4.9 Two-dimensional free mixing layer with supersonic disturbances: $u_2/u_1 = 0.5$, $T_2/T_1 = 1.0$ and $R_2/R_1 = 5.0$. (a) The phase velocity of the most unstable mode C_{pm} and the convective velocity u_c *vs.* the free stream Mach number M_1. (b) The maximum amplification rate $-\alpha_{im}$ *vs.* the free stream Mach number M_1.

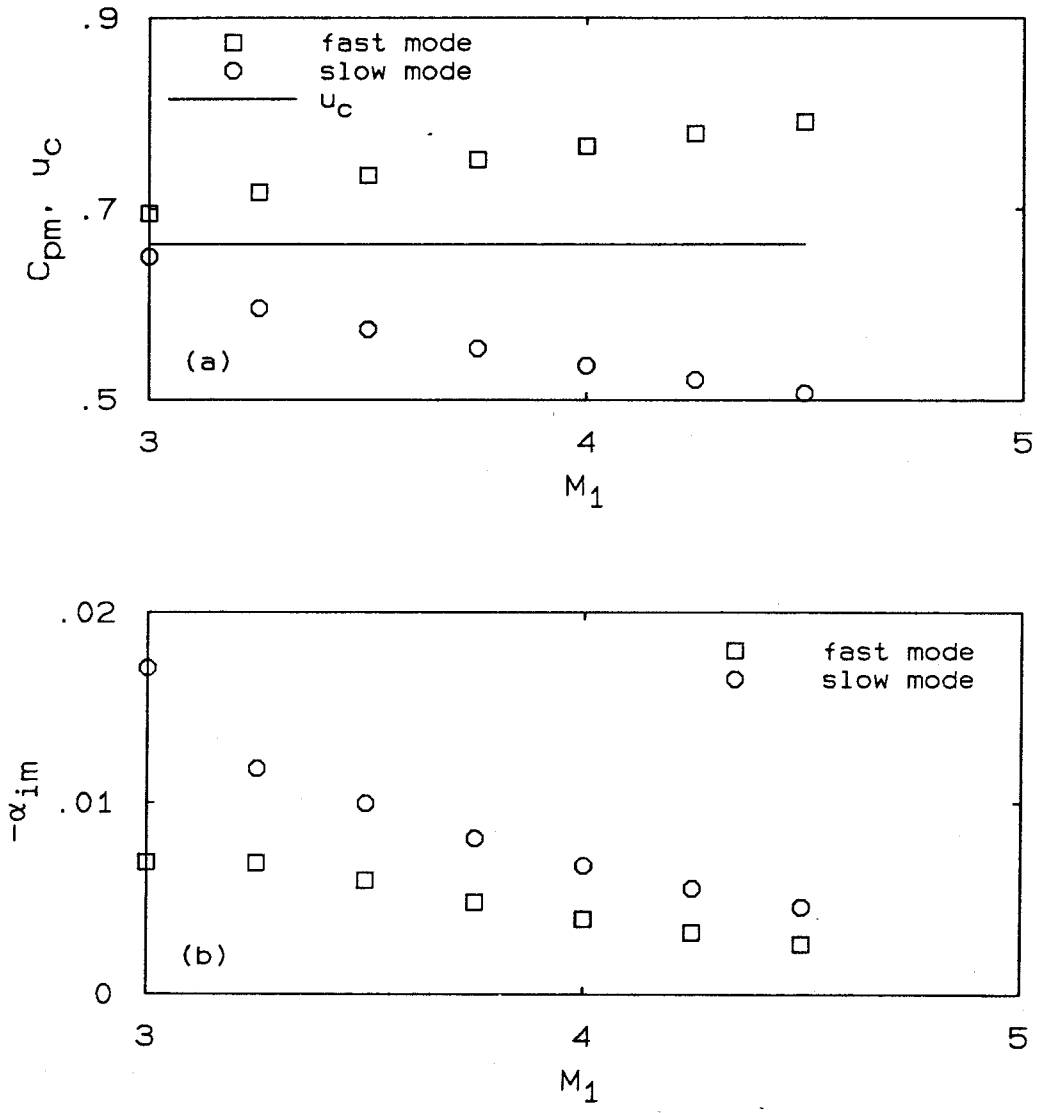

FIG. 4.10 Two-dimensional free mixing layer with supersonic disturbances: $u_2/u_1 = 0.25$, $T_2/T_1 = 1.5$, $R_2/R_1 = 1.0$. (a) The phase velocity of the most unstable mode C_{pm} and the convective velocity u_c *vs.* the free stream Mach number M_1. (b) The maximum amplification rate $-\alpha_{im}$ *vs.* the free stream Mach number M_1.

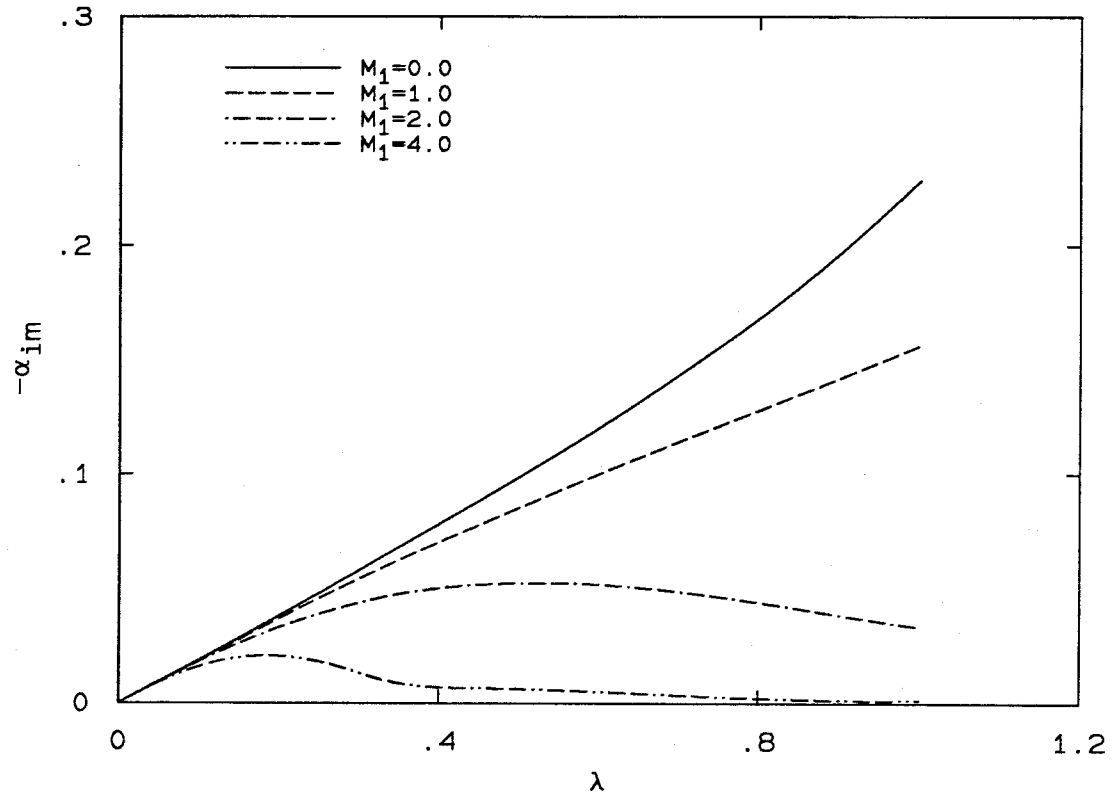

FIG. 4.11 The maximum amplification rate $-\alpha_{im}$ *vs.* $\lambda = (1 - u_2/u_1)/(1 + u_2/u_1)$, for the case $T_2/T_1 = 1.0$ and $R_2/R_1 = 1.0$.

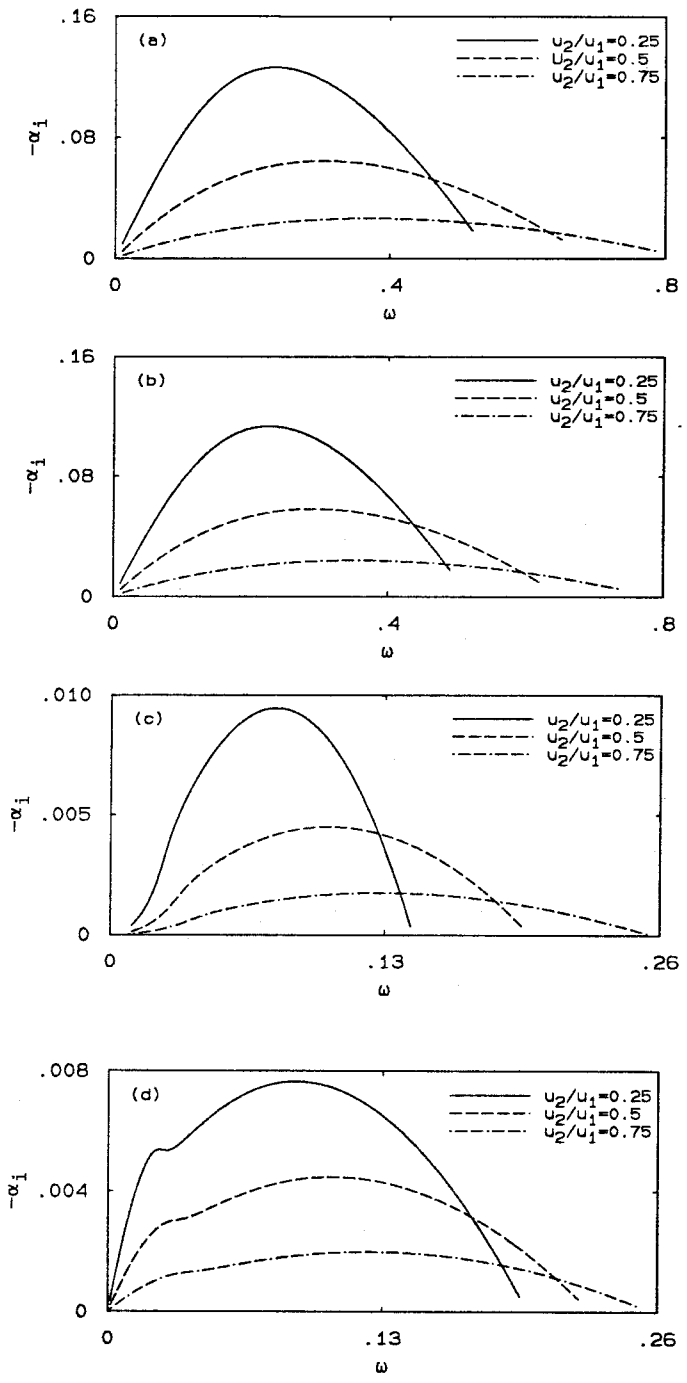

FIG. 4.12 The amplification rate: $T_2/T_1 = 0.5$ and $R_2/R_1 = 1.0$. (a) The subsonic mode $M_{c1} = 0$. (b) The subsonic mode $M_{c1} = 0.3$. (c) The slow supersonic mode $M_{c1} = 1.36$. (d) The fast supersonic mode $M_{c2} = 1.51$.

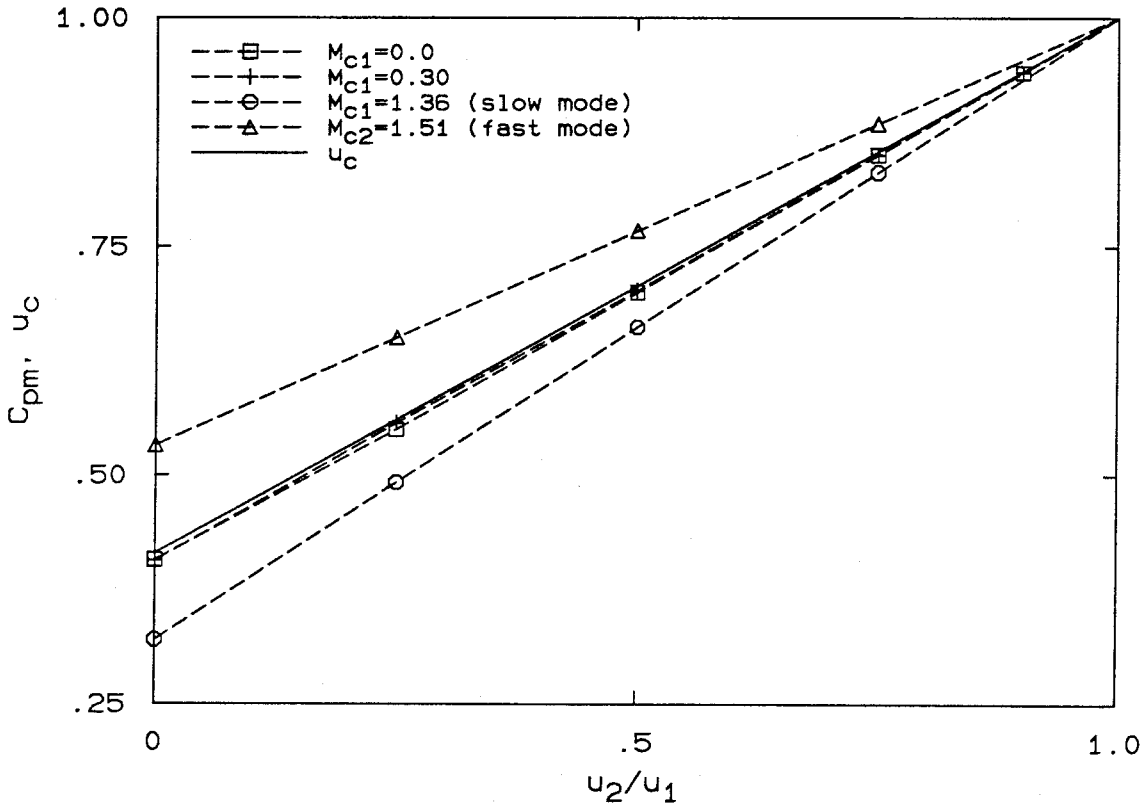

FIG. 4.13 Phase velocity of the most unstable mode C_{pm} and the convective velocity u_c *vs.* the velocity ratio u_2/u_1 for the case $T_2/T_1 = 0.5$ and $R_2/R_1 = 1.0$.

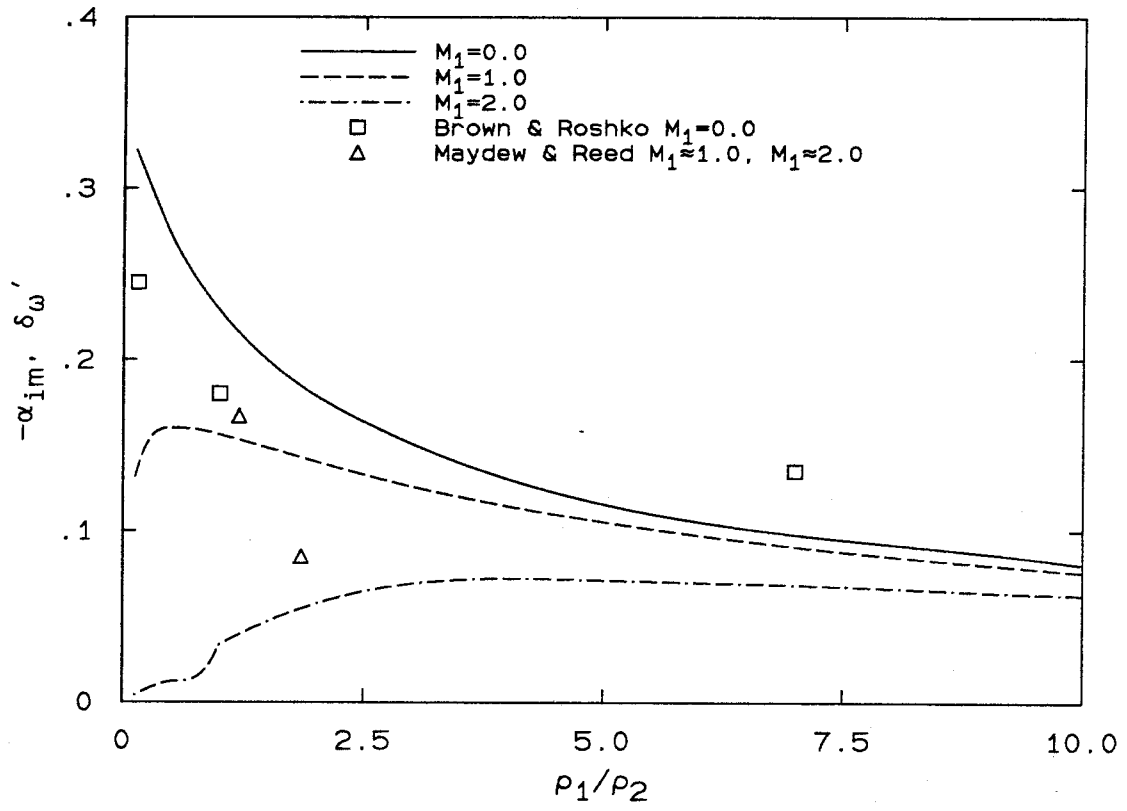

FIG. 4.14 Growth rate plotted against the density ratio ρ_1/ρ_2, for the case $u_2/u_1 = 0$.

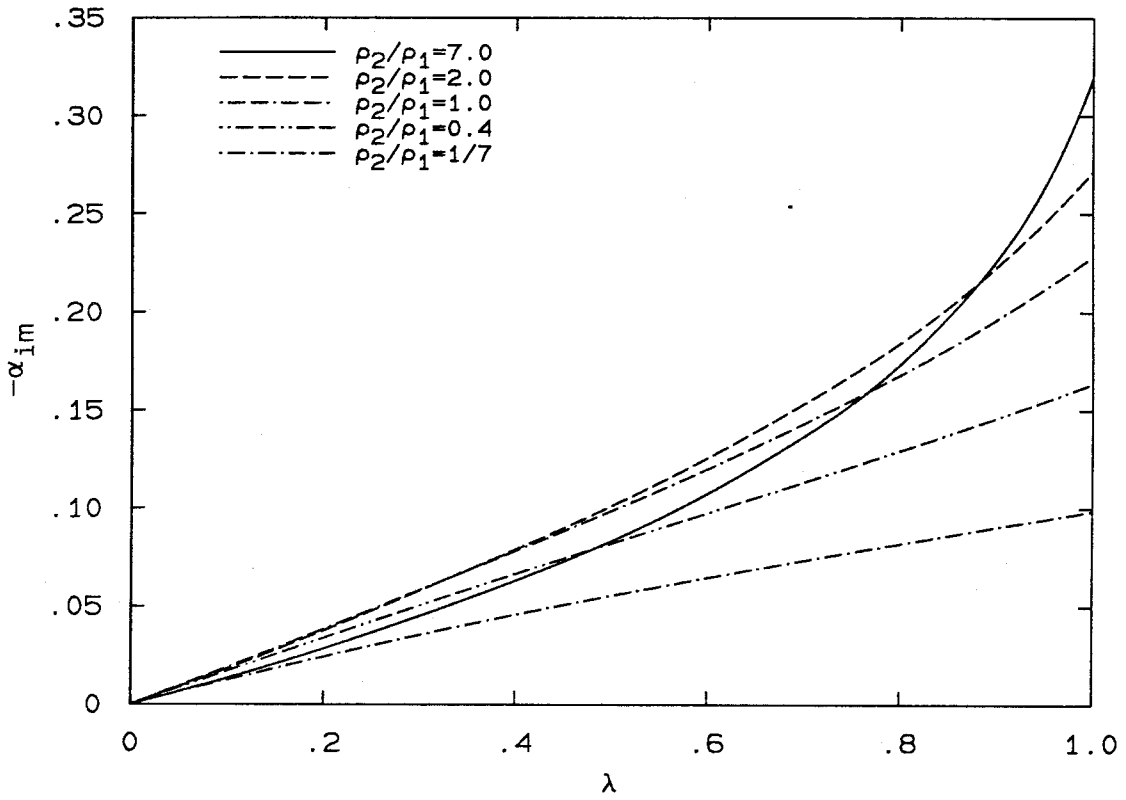

FIG. 4.15 Maximum amplification rate $-\alpha_{im}$ *vs.* $\lambda = (1 - u_2/u_1)/(1 + u_2/u_1)$.

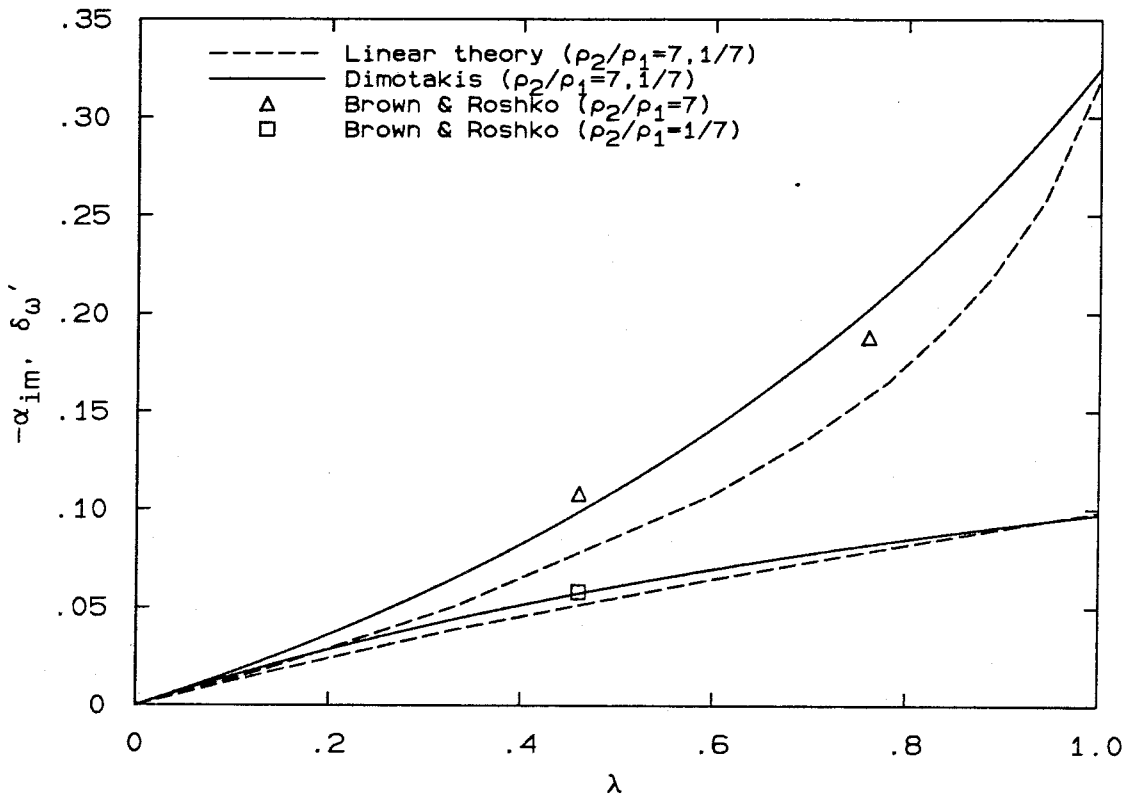

FIG. 4.16 Growth rate plotted against $\lambda = (1 - u_2/u_1)/(1 + u_2/u_1)$.

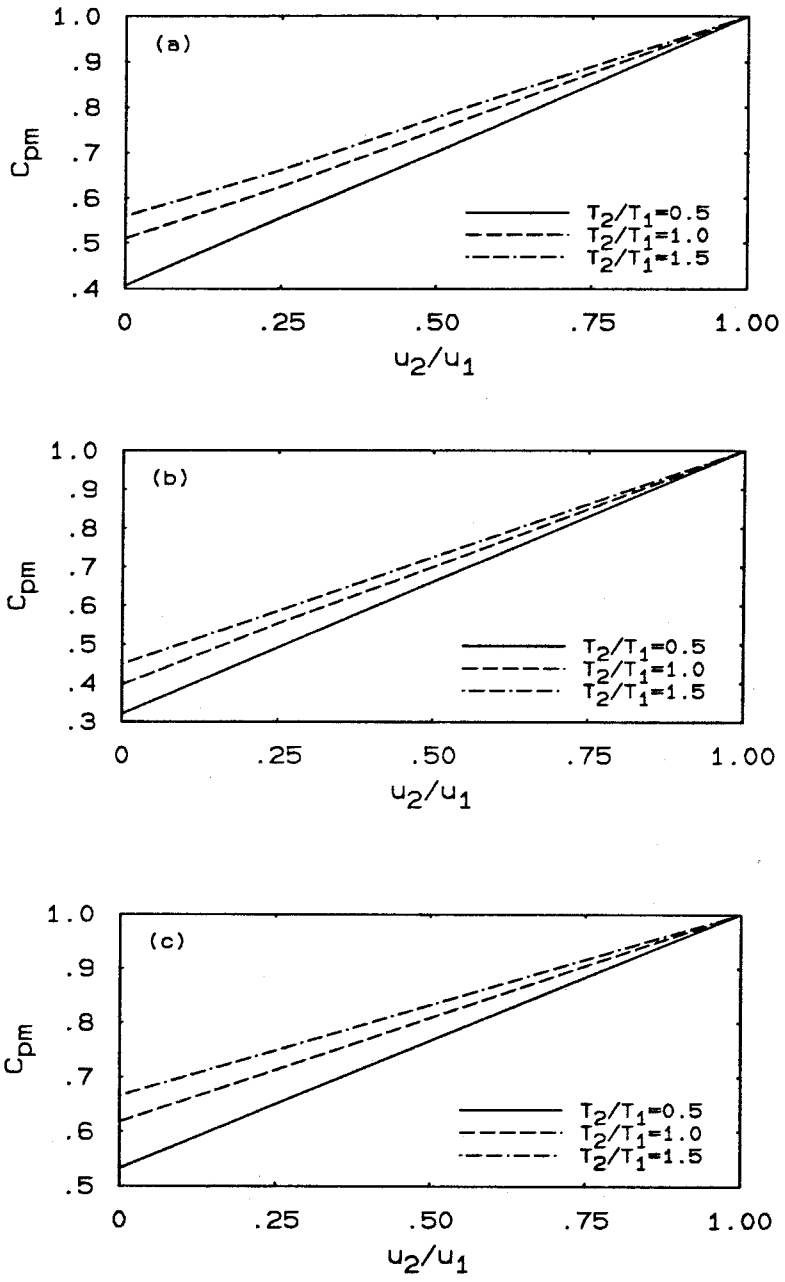

FIG. 4.17 Phase velocity of the most unstable mode C_{pm} *vs.* the velocity ratio u_2/u_1 for the case $R_2/R_1 = 1.0$. (a) The subsonic mode $M_{c1} = 0.3$. (b) The slow supersonic mode $M_{c1} = 1.36$. (c) The fast supersonic mode $M_{c2} = 1.51$.

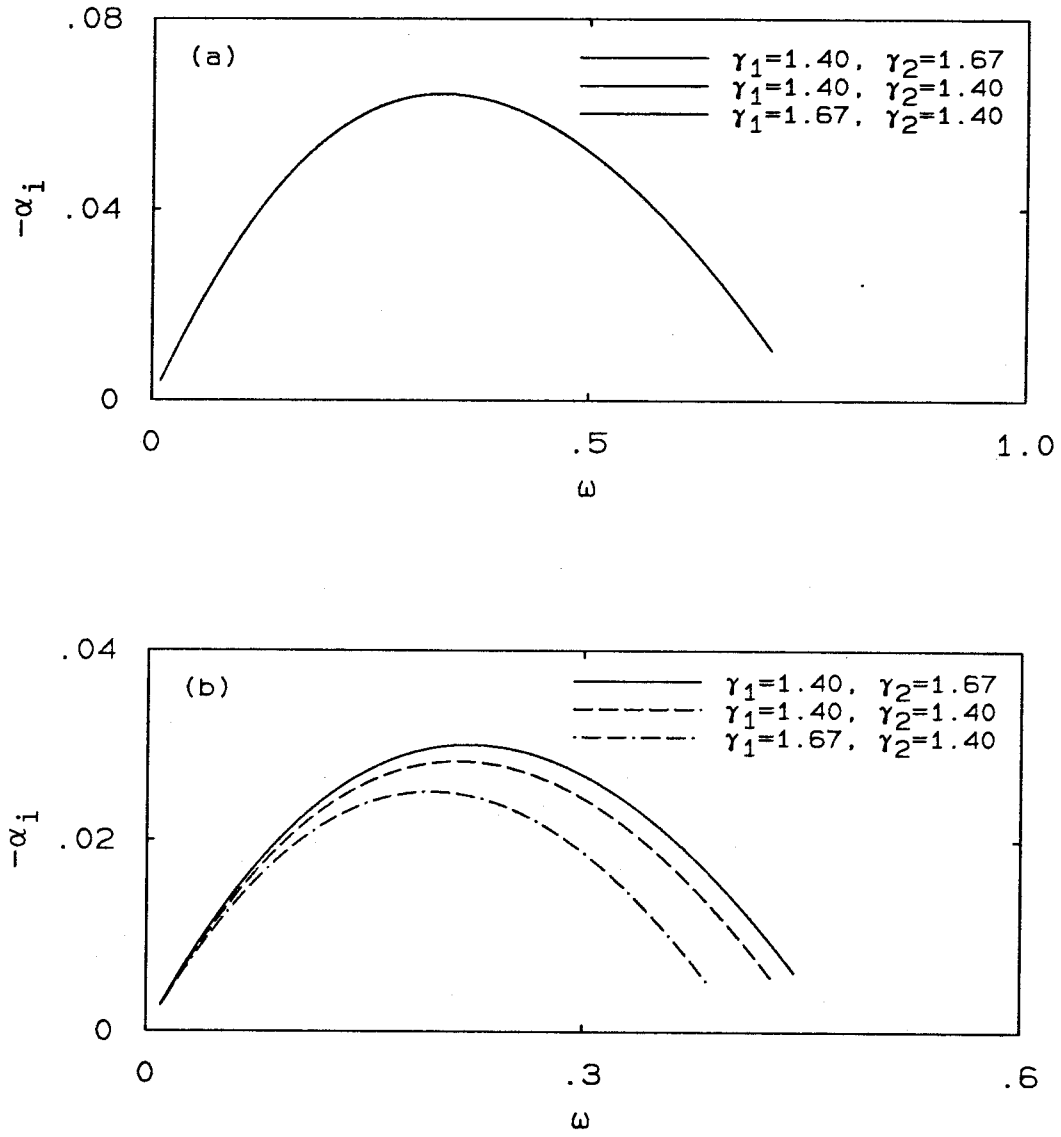

FIG. 4.18 The amplification rate: $u_2/u_1 = 0.5$, $T_2/T_1 = 1.0$ and $R_2/R_1 = 1.0$. (a) The subsonic mode $M_{c1} = 0.0$. (b) The subsonic mode $M_{c1} = 0.75$.

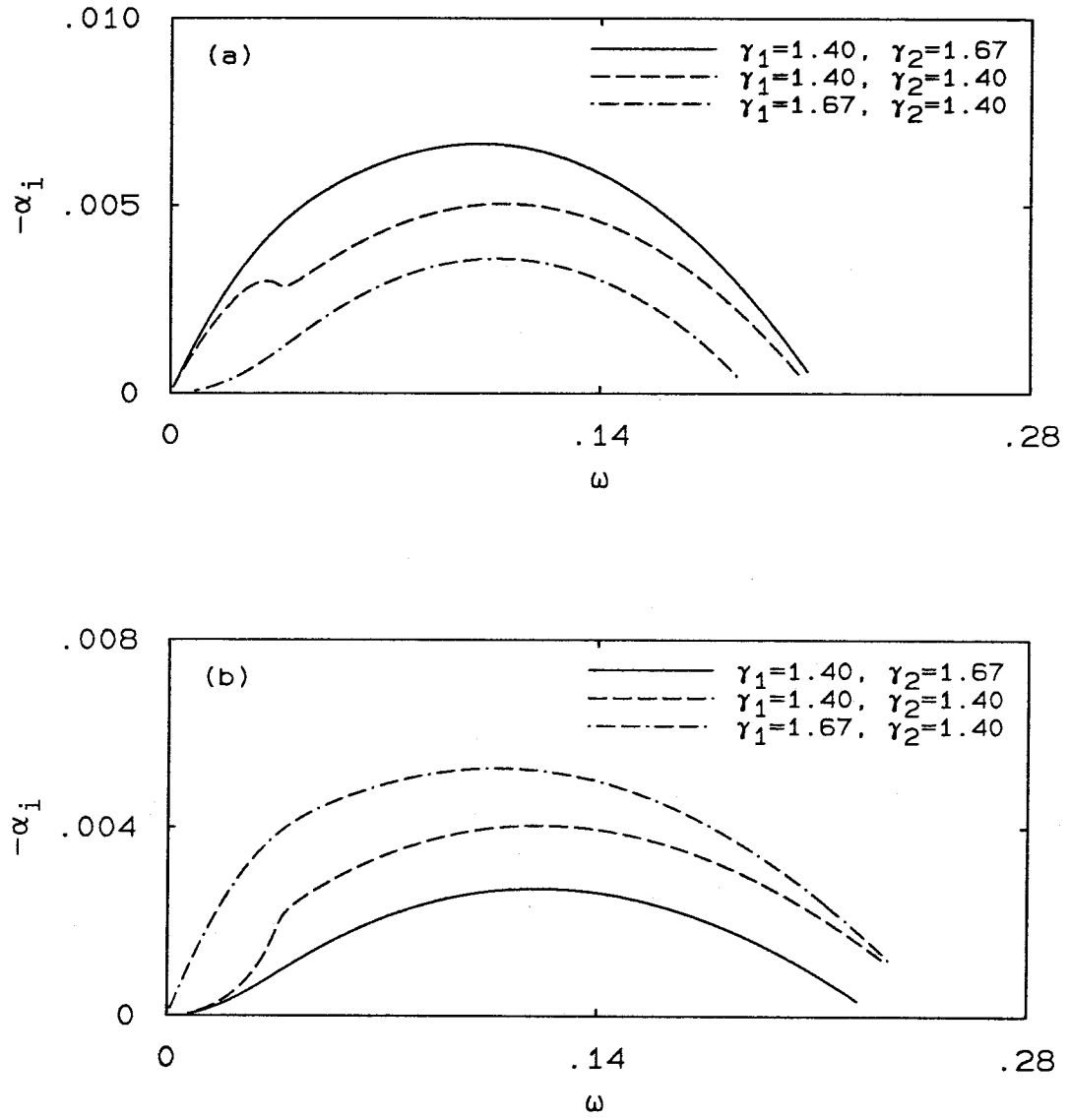

FIG. 4.19 The amplification rate: $u_2/u_1 = 0.5$, $T_2/T_1 = 1.0$ and $R_2/R_1 = 1.0$. (a) The slow supersonic mode $M_{c1} = 1.40$. (b) The fast supersonic mode $M_{c2} = 1.42$.

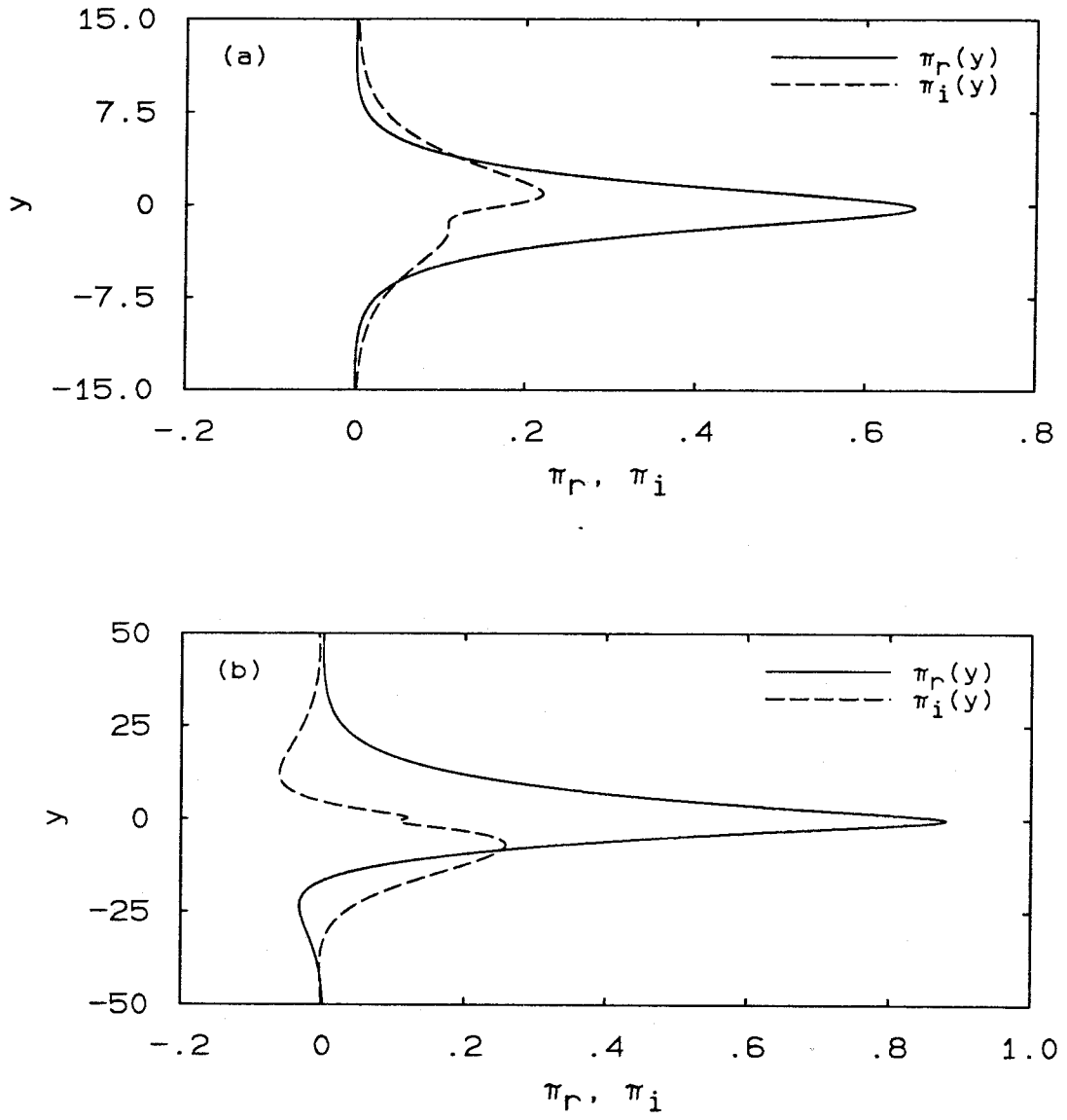

FIG. 4.20 Eigenfunction of the pressure disturbances $\pi(y) = \pi_r(y) + i\pi_i(y)$ for subsonic disturbances: $u_2/u_1 = 0.25$, $T_2/T_1 = 0.5$ and $R_2/R_1 = 1.0$. (a) $M_1 = 0$. (b) $M_1 = 2$.

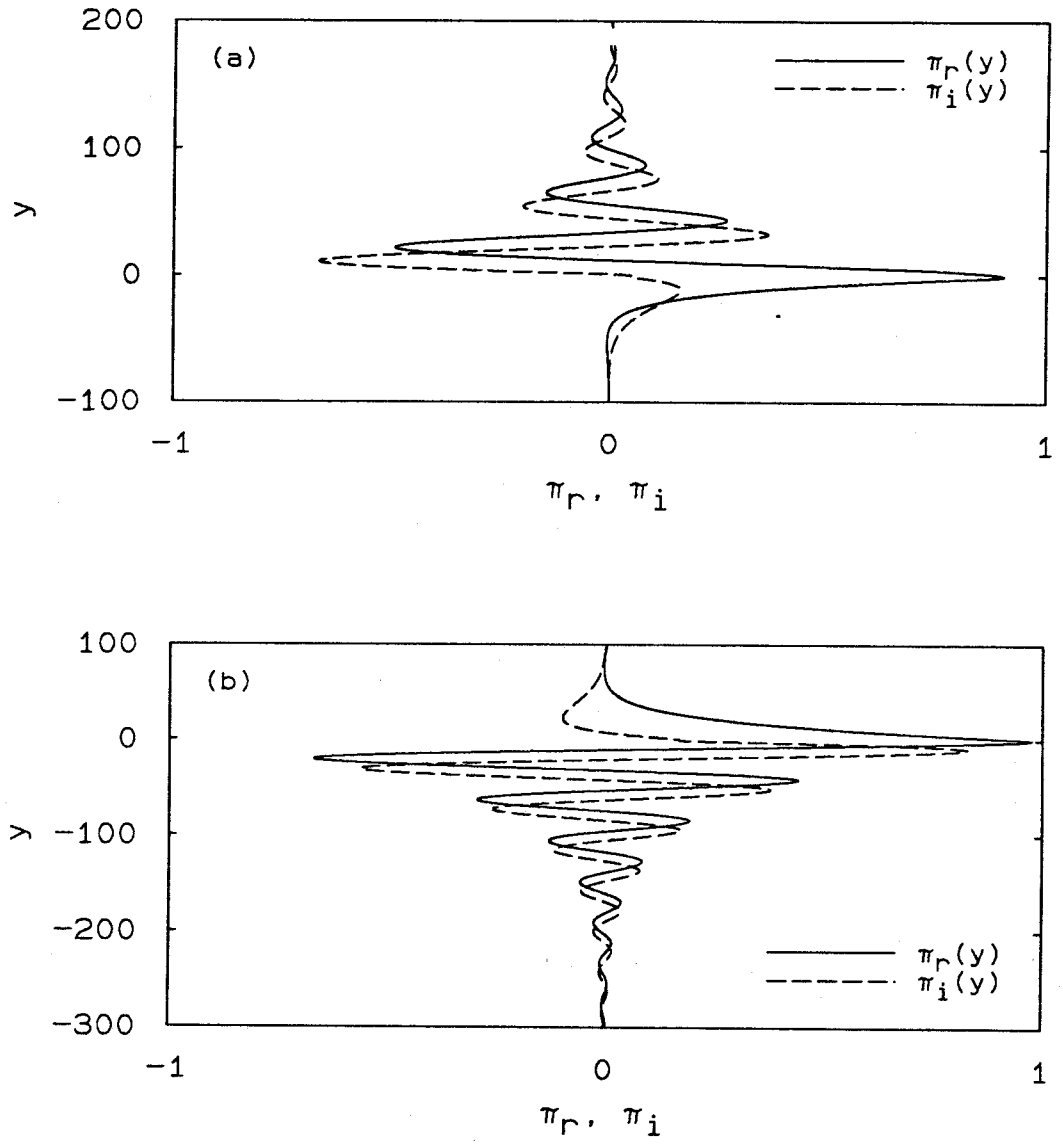

FIG. 4.21 Eigenfunction of the pressure disturbances $\pi(y) = \pi_r(y) + i\pi_i(y)$ for supersonic disturbances: $u_2/u_1 = 0.25$, $T_2/T_1 = 0.5$ and $R_2/R_1 = 1.0$. (a) The supersonic slow mode $M_1 = 2.6$. (b) The supersonic fast mode $M_1 = 2.6$.

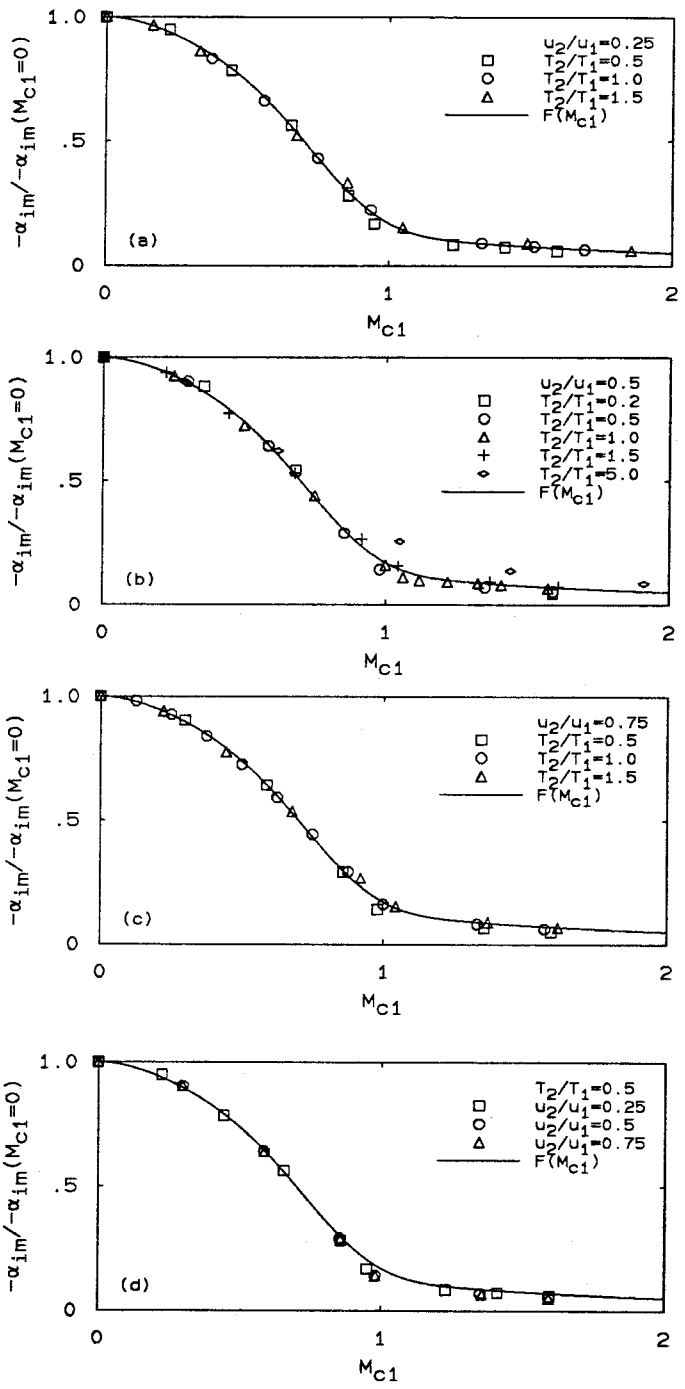

FIG. 4.22 Normalized maximum amplification rate *vs.* M_{c1}. (a) - (f) $R_2/R_1 = 1.0$ and $\gamma_1 = \gamma_2 = 1.4$. (g) $T_2/T_1 = 1.0$ and $\gamma_1 = \gamma_2 = 1.4$. (h) $T_2/T_1 = 1.0$ and $R_2/R_1 = 1.0$.

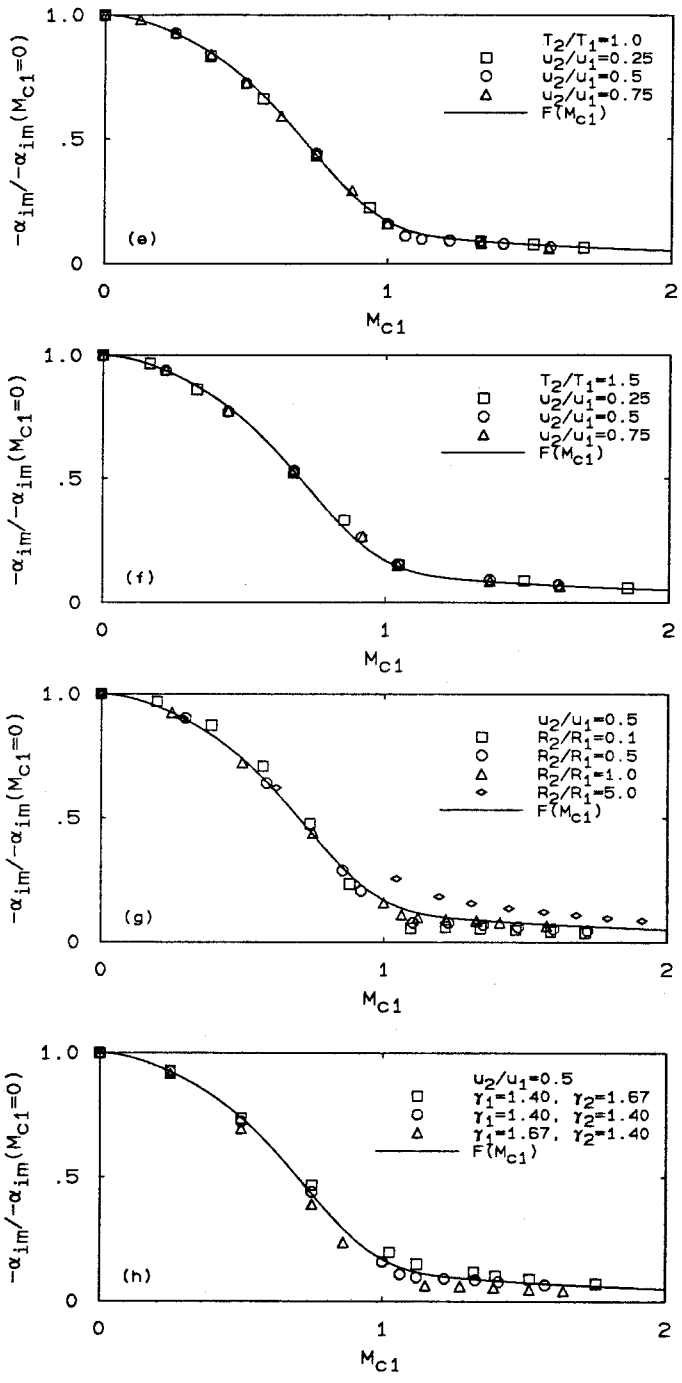

FIG. 4.22 Continued.

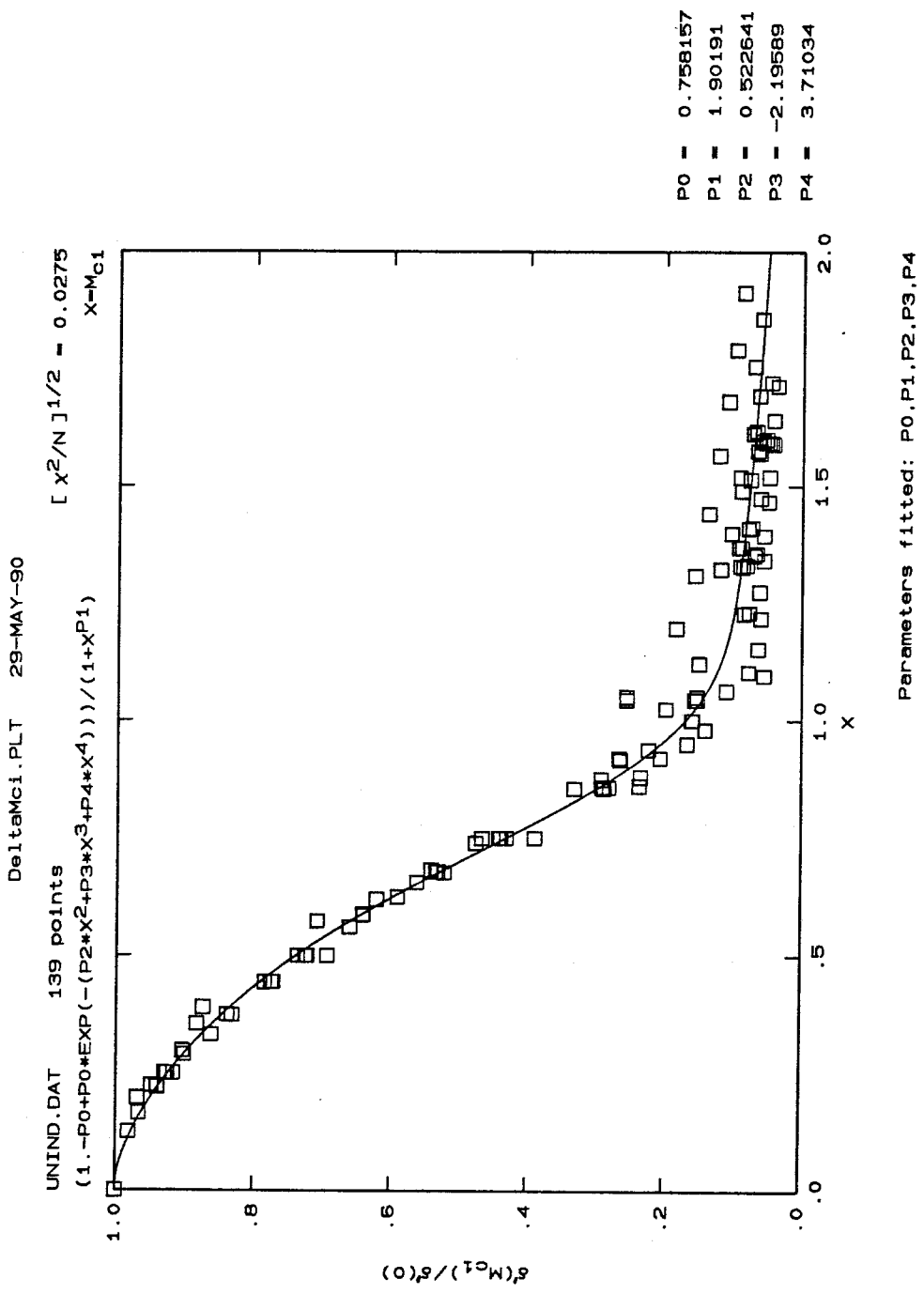

FIG. 4.23 Least squares fitting the normalized maximum amplification rate *vs.* the convective Mach number M_{c1}.

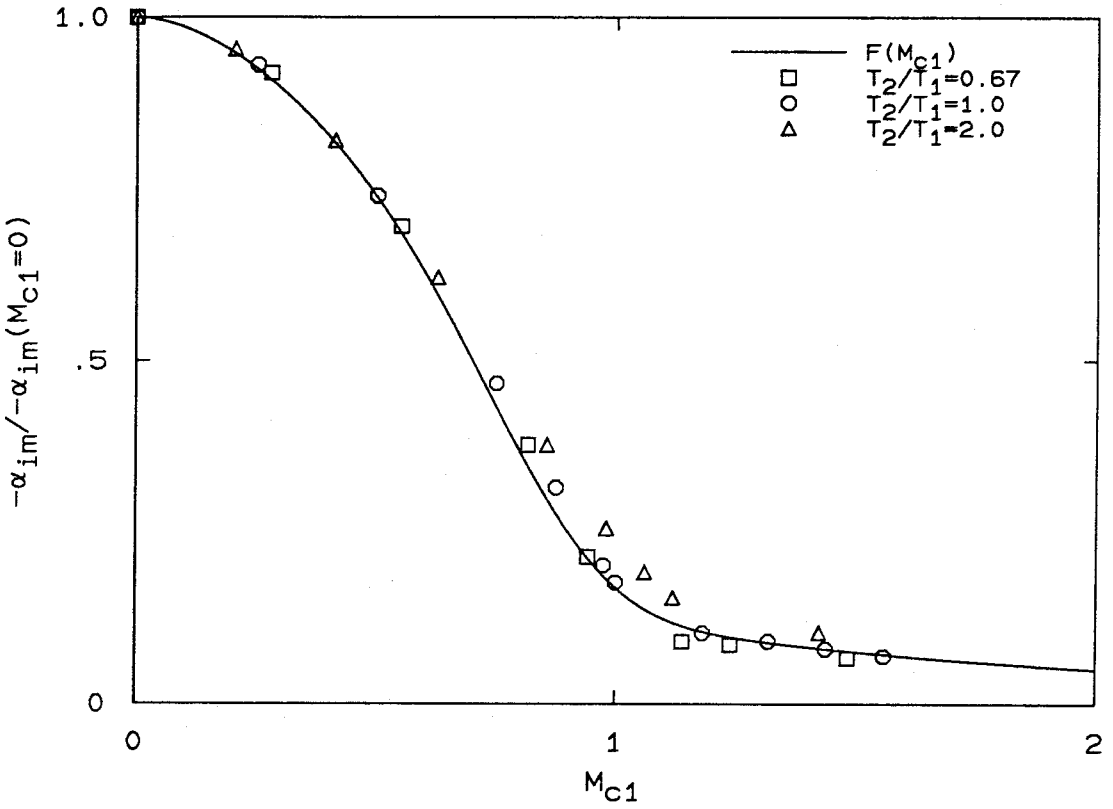

FIG. 4.24 Normalized maximum amplification rate *vs.* M_{c1} for hyperbolic tangent mean temperature profiles comparison with $F(M_{c1})$.

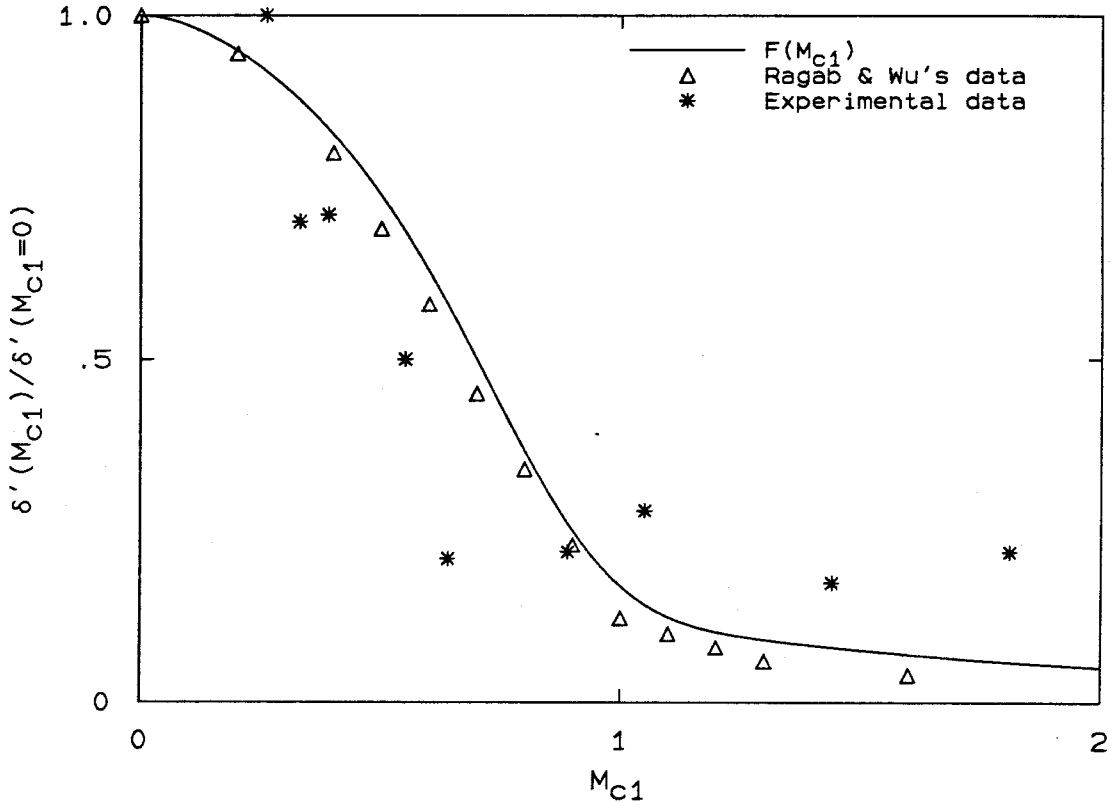

FIG. 4.25 A comparison of $F(M_{c1})$ with Ragab & Wu's numerical data and with Papamoschou & Roshko's experimental data.

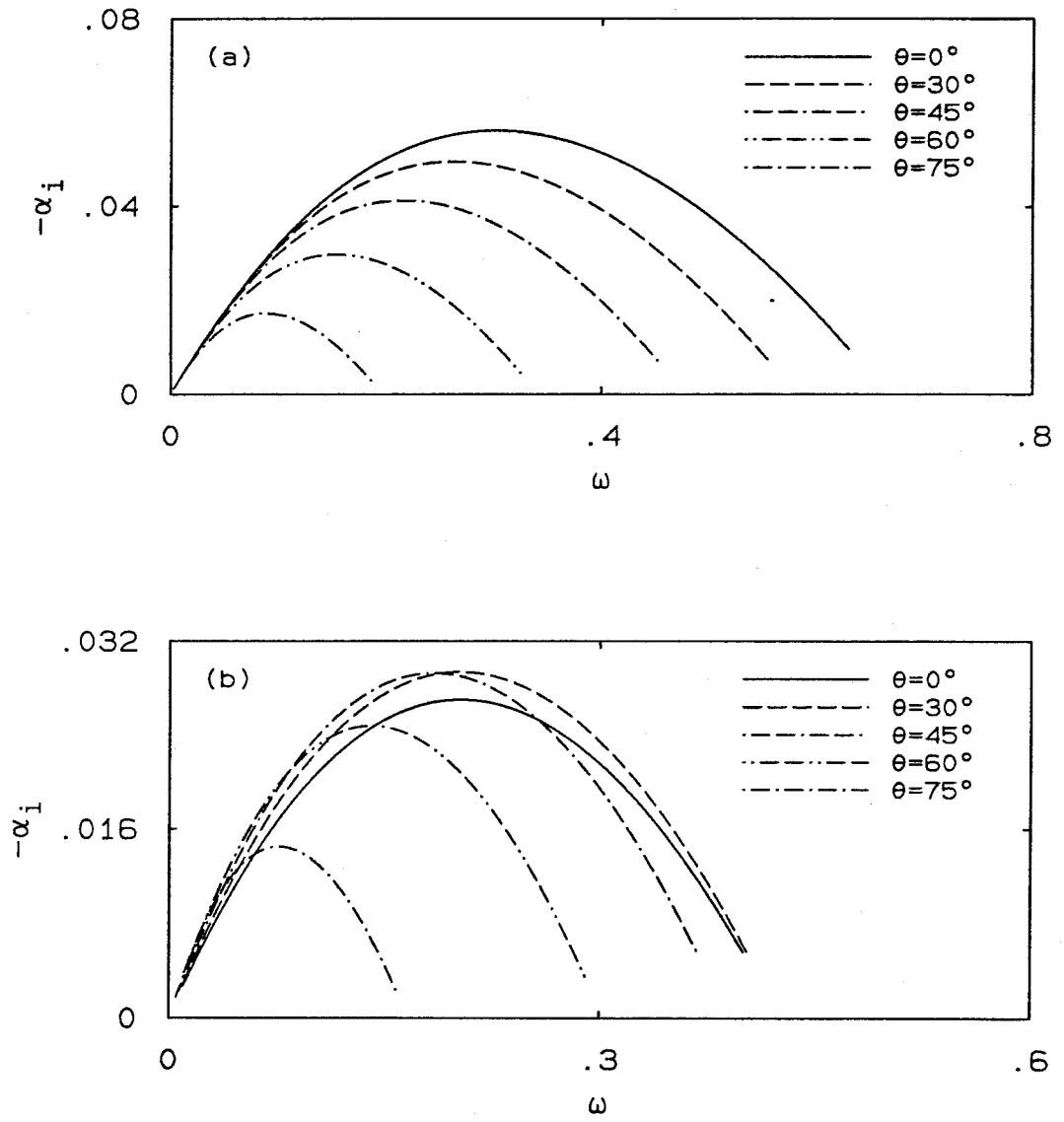

FIG. 4.26 Amplification rate for 3-D disturbances: $u_2/u_1 = 0.5$, $T_2/T_1 = 2.0$ and $R_2/R_1 = 0.5$. (a) $M_{c1} = 0.25$. (b) $M_{c1} = 0.75$.

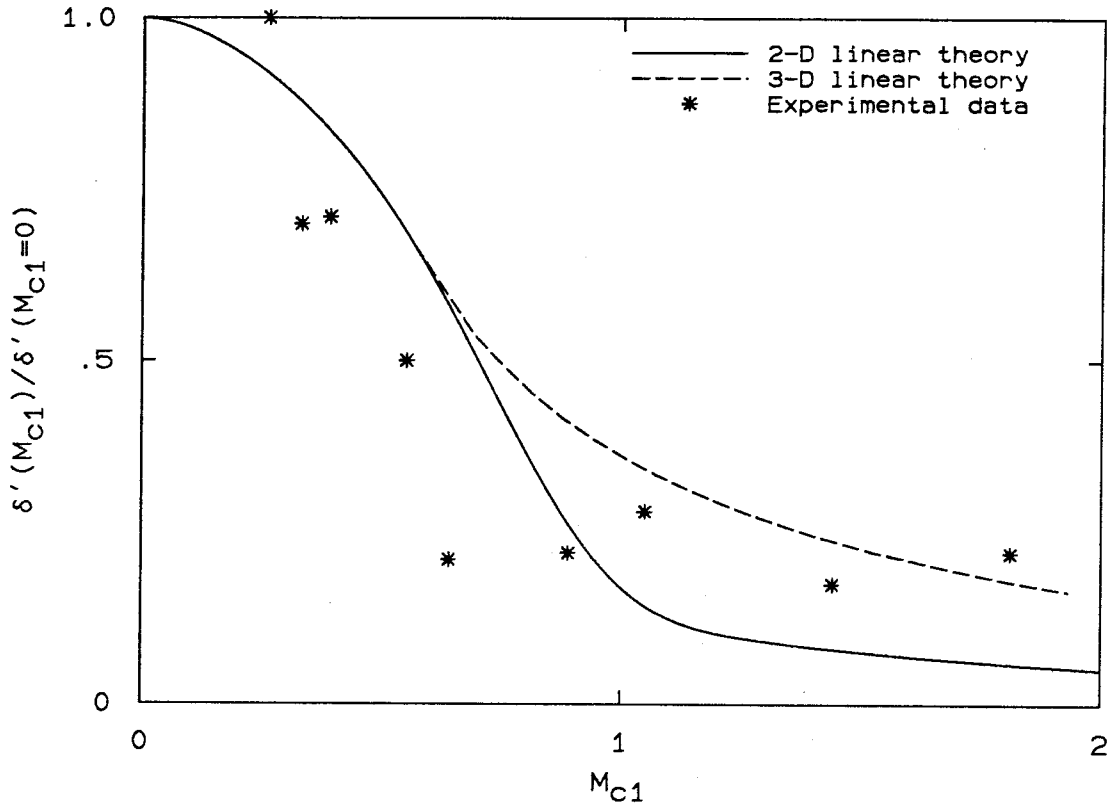

FIG. 4.27 Normalized growth rate *vs.* M_{c1}.

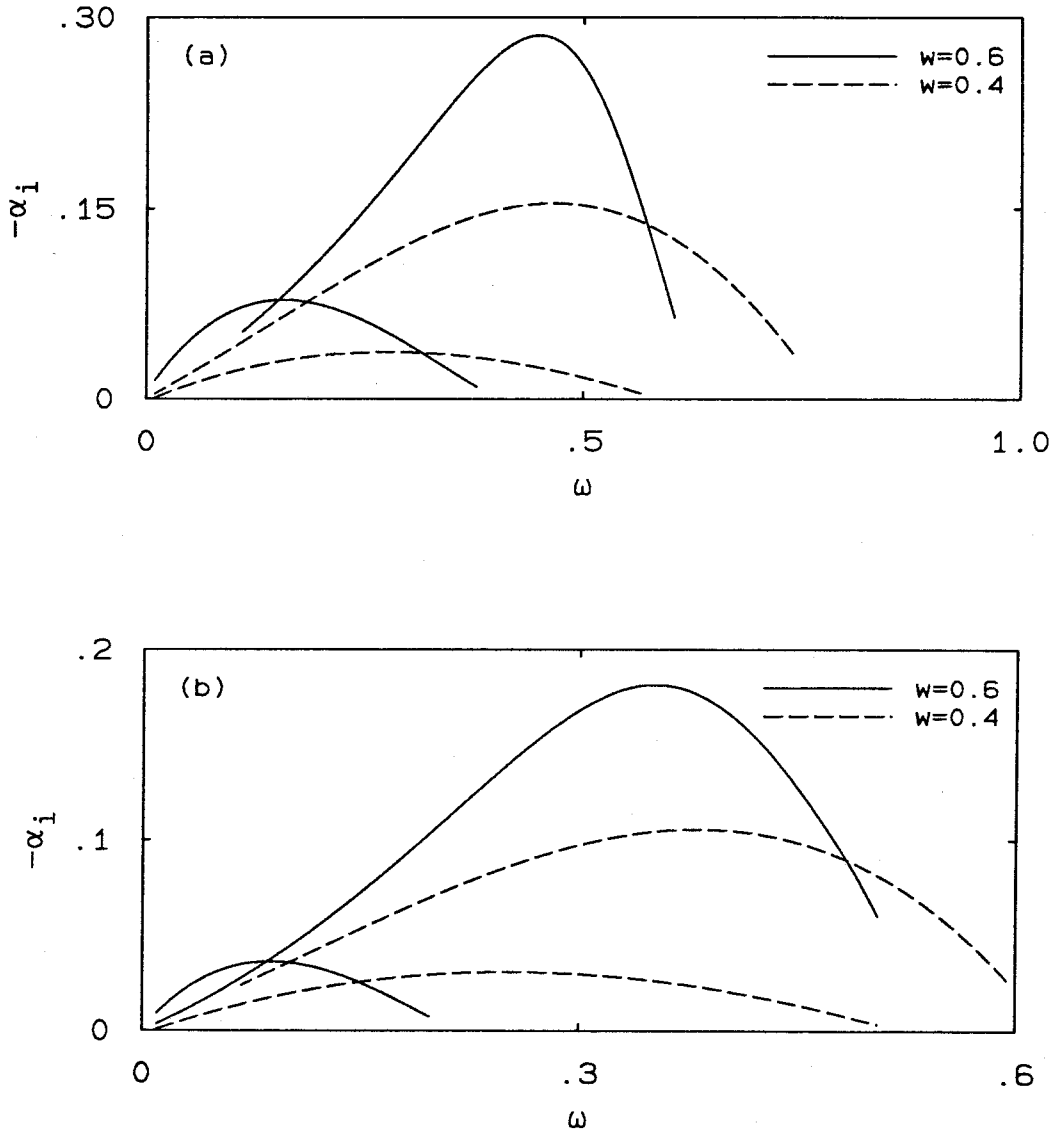

FIG. 4.28 Instability characteristics of the shear layer mode and the wake mode for different values of the normalized wake deficit w: $u_2/u_1 = 0.5$, $T_2/T_1 = 1.0$ and $R_2/R_1 = 1.0$. (a) $M_1 = 1.0$. (b) $M_1 = 2.0$.

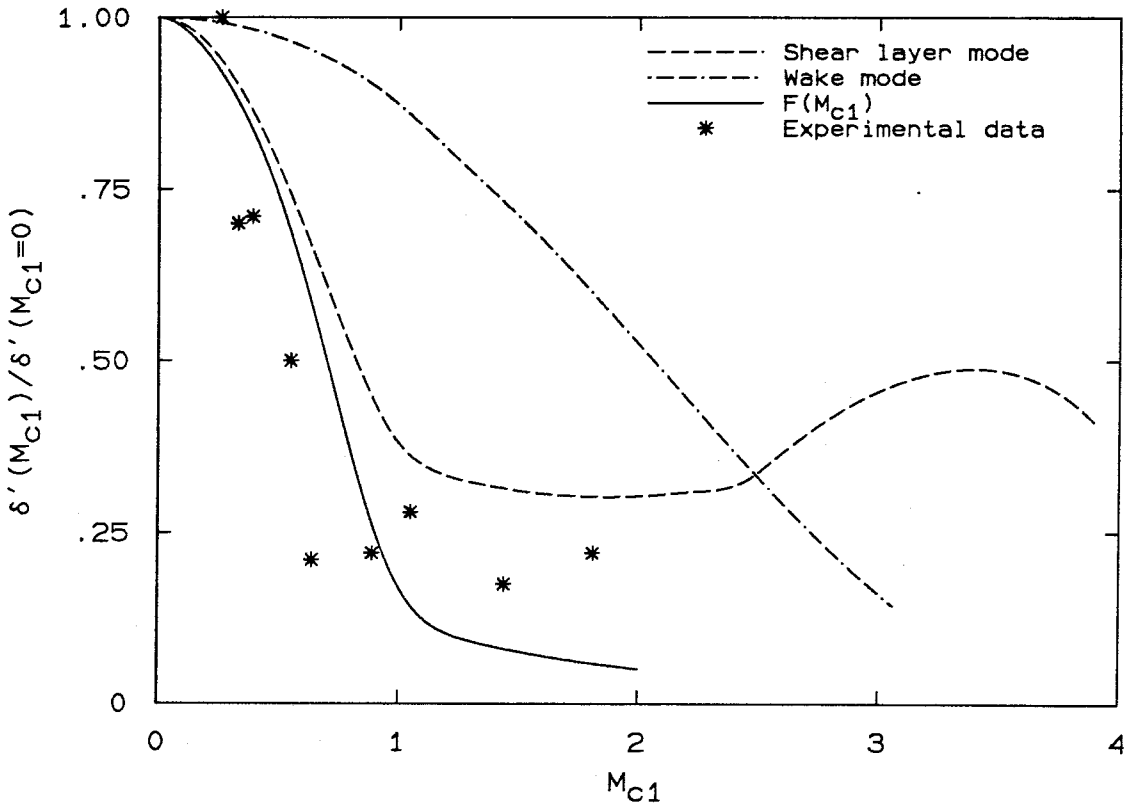

FIG. 4.29 A comparison of the results of the shear layer mode and the wake mode for the case $w = 0.4$ with $F(M_{c1})$ and with Papamoschou & Roshko's experimental data.

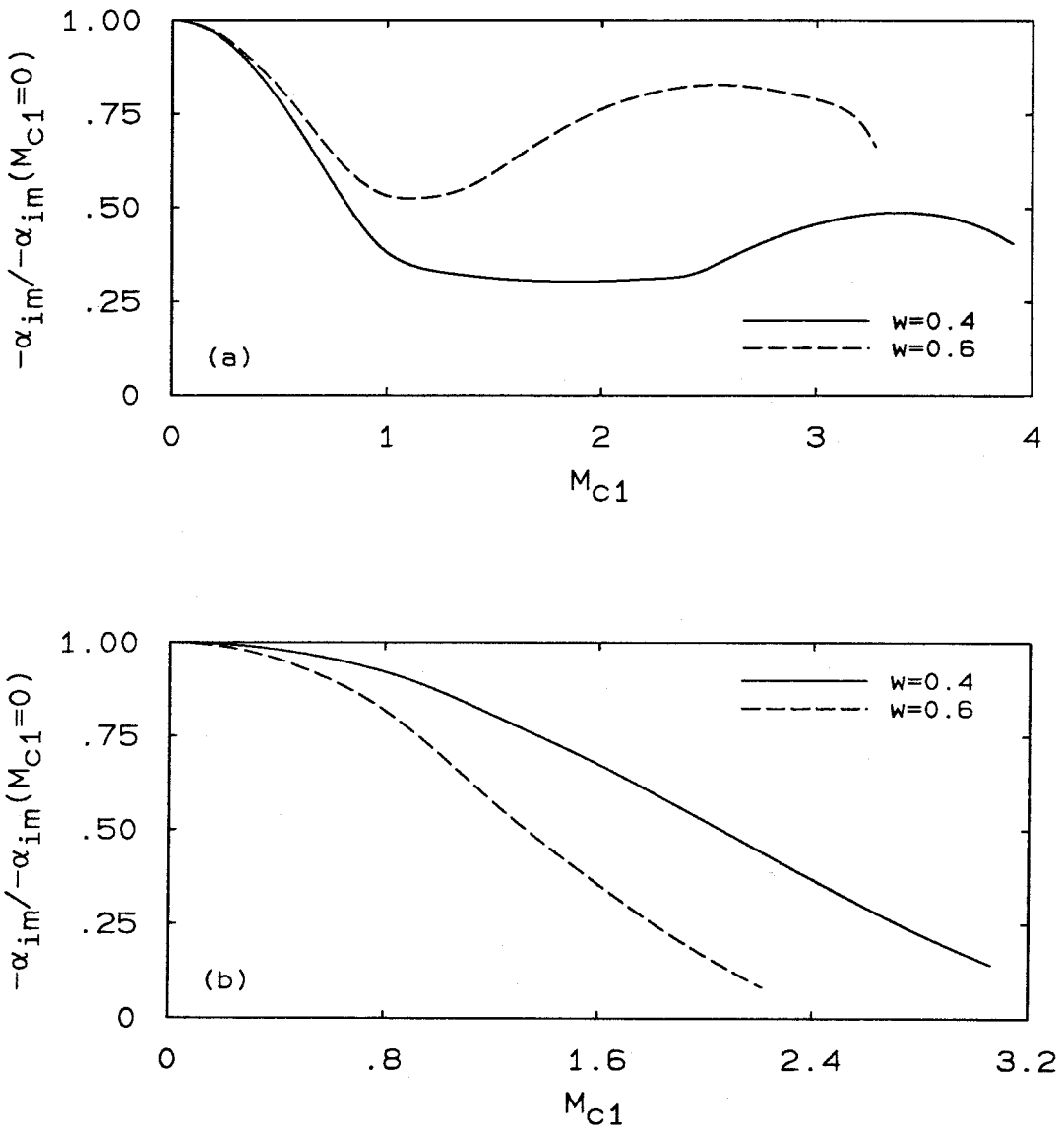

FIG. 4.30 Normalized maximum amplification rate *vs.* M_{c1}: $u_2/u_1 = 0.5$, $T_2/T_1 = 1.0$ and $R_2/R_1 = 1.0$. (a) The shear layer mode. (b) The wake mode.

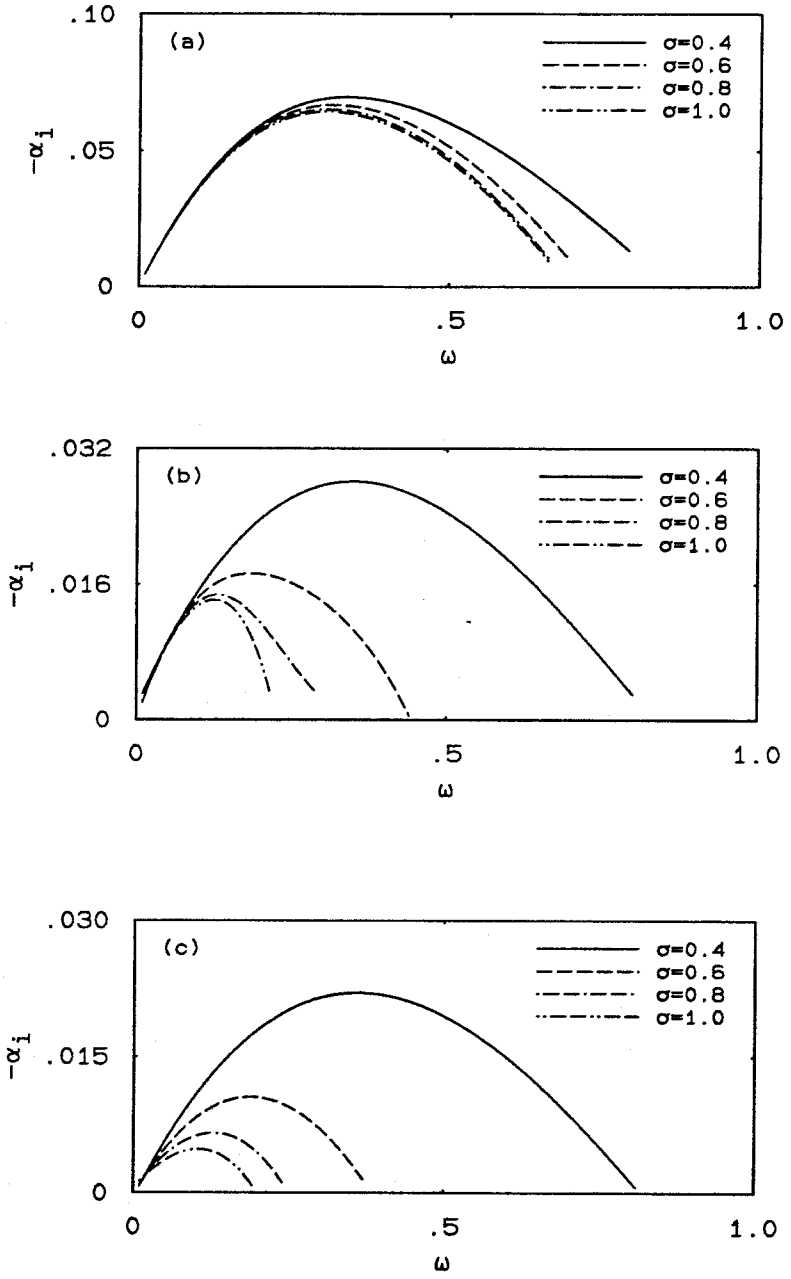

FIG. 4.31 Effect of the thickness of the total temperature profile σ on the amplification rate of the mixing layers: $u_2/u_1 = 0.5$, $T_{t2}/T_{t1} = 0.5$ and $R_2/R_1 = 1.0$. (a) $M_1 = 0.0$. (b) $M_1 = 4.0$. (c) $M_1 = 6.0$.

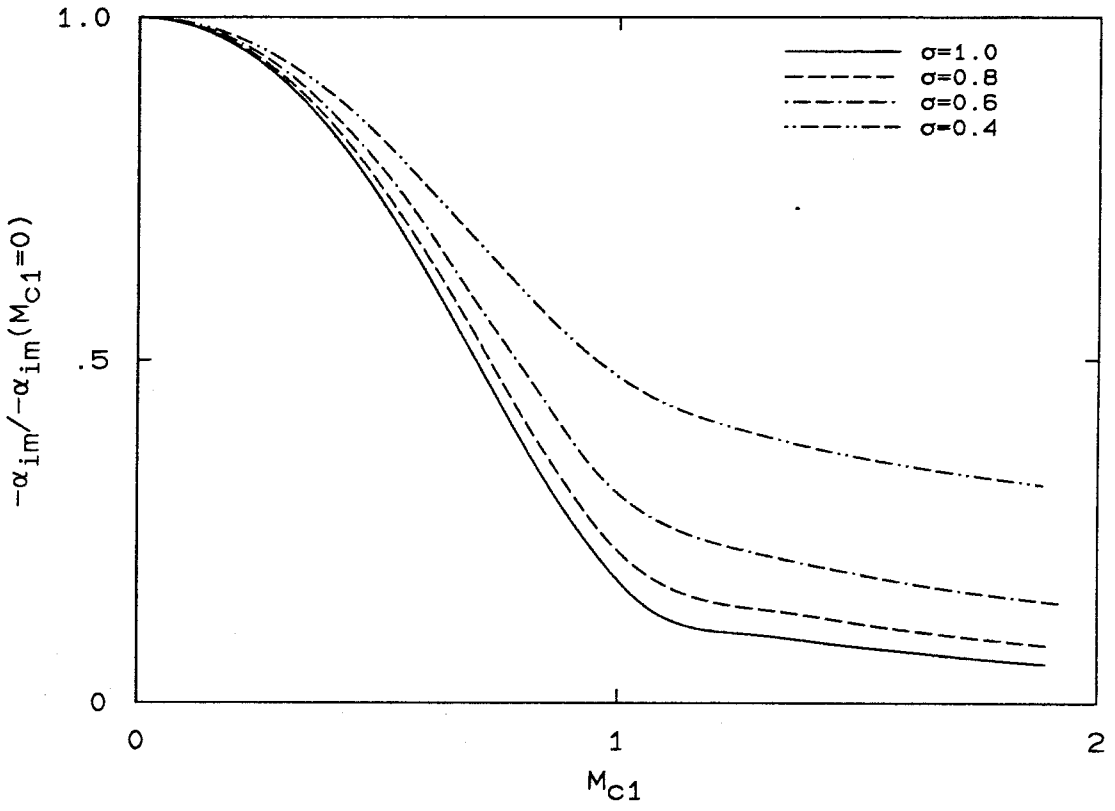

FIG. 4.32 Normalized maximum amplification rate *vs.* M_{c1} for the case $u_2/u_1 = 0.5$, $T_{t2}/T_{t1} = 0.5$ and $R_2/R_1 = 1.0$.

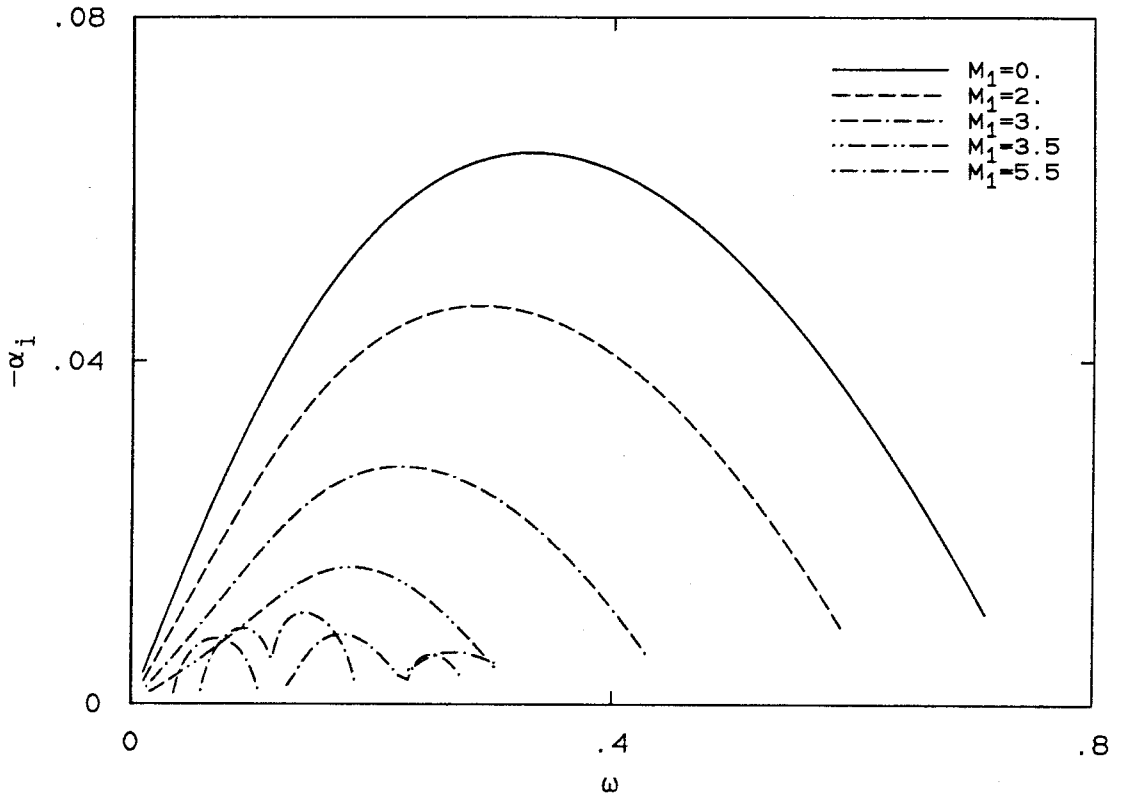

FIG. 5.1 Instability characteristics of the mixing layer for the case $u_2/u_1 = 0.5$ and $T_2/T_1 = 1.0$ at $d = 12$ unit lengths and $\delta = 3$ unit lengths.

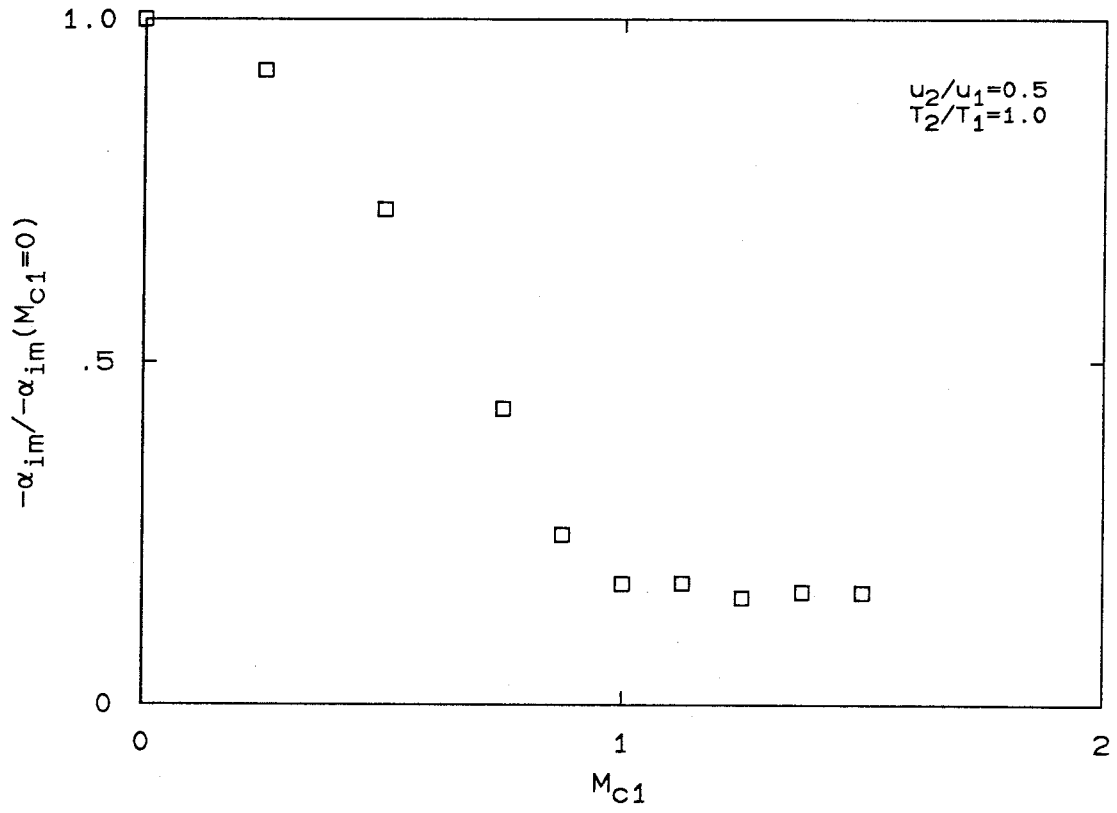

FIG. 5.2 Normalized maximum amplification rate *vs.* M_{c1} at $d = 12$ unit lengths and $\delta = 3$ unit lengths.

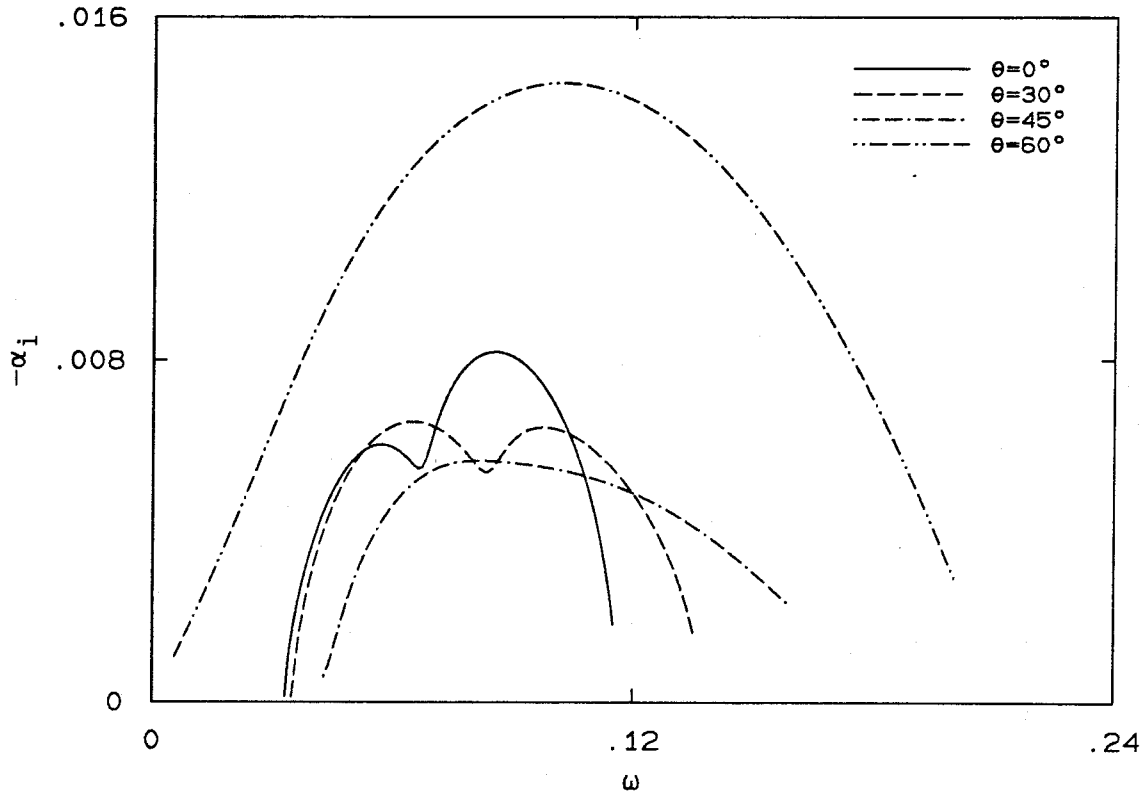

FIG. 5.3 Instability characteristics for 3-D spatially growing disturbances for the case $u_2/u_1 = 0.5$, $T_2/T_1 = 1.0$ and $M_1 = 5.5$ at $d = 12$ unit lengths and $\delta = 3$ unit lengths.

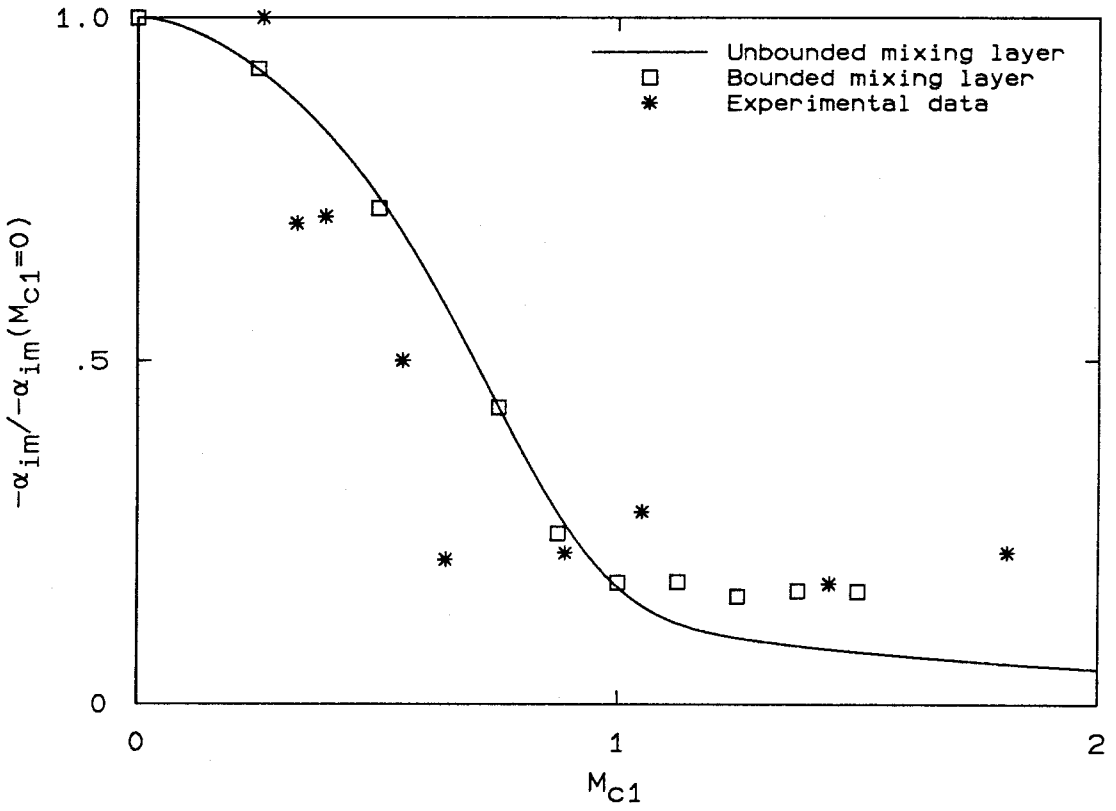

FIG. 5.4 A comparison of the data for 2-D bounded mixing layer with Papamoschou & Roshko's experimental data and with the function $F(M_{c1})$, which was obtained by least squares fitting the data from the calculations of 2-D mixing layers.

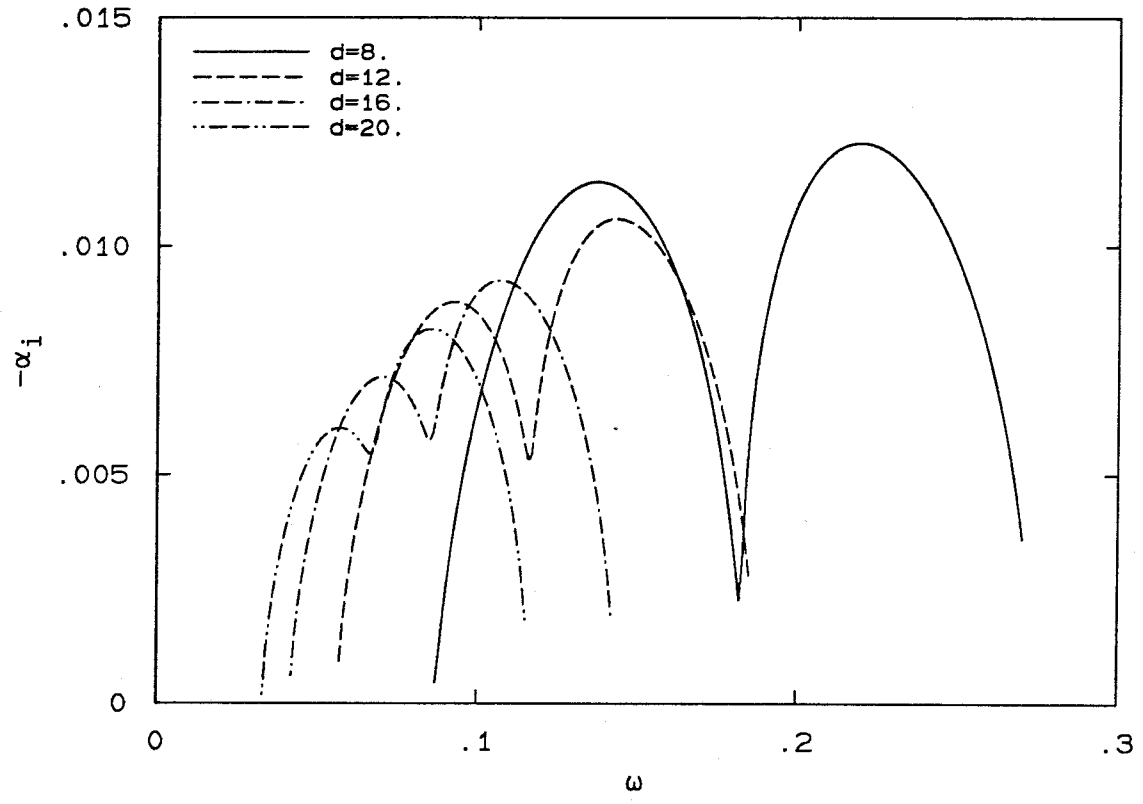

FIG. 5.5 Instability characteristics of the most unstable mode of the case $u_2/u_1 = 0.5$, $T_2/T_1 = 1.0$ and $M_1 = 5.5$ for different values of d at $\delta = 3$ unit lengths.

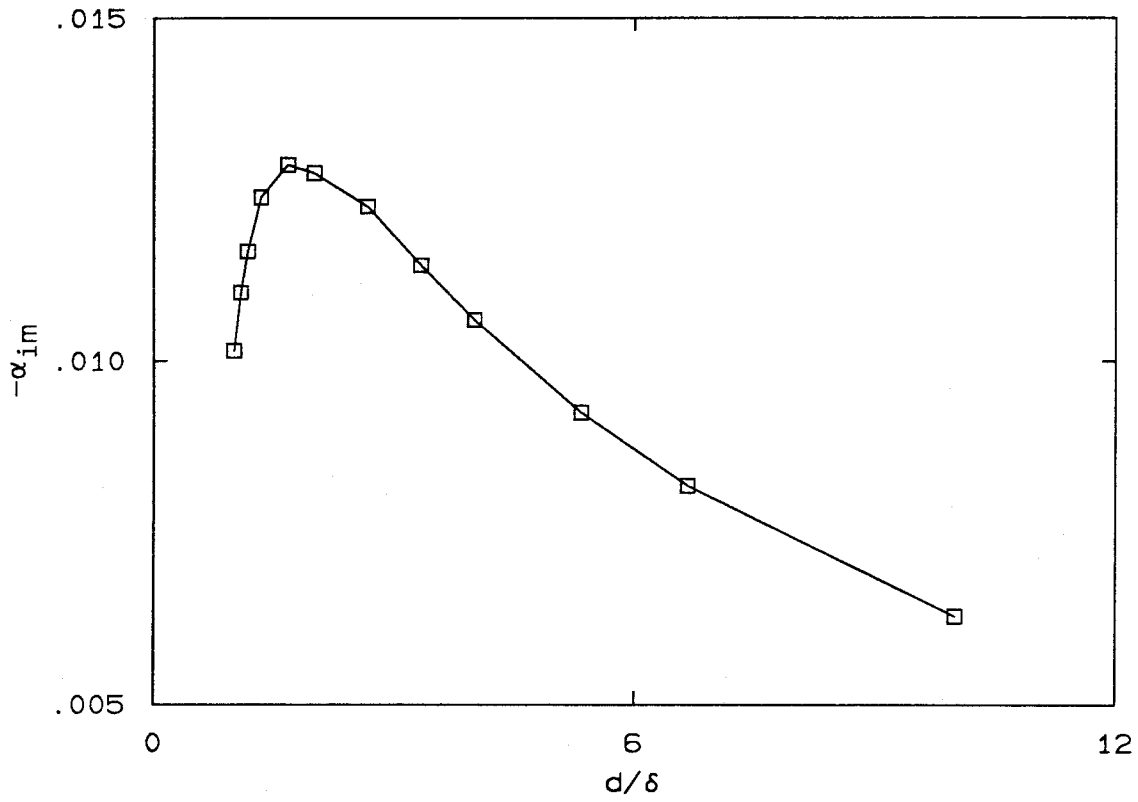

FIG. 5.6 The maximum amplification rate of supersonic instability mode *vs.* d/δ at $\delta = 3$ unit lengths and $M_1 = 5.5$.

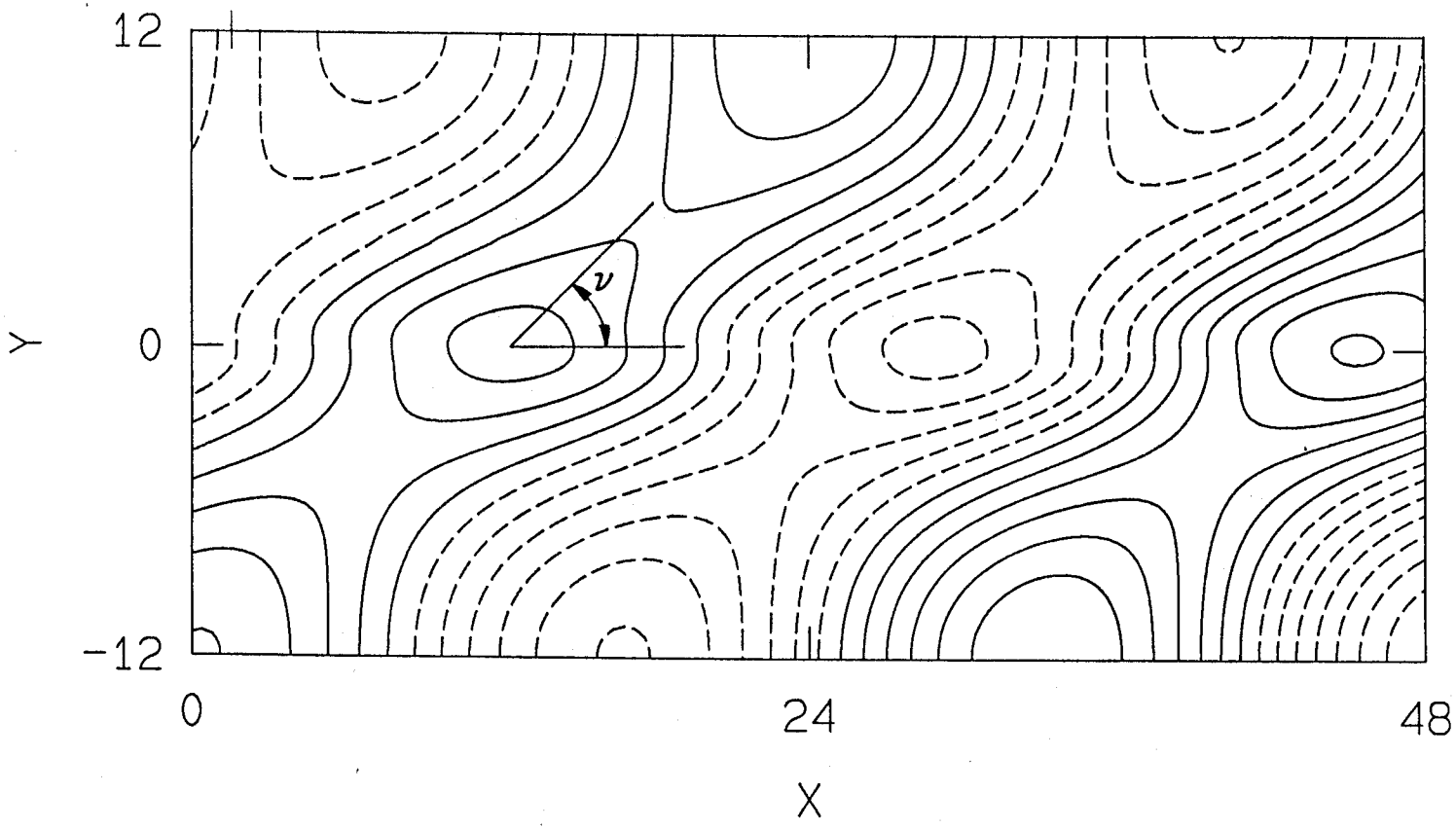

FIG. 5.7 Pressure perturbation field of the most unstable mode for $\delta = 3$ unit lengths, $d = 12$ unit lengths and $M_1 = 5.5$.

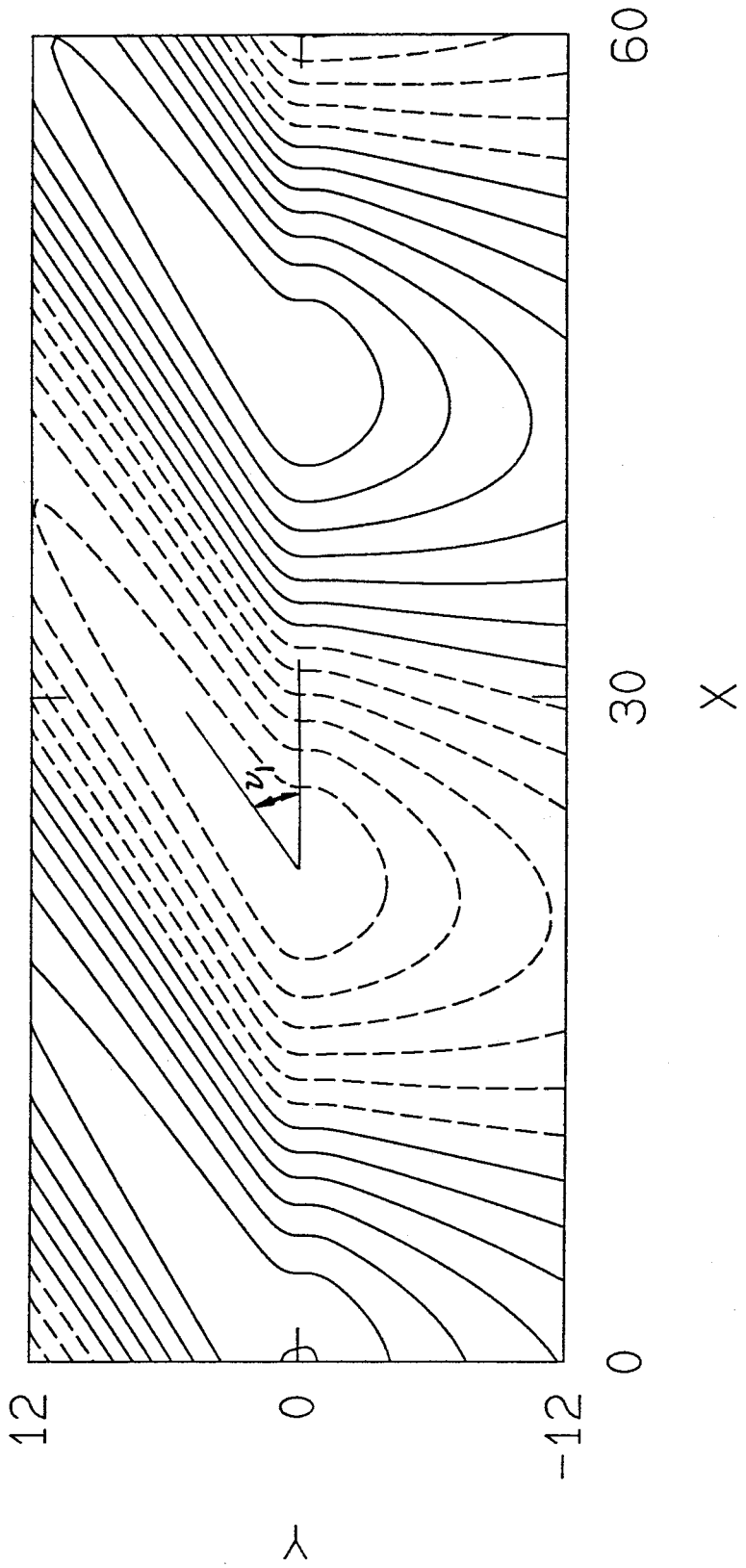

FIG. 5.8 Pressure perturbation field of the most unstable mode for the free mixing layer at $M_1 = 5.5$.

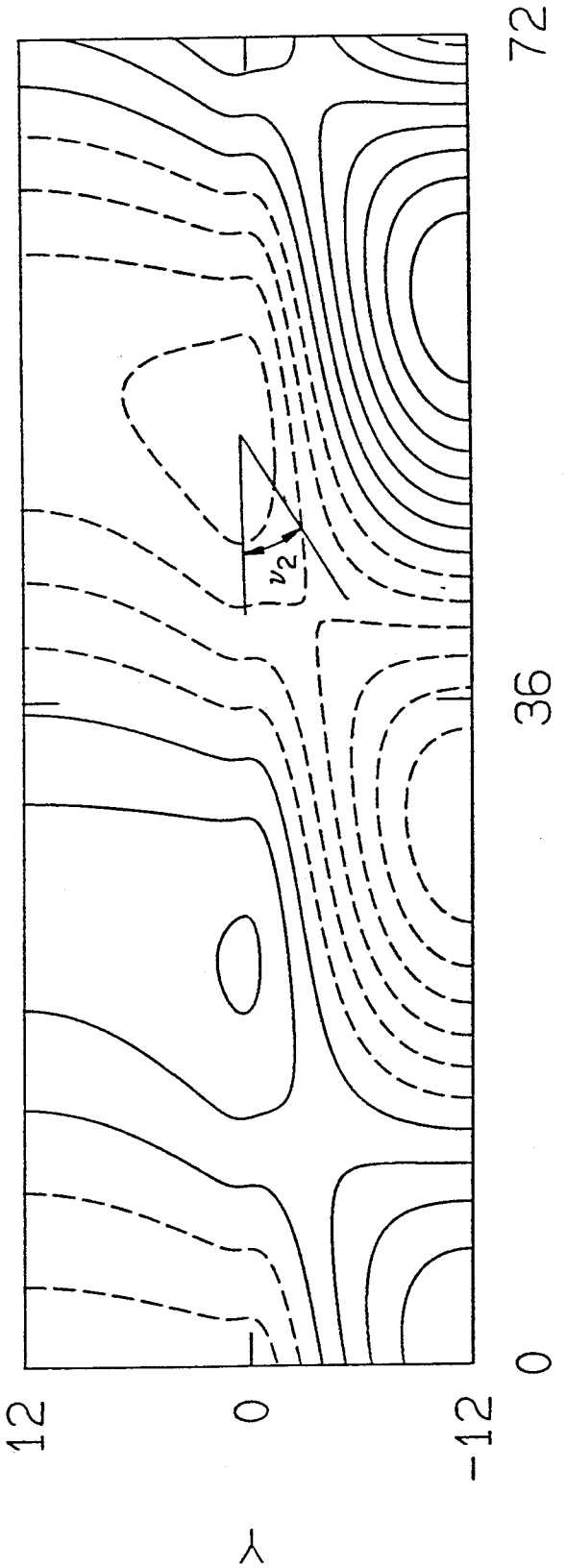

FIG. 5.9 Pressure perturbation field of the second unstable mode for $\delta = 3$ unit lengths, $d = 12$ unit lengths and $M_1 = 5.5$.

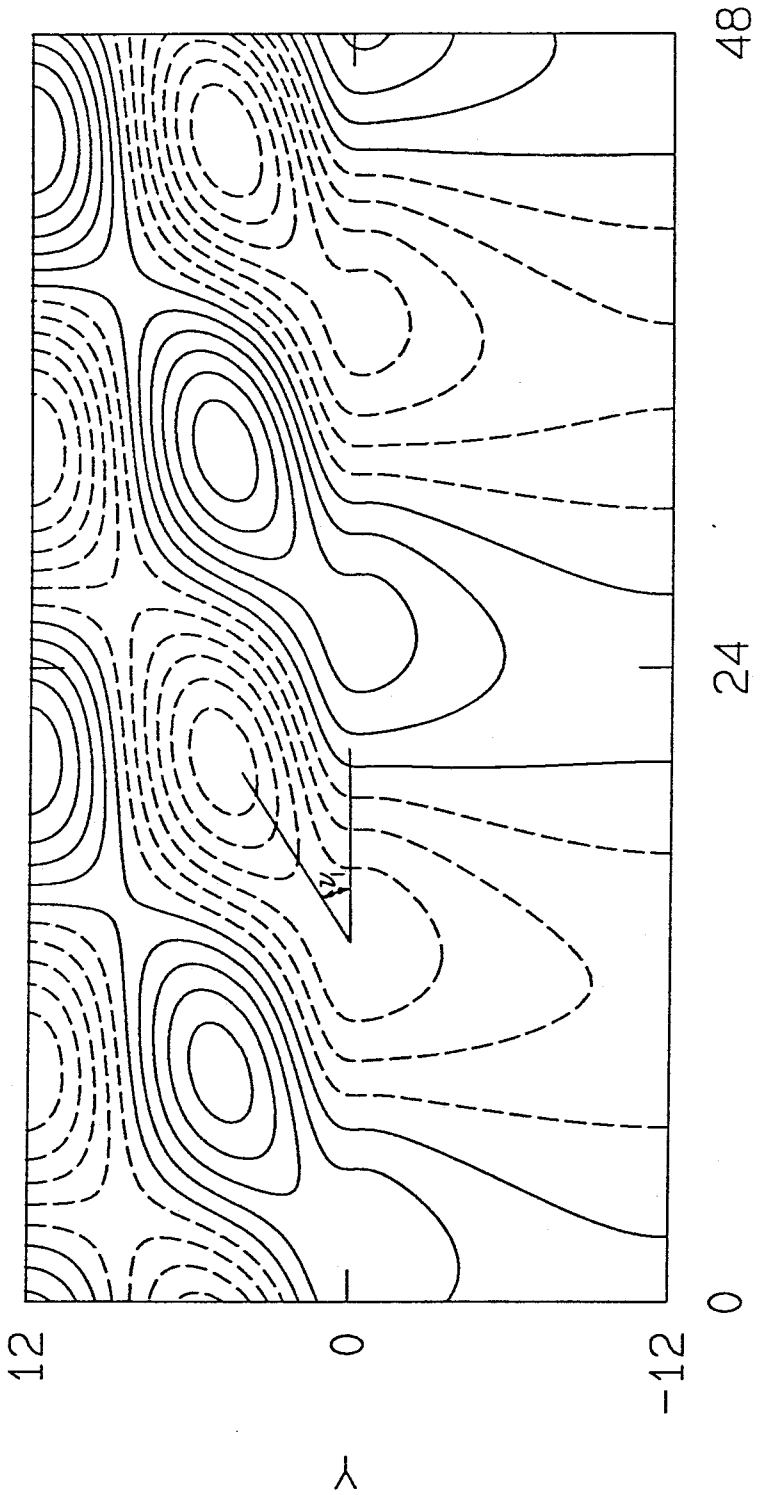

FIG. 5.10 Pressure perturbation field of the third unstable mode for $\delta = 3$ unit lengths, $d = 12$ unit lengths and $M_1 = 5.5$.

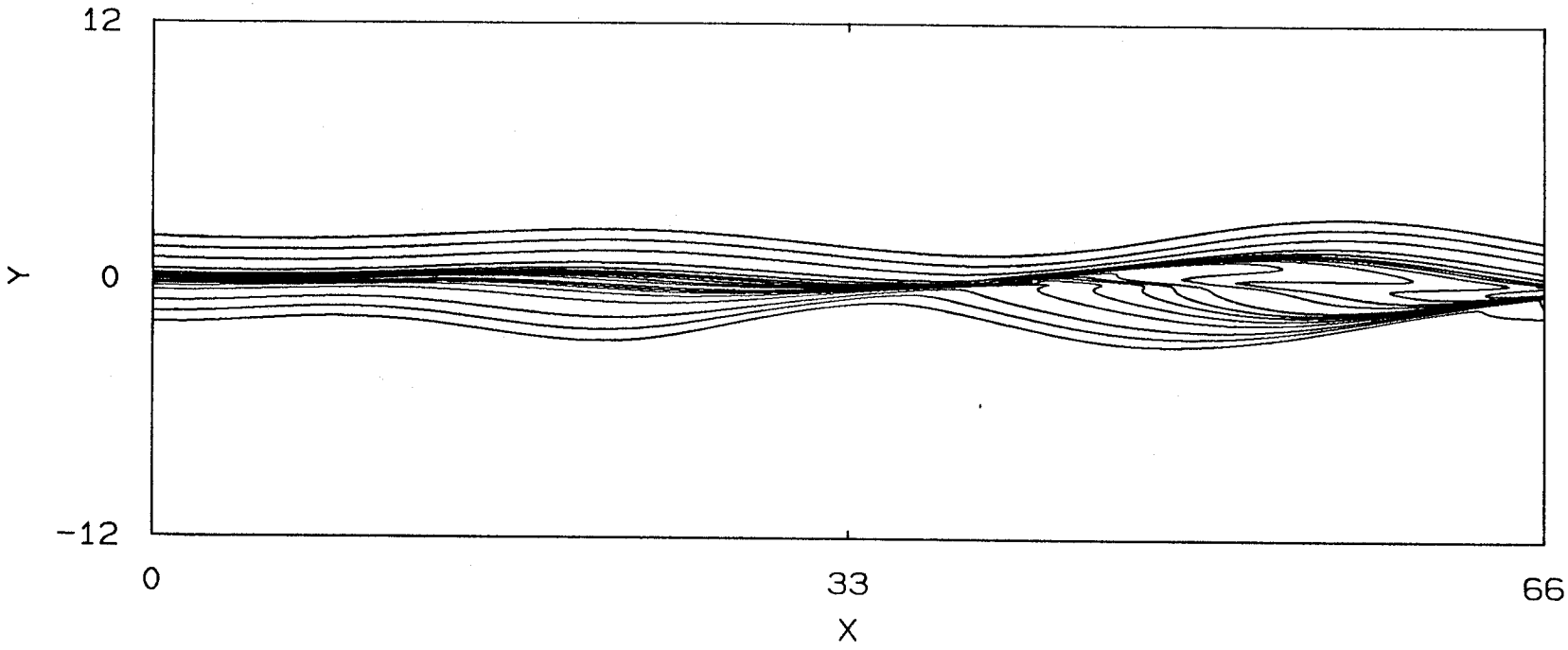

FIG. 5.11 Streaklines for the case $u_2/u_1 = 0.5$ and $T_2/T_1 = 1.0$ at $\delta = 3$ unit lengths, $d = 12$ unit lengths and $M_1 = 5.5$ (supersonic convective Mach numbers $M_{c1} = M_{c2} = 1.375$).

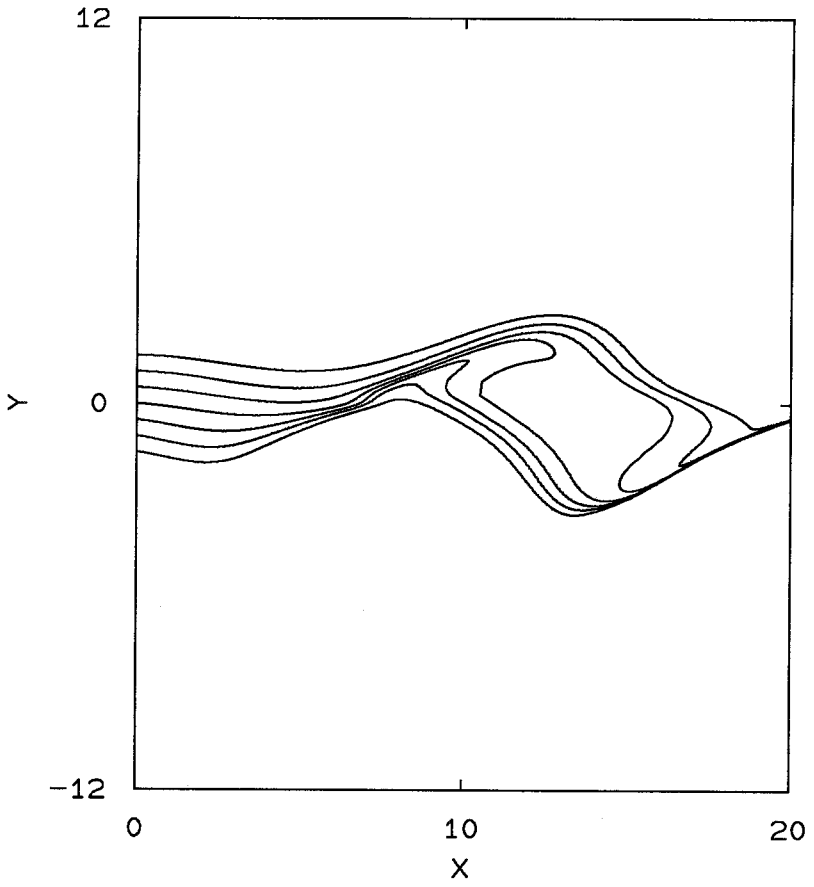

FIG. 5.12 Streaklines for the case $u_2/u_1 = 0.5$ and $T_2/T_1 = 1.0$ at $\delta = 3$ unit lengths, $d = 12$ unit lengths and $M_1 = 2.0$ (subsonic convective Mach numbers $M_{c1} = M_{c2} = 0.5$).